

**CHARACTERISATION OF SPATIO-TEMPORAL PATTERN OF RAINFALL
AND TEMPERATURE OVER THE LOWER NIGER RIVER BASIN**

BY

**ONYEISI, Joseph Onochie
MEng/SEET/2017/7167**

**DEPARTMENT OF AGRICULTURAL AND BIORESOURCES ENGINEERING
FEDERAL UNIVERSITY OF TECHNOLOGY,
MINNA**

JANUARY, 2022

ABSTRACT

The regional climate has been changing with attendant physical, social and environmental consequences culminating in extreme like flood, drought and other climate related hazards. Rainfall and temperature (maximum and minimum) plays fundamental role in agricultural development of Lower Niger River Basin and indeed Nigeria. In view of this, temporal rainfall and temperature patterns over the Lower Niger River Basin (LNRB) was examined. Thirty-five years (1979-2013) of rainfall and temperature time series data from six synoptic stations within the Basin was obtained from Lower Niger River Basin Development Authority, (LNRBDA) Ilorin. Analysis carried out includes Descriptive, homogeneity, autocorrelation, potential trend and spatial variability. Standardized anomaly was employed to determine the anomaly in rainfall and temperature. Similarly, regionalization of the Basin was done using the Principal Component Analysis (PCA) and K-Clustering Analysis to determine major modes of variability and partitioned to find the coherent zones within the Basin. From the result, mean annual rainfall ranges from 1120.5 mm to 1780.6 mm. Time series data analysis revealed homogeneity of rainfall and inhomogeneity in maximum and minimum temperature except at Oke Oyi station. There was positive autocorrelation across the Basin at lag1 = 0.301153 < 2 at Ganaga and was least at Oke Oyi in maximum and minimum temperature. Trend analysis was carried out using Mann-Kendall in annual and monthly bases, though the annual result showed statistically insignificant trend across the Basin in rainfall, maximum and minimum temperature. Monthly Mann-Kendall revealed marked variability in some months that were significant. The spatial variability of rainfall revealed Ekirin Ade having the highest in annual and seasonal times. The standardized anomaly showed marked transition in temperature regime; specifically, characterised by changing from colder than normal to warmer than normal conditions. The last decades depicted 80% colder than normal while the last fifteen years showed 90% warmer than normal. The anomaly result revealed 55% more rain, 41% Little Dry Spell and 4% normal within the last 35 years. The year to year variation that contributed to the anomalies were 34.68, 13.24 and 16% for maximum, minimum and rainfall. This increase portends a disturbing signal which could result in evaporation, heat related hazards and consequently extreme hazards associated with flooding and drought. Based on the regionalization analysis, using PCA and K-means Clustering, the result showed that the entire Basin is one coherent homogeneous zone. An understanding of this implication is central to Agricultural food security, water resources planning and management, and help to simplify the larger analysis of water budget.

TABLE OF CONTENTS

Content	Page
Title Page	i
Declaration	ii
Certification	iii
Dedication	iv
Acknowledgments	v
Abstract	vi
Table of Contents	vii
List of Tables	xiii
List of Figures	xv
List of Plates	xvi
Abbreviation	xvii
 CHAPTER ONE	
1.0 INTRODUCTION	1
1.1 Background to the Study	1
1.2 Statement of the Research Problem	4
1.3 Aim and Objectives of the Study	4
1.4 Justification of the Study	5
1.5 Scope of the Study	6
 CHAPTER TWO	
2.0 LITERATURE REVIEW	7
2.1 Precipitation	7
2.1.1 Forms of precipitation	7

2.1.1.1	<i>Rainfall</i>	7
2.1.1.2	<i>Drizzle</i>	7
2.1.1.3	<i>Hail</i>	8
2.1.1.4	<i>Sleet</i>	8
2.1.1.5	<i>Graupel</i>	8
2.2	Tropical Rainfall	9
2.2.1	The origin of tropical rainfall	9
2.2.2	Climate of Nigeria (rainfall)	10
2.2.3	Causes of rainfall in Nigeria	11
2.2.4	Changing rainfall pattern in Nigeria	12
2.3	Rainfall Characteristics	13
2.3.1	Physical characteristics	13
2.3.1.1	<i>Amount</i>	13
2.3.1.2	<i>Intensity</i>	13
2.3.1.3	<i>Rainfall duration</i>	13
2.3.1.4	<i>Frequency</i>	14
2.3.1.5	<i>Time distribution (intensity hyetograph)</i>	14
2.3.2	Climate change & variability	14
2.3.3	Rainfall and temperature extreme	15
2.3.4	Climate change variability and extreme impact	17
2.4	Trend	19
2.4.1	Indices of extreme rainfall event	20
2.4.2	Rainfall indices	21
2.4.3	Importance of rainfall indices	22
2.4.4	Characteristics of extreme rainfall indices	23

2.4.4.1	<i>Precipitation Total</i>	24
2.4.4.2	<i>Simple daily intensity index (SDII)</i>	24
2.4.4.3	<i>Precipitation above 95- percentile (R95P)</i>	24
2.4.4.4	<i>Precipitation above 99-percentile (R99P)</i>	25
2.4.4.5	<i>Precipitation in one day (RX1day)</i>	25
2.4.4.6	<i>Precipitation on consecutive five days (RX5day)</i>	25
2.4.4.7	<i>Consecutive wet days (CWD)</i>	25
2.4.4.8	<i>Intense precipitation above 10 mm (R10 mm)</i>	26
2.4.4.9	<i>Intense precipitation above 20 mm (R20 mm)</i>	26
2.4.4.10	<i>Days with NN mm of rainfall (RNN mm)</i>	26
2.5	Quality of Rainfall Data	27
2.5.1	Consistency of rainfall data	27
2.5.1.1	<i>Correlation</i>	27
2.5.2	Direct method of homogeneity testing	28
2.5.2.1	<i>Use of metadata</i>	28
2.5.2.2	<i>Side by side comparison of instrument</i>	29
2.5.3	Indirect methodologies for homogeneity testing	30
2.5.3.1	<i>Use of station data</i>	30
2.6	Spatial Temporal Variation of Rainfall	30
2.6.1	Spatial variation	31
2.6.1.1	<i>Temporal variation</i>	31
2.6.2	Assessment of spatial temporal rainfall variation	32
2.6.2.1	<i>Spatial distribution</i>	32
2.6.2.2	<i>Spatial interpolation</i>	32
2.6.2.3	<i>Thiessen polygon</i>	33

2.6.2.4	<i>Smoothing splines</i>	33
2.6.2.5	<i>Kriging method</i>	34
2.6.2.6	<i>Principal component analysis</i>	35
2.6.2.7	<i>Temporal distribution</i>	36
2.7	Regression Analysis	37
2.7.1	Spearman's rank correlation coefficient	39
2.7.2	Mann kendall test	41
2.7.3	The Sen's estimator of slope	42
2.8	Standardised Anomaly Index	42
2.9	Regionalisation of Rainfall	43
2.9.1	Approaches to rainfall regionalisation	44
2.9.1.1	<i>Correlation analysis</i>	44
2.9.1.2	<i>Principal component analysis</i>	44
2.9.1.3	<i>Common factor analysis (CFA)</i>	45
2.9.1.4	<i>Cluster analysis procedure</i>	46
2.9.1.5	<i>Spectral analysis</i>	46
2.9.1.6	<i>Hierarchical regionalisation approach</i>	47
2.9.1.7	<i>Region of influence approach</i>	47
 CHAPTER THREE		
3.0	MATERIAL AND METHODS	48
3.1	Materials	48
3.1.1	Dataset	48
3.1.2	Location of the study area	48
3.1.3	Hydrometeorology of the study area	49
3.2	Methods	50

3.2.1	Data collection	50
3.2.2	Data quality analysis (preliminary)	50
3.2.2.1	<i>Homogeneity test</i>	51
3.2.2.2	<i>Kruskal - Wallis homogeneity test</i>	50
3.2.2.3	<i>Wald – Wolfowitz run test</i>	52
3.2.2.4	<i>Persistence test</i>	52
3.3	Spatial Variation	52
3.3.1	Kriging method for producing spatial of LNRB	52
3.3.2	Temporal variation	53
3.3.2.1	<i>Analysis of serial dependence (autocorrelation)</i>	53
3.3.3	Temporal resolution for trend analysis	54
3.3.3.1	<i>Mann – Kendall test</i>	54
3.3.3.2	<i>Mann – Kendall for monthly or seasonal</i>	55
3.3.3.3	<i>Determination of the magnitude of change in trend (Sen’s slope)</i>	57
3.3.3.4	<i>Statistical change point (SCP) mutation detection</i>	59
3.4	Standardised Anomaly Index (SAI)	61
3.5	Principal Component Analysis	62
 CHAPTER FOUR		
4.0	RESULTS AND DISCUSSION	64
4.1	Preliminary Analysis of Result	64
4.1.1	Geographical autocorrelation	67
4.2	Descriptive Statistics of Time Series Characterisation of Rainfall	68
4.2.1	Annual and seasonal time series Plot for the stations and their statistics	68
4.3	Characterisation of Extreme Rainfall Indices	69
4.3.1	Trend and magnitude of rainfall and temperature	69

4.3.2	Spatial distribution of the mean annual and seasonal rainfall	76
4.4	Determination of Flood and Dry Spell using Standardised Anomaly Index	78
4.5	Regionalisation of Rainfall into Coherent Zones	85
4.5.1	Results principal component analysis of rainfall	85
4.5.2	Component coefficients	87
4.6	Regionalisation of Coherent Rainfall	92
 CHAPTER FIVE		
5.0	CONCLUSION AND RECOMMENDATIONS	94
5.1	Conclusion	94
5.2	Recommendations	95
5.3	Contribution to Knowledge	95
REFERENCES		97
APPENDICES		103

LIST OF TABLE

Table	Title	Page
2.1	Standardised anomaly index value classification	43
3.1	Study Area Station with Longitude and Latitude	49
4.1	Rainfall Homogeneity test result for the LNRB at 95% significance level	64
4.2	Maximum Temperature Homogeneity Test Result for the LNRB at 95% Significance Level	66
4.3	Minimum Temperature Homogeneity test result for the LNRB at 95% significance level	67
4.4	Minimum Temperature Homogeneity Test Result for LNRB at 95% Significance	67
4.5	Descriptive Statistics for Maximum Temperature	68
4.6	Descriptive Statistics for Minimum Temperature	69
4.7	Descriptive Statistics for Rainfall	69
4.8	Maximum Temperature Trend Result of the LNRB	70
4.9	Minimum Temperature Trend Result of the LNRB	70
4.10	Annual Rainfall Trend Result in the LNRB	70
4.11a	Monthly Rainfall, Maximum Temperature and Minimum Temperature Trend Result Ekirin Ade	71
4.11b	Monthly Rainfall, Maximum Temperature and Minimum Temperature Trend Result at Ganaga	71
4.11c	Monthly Rainfall, Maximum Temperature, Minimum Temperature, and Trend Result at Lafiagi	72
4.11d	Monthly Rainfall, Maximum Temperature and Minimum Temperature Trend Result at Obangede	72
4.11e	Monthly Rainfall, Maximum Temperature and Minimum Temperature Trend Result at Oke Oyi	73
4.11f	Rainfall, Maximum Temperature and Minimum Temperature Trend Result at Olamaboro	74

4.12	Maximum Temperature Standardised Anomalies for LNRB	79
4.13	Warmer than normal maximum Temperature Standardized Anomaly	80
4.14	Colder than Normal maximum Temperature Standardized Anomaly	80
4.15	Minimum Temperature Standardised Anomalies for LNRB	81
4.16	Summary Six years Warmer than Normal Minimum Temperature Standardized Anomaly	82
4.17	Summary of Six years Colder than Normal Minimum Temperature Standardized Anomaly	82
4.18	Rainfall Standardized Anomalies values for the LNRB	84
4.19	Summary of wetter years and little dry spell of rainfall from 1979-2013 in the LNRB	85
4.20	Eigenvalues and Variance of the Non-Rotated first six principal components (PCs) for monthly precipitation series from 1979 – 2013	87
4.21	Principal Components Coefficients of the LNRB Rainfall Series	88
4.22	Factor loading	90
4.23	Cluster Analysis	93
4.24	Cluster Centroid (mm)	93
4.25	Distance between Cluster Centroids (mm)	93
4.26	Final Partition	93

LIST OF FIGURES

Figure	Title	Page
3.1	Map of Nigeria showing the Lower Niger River Basin	49
4.1(a)	Rainfall Pettit's Test	65
4.1(b)	Rainfall Pettit's Test	65
4.1(c)	Rainfall Pettit's Test	65
4.2(a)	Pettit's Test	66
4.2(b)	Pettit's Test	66
4.2(c)	Pettit's Test	66
4.3	Sen's slope of Ekirin Ade maximum temperature from 1979-2013	75
4.4	Sequential Mann-Kendall change per unit time of Ekirin Ade from 1979-2013	75
4.5a	Total Annual Spatial Rainfall (Mar-Nov)	76
4.5b	Seasonal Spatial Rainfall (April –June)	77
4.5c	Seasonal Spatial Rainfall (July –Sept)	77
4.5d	Seasonal Spatial Rainfall (Oct-Nov)	78
4.6	Rainfall Standardised Anomaly of Oke Oyi from 1979-2013	83
4.7	Scree Plot diagram	86
4.8	Principal Component 1	88
4.9	Principal Component 2	89
4.10	Principal Component 3	89
4.11	Factor Loading D1	90
4.12	Factor Loading D2	91
4.13	Biplot Map	91
4.14	Correlation of stations	92

LIST OF PLATE

Plate	Title	Page
I	Flood Farm in Kogi State Nigeria (2018)	20

ABBREVIATION

HRU	Hydrological Response Unit
LNRB	Lower Niger River Basin
DTR	Diurnal Temperature Range
IPCC	Intergovernmental Panel for Climate Change
ITD	Intercontinental Tropical Discontinuity
UNFCCC	United Nation Framework Convention on Climate Change
GHG	Green House Gases
MWR	Moving Window Regression
LAUO	Linear Unauthorised Unbiased Optimal
WMO	World Meteorological Organization
MSD	Monsoon Spectra Density
PSD	Power Spectra Density
LNRBDA	Lower Niger River Basin Development Authority

CHAPTER ONE

1.0 INTRODUCTION

1.1 Background to the Study

Rainfall and Temperature variations are the most evident effect of climate change (Sarwar *et al.*, 2014). In the recent past, Africa and Nigeria in particular, the emphasis of many scholars in the study of tropical climatology has been the consideration of rainfall characteristics, such as rainfall amount, duration and intensity. Climate change seems to be the foremost global challenge facing humans at the moment, even though it seems that not all places on the globe are affected. The scientific community has not been left out as causes and solutions are being proffered and it is expected to linger on for a long time (Obot *et al.*, 2010). Two major indicators of climate change are rainfall and temperature. Rainfall is a climate parameter that affects the way and manner man lives. It affects every facet of the ecological system, flora and fauna inclusive. Hence, the study of rainfall is important and cannot be over emphasized. Aside the beneficial aspect of rainfall, it can also be destructive in nature; natural disasters like floods and landslides are caused by rain (Ratnayake and Herath, 2005).

Climate variability is the variations of the normal state and other statistics of the climate on all temporal and spatial scales beyond that of individual weather events. Variability may result from natural internal processes within the climate system (internal variability) or from anthropogenic external forces (external variability) (IPCC, 2005). The global climate has changed rapidly with the global mean temperature increasing by 0.7 °C within the last century, but the rates of change are significantly different among regions (IPCC 2007). This is primarily due to the varied types of land surfaces with different surface albedo, evapotranspiration and carbon cycle affecting the climate in different ways (Meissner *et al.*, 2003; Snyder *et al.*, 2004). Several studies have been

carried out at different temporal and spatial scales in different part of the globe. For example, Adepitan *et al.* (2017) examined and confirmed changes in trend of some cities in South Western Nigeria. Hasanean (2001) examined trends and periodicity of air temperature from eight meteorological stations in the east Mediterranean and observed positive significant trends in Malta and Tripoli, and negative trend in Amman. Turkes *et al.* (2002) evaluated mean, maximum and minimum air temperature data in Turkey during the period 1929 –1999. Their analysis revealed spatial temporal patterns of long-term trends, change points, and significant warming and cooling periods. (Fan *et al.*, 2010) reported separately that Diurnal Temperature Range (DTR) has been on the decrease in most region of the world. Karl *et al.* (1993) analyzed temperature data from 37% of global land mass and found high increment in the minimum compared to the maximum temperature. Studies on the spatial-temporal variability and trend in temperature are very limited in Africa. Several studies have attributed extreme rainfall to be the major cause of flooding worldwide. Such studies include; Odekunle (2001); Ologunorisa, (2004). Other studies had identified the characteristics of extreme rainfall that are associated with flood frequency to include duration, intensity, frequency, seasonality, variability, trend and fluctuation Olaniran (1983); Ologunorisa. (2001); Ayansina *et al.* (2009) also investigated the seasonal rainfall variability in Guinea savannah part of Nigeria and concluded that rainfall variability continues to be on the increase as an element of climate change.

Global climate changes have potential to cause devastating impact on society natural systems and infrastructure on a larger scale. In the last decades, we had witness extreme rainfall and temperature leading to flooding in many parts of Nigeria especially along the Niger-Benue trough, the continental shelves, along Niger delta in the Southern part of Nigeria and drought leading to desertification in certain Northern States of the

country. Precipitation is considered as one of the most important variables for characterization and understanding climate impacts on the hydrologic system. Sustainable socioeconomic development on the Lower Niger River Basin (LNRB) could be threatened by erratic rainfall and extreme temperature. Serious water stress and population increase can bring conflict among the local communities because agriculture is their major activities within the basin, available lands for irrigation and other integrated farming could be put under serious water stress. The incomprehensive analysis on the variation of rainfall and temperature in time and space resulting in inefficient utilization of water resource within the basin. Favourable conditions to the development of the LNRB are predicted for the near future, but they are associated with great uncertainties. It is projected that climatic factors will increase in the 21st century according (Sarwar *et al.*, 2014). The actual effect of climate on the hydrologic cycle and water resources are associated with uncertainties.

Characterization of the spatial variability of rainfall, temperature and its association with local and global stressor are required for effective water management including control and utilization of flood water. An understanding of spatial rainfall and temperature characteristics is central to water resources planning and management in the face of global climate change (Lin *et al.*, 2015). This information is important in Agricultural planning, flood frequency analysis, flood hazard mapping, alert systems or information for ungauged basins, hydrological modeling and water resource assessment Rakib. (2018). The knowledge of rainfall and temperature variation patterns will help to maximize various water resources endowment. In addition, characterisation of climate variables will enhance better understanding of the regional climate. Moreover, it allows for the simplification of larger analysis such as; water budget and agricultural production which depends on this kind of data as input Rakib (2013). In view of all this,

to avoid further losses arising from extreme weather events (Flooding and Drought), characterisation of climate change had to be carried out. The whole essence of this study is to understand the variation of rainfall and temperature patterns over Lower Niger River Basin using data from 1979 - 2013 and their associated mechanism. This study will add knowledge to the obvious effect of climate change, in addition to local conditions that also affect the spatial variations of season precipitation. Hence the focus of this study is to characterised spatial rainfall and temperature patterns for hazard analysis in the Lower Niger River Basin.

1.2 Statement of the Research Problem

The problems that drive the motivation for this study in real-time can be summarized as follows:

- i. Lack of adequate information on the spatial mode of rainfall and temperature variability in the Lower Niger River Basin (LNRB).
- ii. Undefinable change in temperature regime with serious rainfall anomaly.
- iii. Conventional practice was to delineate regions as geographically contiguous area based on physiography that may not have causal/explanatory variables influencing rainfall

1.3 Aim and Objectives of the Study

The aim of this study is to characterise spatio-temporal patterns of rainfall and temperature for hazard analysis over LNRB.

The specific objectives of this study are as follows:

1. Ascertain potential long-term trends and statistical change point in rainfall and temperature patterns
2. Determine flood Wet and dry spell for hazard analysis.

3. Regionalize rainfall pattern over the LNRB.

1.4 Justification of the Study

Studies has showed that climate change effect is not just threatening food security but the existence of human globally. Farmers in the Lower Niger River Basin are yet to understand the effect of climate change on the planting and harvesting seasons of crops. Traditional methods of cultivation, use of local seeds with long duration coupled with extreme temperature and serious rainfall anomalies has led to monumental loss in terms of yield. Moreover, farmers mostly regionalise homogeneous zones based on simple physiography and not on causal/explanatory factors responsible for the changes within the Basin. Most studies carried out has been on trend, year and year variation (time and space) on certain cities in Nigeria, but no documented evidence of analysis taking into consideration step-wise change, sequential trend to identify starting point in rainfall and temperature trajectories, over the LNRB which rely wholly on rainfall for their Agricultural activities. The study of climate variables is good tool for policy makers, in order to estimate among other factors, erosion and desertification that appear as consequence of climate change.

In addition, the study is designed to enhance our understanding of climate variability focusing on annual, seasonal, decadal and spatial patterns in the face of global climate change. An understanding of spatio-temporal rainfall and temperature characteristics is central to water resources planning and management, hydrological design, forecast issues, alert systems or information for un-gauged basin, flood frequency analysis, hydrological modeling and water resources assessment (Lin *et al.*, 2015), in the face global climate changes.

1.5 Scope of the Study

The scope of this study is only limited to the assessment of spatial rainfall and temperature change (maximum and minimum) within the basin. The entire basin is considered as a single spatial Hydrologic Response Unit (HRU). The study employed the use of secondary data for analysis. The limitation of this study is basically the lack of extensive and continuous data pool as well as the integrity of available data which affect result. Quality test was employed to ensure the quality of data.

CHAPTER TWO

2.0 LITERATURE REVIEW

2.1 Precipitation

This is any product of the condensation of atmospheric water vapour that falls under gravity. The main forms of precipitation include drizzle, rain, sleet, snow, graupel and hail. It is recognized that evaporation from ocean surfaces is the chief source of moisture for precipitation. Generally speaking, location of a region with respect to circular latitude and distance to moisture source is primarily responsible for its climate.

2.1.1 Forms of precipitation

2.1.1.1 Rainfall

Rain is liquid water in the form of droplets that have condensed from atmospheric water vapor and then become heavy enough to fall under gravity. Rain is a major component of the water cycle and is responsible for depositing most of the fresh water on the Earth. Drops of liquids water fall from the cloud when water vapour condenses around dust particle in the cloud resulting in tiny droplet that combines to form larger droplet and breaks the gravitational forces thereby falling as rain. Rainfall droplets are usually 0.5 mm (0.2 in) in diameter and above. It can be classified based on intensity as

Light rain – up to 2.5 mm/h

Moderate rain- 2.5 mm/h to 7.5 mm/h

Heavy rain- above 7.5 mm/h

2.1.1.2 Drizzle

Liquid precipitation that consists of very small and uniformly dispersed droplets of liquid water that appears to "float" while following air currents. Drizzle sometimes

called mist is usually 0.1 to 0.5 mm (0.004 to 0.2 in) with slow settling rates that they occasionally appear to float.

2.1.1.3 Hail

A clear opaque ball of hard ice, ranging in diameter from 1/8 inch or so to 5 inches or larger produced by convective clouds. Hailstone size may be conical or irregular in shape and ranges (0.2 to 0.5 in) in diameter. They are generally composed of alternating layers of glaze and rime. It is measured and reported in inches, but hailstones are usually compared to common objects when reported to the public by television or radio, such as pea size, walnut size, golf-ball size, baseball size, Hail frequently displays a layered appearance of alternate opaque.

2.1.1.4 Sleet

Generally globular transparent ice pellets that have diameters of 5 mm (0.2 inch) or less and that form as a result of the freezing of raindrops or the freezing of mostly melted snowflakes. Sleet may occur when a warm layer of air lies above a below-freezing layer of air at the Earth's surface Sleet is frozen raindrops that strike the earth surface. It is frozen raindrops of transparent grains which form at a subfreezing temperature. The lowest layer part of the troposphere will freeze in sleet situation and deep to freeze drops.

2.1.1.5 Graupel or Snow

Graupel is composed of ice-crystal chiefly in complex branched hexagonal form and often agglomerated into snow-flakes which may reach several inches in diameter. The density of freshly fallen snow varies greatly; 125 to 500 mm (5 to 20 in) which undergo riming upon collision with super cooled water. Graupel is almost like hail except for their size, which is 5 mm less in diameter.

2.2 Tropical Rainfall

Tropical rainfall is of prime importance as it can either be life-giving or life taking as the case may be if excess rainfall produces floods or insufficient rainfall results in drought. Apart from its relevance on life, tropical rainfall is also important for global climate and weather. Over two-thirds of global precipitation falls in the tropics. As a result, a large amount of energy in the latent heat form is released in the low latitudes. The energy not only balances radiation heat losses but it is used to power the global atmospheric circulation. Thus, an understanding of the geographical distribution of rainfall is a leeway to understanding the global distribution of heat sources that drive the global atmospheric heat regime. Rainfall is probably the most variable element of tropical climates. The annual total differs from year to year and from one place to another. Its spatial and temporal variations are also demonstrated by characteristic seasonal and diurnal distribution, intensity, duration and frequency of rain-days, (Udo, *et al.*, 2002).

2.2.1 The origin of tropical rainfall

Udo *et al.* (2002) pointed out that the origin of rainfall in the tropics can be classified into three different types namely; conventional, cyclonic and Orographic. Conventional rainfall is the result of free convection due to heating alone, dynamic processes such as convergence or physical forcing over mountain ridge. Conventional rainfall generally occurs over a limited spatial scale of between 10-20 km² and 200 – 300 km². This type of rainfall is characterized, therefore, by considerable spatial variability. Cyclonic rainfall is produced by horizontal convergence of moist air in a circular area of low pressure where the velocity maximum exists. Its most impressive expression is in tropical cyclone where the combined processes of cyclonic inflow and convection produce intense rainfall. Cyclonic storms typically last between one to five days, which

contrasts with the short life span of individual convection cells. The area affected by cyclonic precipitation may be large, as throughout their lifetimes, tropical cyclonic storms can move several hundred kilometers. Orographic rainfall is the result of condensation and cloud formation in moist air that has been physically forced over topographic barriers. Convective processes in the tropics may aid orographic rainfall formation. It finds its best expression on windward slopes that face into a sustained moist flow of air such as the trade winds. Orographic precipitation unlike cyclonic precipitation is not mobile and it's limited to the mountain barrier to which it owes its origin. Regardless of the type of rainfall or climate, all rainfall is the result of upward movements of moist air. Although for uplift to occur, the atmosphere needs to be in a state of conditional potential or convective instability. The stability states depend, however on the relationship of the actual environmental lapse rate to the dry and moist adiabatic lapse rates (Ati *et al.*, 2009).

2.2.2 Climate of Nigeria (rainfall)

Nigeria's climate is characterized by strong latitudinal zones, becoming progressively drier as one moves north from the coast. Rainfall is the key variable, and there is a marked alternation of dry and wet seasons in most areas. The two air masses that control rainfall in the country are; the moist northward moving maritime air coming from the Atlantic Ocean and the dry continental air coming from African landmass. The zone where the two air masses meet constitute the well-known Inter Tropical Discontinuity (ITD). Topographic relief plays a significant role in local climate only around the Jos plateau and along the eastern border highlands. In the coastal and southern portion of Nigeria, the rainy season usually begins in February or March as moist Atlantic air, known as the southwest monsoon that invades the country, Ati *et al.* (2009); Udo *et al.* (2002) shows that the beginning of rain is usually marked by incidence of high winds

and heavy but scattered squall. The scattered quality of this storm's rainfall is noticeable in the north in dry years, when rain may be abundant in some small areas while other contiguous places are completely dry. By April or early May in most years, the rainy season is under way throughout most of the area south of the Niger and Benue river valleys. Farther north, it is usually June or July before rains really commence. The peak of rainy season occurs through most of northern Nigeria in August, when air from the Atlantic covers the entire country. In the southern regions, this period marks the August dip in precipitation. Although rarely completely dry, this dip in rainfall, which is especially marked in the southwest, can be useful agriculturally, because it allows a brief period for grain harvesting, Osang *et al.* (2013). From September through November, the northeast trade wind generally brings a season of clear skies, moderate temperatures, and lower humidity for most of the country. From December through February, however, the northeast trade winds blow strongly and often bring with them a load of fine dust called harmattan from the Sahara. These dust-laden winds often appear as a dense fog and cover everything with a layer of fine particles. The Harmattan is more common in the north but affects the entire country except for a narrow strip along the southwest coast.

2.2.3 Causes of rainfall in Nigeria

According to Udo *et al.* (2002) the distribution of rainfall in Nigeria both in time and space is controlled by four main rain producing factors which are invariably operative in the West Africa region to which Nigeria is a part. The factors include; the monsoonal air from the Atlantic Ocean. The organized belt of thunderstorm, the distribution lines which trade roughly from East to West. The location of the surface position of the Inter-Tropical Discontinuity (ITD) and the Associated Weather zone. The Relief Factors. The major cause of rain production is moisture moving in three dimensional zones of

temperature and moisture contrasts known as Weather Fronts. If enough moisture and upward motions are present, precipitation falls from convective clouds (those with strong upward vertical motion) such as cumulonimbus (thunder clouds) which can organize into narrow rain bands (Udo *et al.*, 2002). The intensity and duration of rainfall are usually inversely related, that is high intensity storms are likely to be of short duration and low intensity storms are likely to have long duration, (Udo *et al.*, 2002).

2.2.4 Changing rainfall patterns in Nigeria

Global warming has brought about changes in weather patterns toward an intensified water cycle with stronger floods and droughts. In Nigeria, global warming has had a significant impact on rainfall-undoubtedly, the most significant component in agricultural practice, and the defining element in seasonal change. Rainfall has grown more intense with frequent and devastating floods. 2012 was indeed a tragic year, country wide, as intense rains left in their wake wanton destruction of lives and properties. On 2, July 2012, many Nigerian coastal and inland cities experienced heavy rains. In mid - July 2012, flooding in Ibadan, Oyo State capital, caused many residents to flee from their homes. In late July 2012, at least 39 people were killed due to flooding in Plateau State. Heavy rainfall caused the Lamingo Dam to overflow near Jos, sweeping across a number of neighborhoods and approximately 200 homes were submerged or destroyed. In that year also, discharge of water from a dam in neighboring Cameroon, as a result of a downpour, triggered one of the most disastrous floods in the northern part of the country. Worst hit was Adamawa State, where no fewer than 89 schools were severely flooded, prompting the state government to indefinitely postpone the resumption of schools for the new academic year. The Nigerian Meteorological Agency, NIMET, had, in March that year, warned about imminent heavy rainfall and the attendant flooding in many parts of the country, but the warning was either ignored

or not taken seriously. Several conferences have been held on the international scene to check the release of harmful gases that are causing increase in global temperatures.

2.3 Rainfall Characteristics

These are characteristics that help hydrologist to access the variability of river flow, evaluate risk of flood and design river regulation structures. Rainfall event characteristics are amount, intensity, duration, frequency, and seasonal distribution. The two most storm characteristics are duration and intensity. Amount is the quantity or depth of rainfall (volume) during the storm

2.3.1 Physical characteristics

2.3.1.1 Amount

The amount is the depth of rainfall in (mm) or cm. It is the accumulation or product of intensity times the duration. Amount is important in the hydrologic circle as it replenishes the soil water. It is the amount that would accumulate on the surface of watershed assuming there were no infiltration and evapotranspiration and land surface is flat without runoff. It is usually expressed in (mm).

2.3.1.2 Intensity

This is the rate at which rainfall takes place, usually expressed in (mm/h). Rainfall intensity is expressed as depth per time (mm/h). Higher rainfall intensity may produce larger raindrop sizes which often impact more energy. Higher intensity storms can damage vegetation and bare soil. High intensity storms can carry soil particles, causing soil crusting and manifest the process of erosion. At high intensity, infiltration is usually less thereby causing runoff. Knowledge of rainfall intensity can be indispensable in design of structures. The effect of climate change is making rainfall intensity measurement more important.

2.3.1.3 Rainfall duration

Duration of rainfall is the total time in minutes or hours taken by a rainfall event or the length of time rainfall occurs. Rainfall of longer duration can affect infiltration, runoff and soil erosion processes. High intensity rainfall for short duration can affect small seedlings, but may not affect erosion. Longer duration rainfall can enhance infiltration capacity during storm.

2.3.1.4 Frequency

Frequency of rainfall event is the time usually in years that it will take for an event to repeat on the average. This is estimated in return periods. It refers to how often rainfall occurs at any amount, intensity and duration. For instance, rainfall return periods are referred to as 100 year-1hour rainfall or 100 year-24 hour to define the probability that a given amount will fall with a given time period.

2.3.1.5 Time Distribution (intensity hyetograph)

The seasonal distribution of rainfall refers to the time of year when various rainfall amounts usually occur. This determines when surface runoff or deep percolation is likely to place. Seasonal distribution of rainfall across the globe varies and recommendations also are not same.

2.3.2 Climate change and variability

Climate change and climate variability are two important characteristics of climate. According to IPCC (2007) report, climate change refers to a statistically significant variation either in the mean state of the climate or in its variability, persisting for a long period (typically decades or longer). The United Nations Framework Convention on Climate Change (UNFCCC) defines climate change as “a change of climate which is attributed directly or indirectly to human activity that alters the composition of the

global atmosphere and which is in addition to natural climate variability observed over comparable time periods. Climate change refers to any systematic change in the long-term statistics of climate elements (such as temperature, pressure, or winds) sustained over several decades or longer time periods. On the other hand, climate variability refers to the variations in the mean state and other statistics of climate on both temporal and spatial scales beyond that of individual weather events. For climate change, human factors are more responsible for change compared with natural processes, but climate variability, natural factors have more effect than human factors (IPCC, 2007).

The climate of the world is changing in a tragic manner; the evidences of these changes are very clear according to most recent climate researches from different regions around the world (Funk *et al.*, 2012). Africa is the most vulnerable continent to the effect of climate change and variability due to low adaptive capacity and weak resilience in different socio-economic sectors, such as lack of adaptation strategies in case of water stress and food insecurity among others, hence increasing vulnerability of the poor communities. Tayanc *et al.* (2009) in their study showed a significant warming trend in southern and southeastern parts of Turkey from 1950 to 2004. Significant decrease in precipitation was observed over the western parts of the country, although the variability of precipitation was substantially different across urban and rural areas. Suggesting that urban stations can experience more frequent and severe droughts and floods compare to rural areas.

Nicholson *et al.* (2013) analyzed temperature variability over Africa during the last 2000 years and observed that near surface temperature had increased by 0.5 °C or more during the last 50 to 100 years over most parts of Africa with minimum temperatures warming more rapidly than maximum temperatures. Near surface air, temperature

anomalies in Africa were significantly higher for the period 1995 – 2010 compared to the period 1979 –1994 (Collins *et al.*, 2017); Cronin *et al.* (2018). The analysis for Sub periods 1974 -1983 and 1999 - 2008 for June and October respectively indicates that these periods were notably drier compared to average conditions. The results of the standardized anomaly index showed that rainfall amount is declining. Analysis of observed trends revealed that the decline in the annual rainfall amount is mainly because of the considerable decline in July, September, and October rainfall.

2.3.3 Rainfall and temperature extremes

Climate change have a strong effect on socio-economic sectors like agriculture, water resources and energy among others through occurrence of extreme climate events, which are responsible for a major part of climate-related economic losses (Kunkel *et al.*, 1999; Easterling *et al.*, 2000). The major extreme climate events that are categorized under extreme precipitation and temperature are flood, drought, frost cold and heat waves. These extreme events affect property, society and the entire ecosystems in different ways. For example, Extra-ordinary rainfall can cause floods due to change in rainfall patterns such as changes in frequency or in intensity while extreme temperature events can affect crop growth and reduce production differently with changes in frequency, with an increase in recurrent days of extreme maximum and minimum temperature (Ning *et al.*, 2012).

Lee *et al.* (2020) examined changes in climate and extreme climate indices in present and Future Projected climate in Korea, the model results pointed out in a clear and sensible way that the spatial change in extreme climate indices is significantly modulated by geographical characteristics in relation to land-ocean thermal inertia and topographical effects.

The summer-based indices showed an increasing trend, while the winter-based indices show a decreasing trend. Ning *et al.* (2012) studied the changes of temperature and precipitation extremes in Hengduan Mountain, and detected a significant increase in the temperature of the coldest and warmest nights and in the recurrence and intensities of extreme warm days and nights. While there is clear decrease in diurnal temperature range and number of frost and ice days, averages of increasing season length also showed that trend is harmonious and significant with temperature warming? Minimum temperature warming trends are greater than those of maximum temperature but variations of extreme precipitation events are unclear. De Jesus *et al.* (2020) examined the current and future characteristics of extreme events in California and found a significant increase in the frequency and intensities of both high maximum and high minimum temperature extremes in many areas of California. The frequency of extreme temperatures earlier observed once every 100 years are expected to increase by at least ten-fold in many parts of California under a moderate emissions scenario.

2.3.4 Climate change variability and extremes impacts

Climate change and variability Impacts on most of socio-economic such as agriculture sector are expected to steadily manifest directly from changes in land and water regimes, the likely primary conduits of change. Changes and recurrent and intensity of extreme events such as drought, flooding, and storm damage are observed and expected to continues in next a few years (Arnell *et al.*, 2019). Climate change is expected to result in long-term water and other resource shortages, worsening soil condition, drought and decertification, diseases and pest outbreaks on crops and livestock, sea-level rise, among other IPCC (2007). Rainfall and temperature are key features of climate that threaten rain fed agricultural productivity in the tropical and sub-tropical countries. Agricultural production depends on rainfall and carbon dioxide in the

atmosphere among other factors. Rainfall is affected by the change of atmospheric temperature or global warming. In the recent years, scientific research based on reliable world climate data reveal that the climate is being affected by the Green House Gases (GHGs) effect and temperature and precipitation are changing globally (IPCC, 2007).

Climate change has already caused significant impacts on water resources, food security, hydropower, human health especially for African countries, as well as to the whole world Mukwada and Manatsa, (2019). Studies on climate impacts and adaptation strategies are increasingly becoming major areas of scientific concern, such as impacts on the production of crops such as maize, wheat and rice, water resources in the river basin catchments, forests, industry and the native landscape (Prober *et al.*, 2017). Climate variability adversely impacts crop production and imposes a major constraint on farming planning, mostly under rain-fed conditions across the world. Higher growing season temperatures can significantly impact agricultural productivity, farm incomes and food security (Tigchelaar *et al.*, 2018). However, more severe warming, floods, and drought may reduce yields. Livestock may be at risk, both directly from heat stress and indirectly from reduced quality of their food supply. Fisheries will be affected by changes in water temperature that shift species ranges, make waters more hospitable to invasive species, and change lifecycle timing Ankrah (2018).

Water availability is a critical factor in determining the impacts of climate change and variability in many places, especially in Africa. Also, temperature in Africa is projected to increase at least more than global, this will have varying impacts depending upon ecological zones (IPCC, 2007). The predicted variability of temperature, precipitation, atmosphere carbon oxide and extreme events are anticipated to have profound effect on plant grows and yield, crops, soil, weed, diseases, livestock and water availability in

Sub-Saharan Africa (IPCC, 2007). The contribution of agriculture to Gross Domestic Product varies across countries.

2.4 Trend

The trend analysis of rainfall, temperature and other climatic variables on different spatial scales will help in the construction of future climate scenarios. Using this, water availability in different basins can be assessed in the context of future requirements. Most tests for detecting change assume independence of sample value. Independence means that current value of a variable cannot provide information about what next value will be. Trend analysis of a time series consists of the magnitude of trend and its statistical significance. Obviously, different workers have used different methodologies for trend detection. In general, the magnitude of trend in a time series is determined either using regression analysis (parametric test) or using Sen's estimator method (non-parametric method).

Both of these methods assume a linear trend in the time series. Regression analysis is conducted with time as the independent variable and rainfall/temperature as the dependent variable. The regression analysis can be carried out directly on the time series or on the anomalies (i.e. deviation from mean). A linear equation, $y = mt + c$, defined by c (the intercept) and trend m (the slope), can be fitted by regression. The linear trend value represented by the slope of the simple least-square regression line provided the rate of rise/fall in the variable. Sen's estimator has been widely used for determining the magnitude of trend in hydro-meteorological time series. One way to calculate the extent of correlation (dependence) is to calculate the autocorrelation function ACF (Kendall & Ord, 1990). Autocorrelation is a measure of the correlation of a variable with itself, but time shifted. To aid interpretation of a correlogram, it is advisable to add horizontal

lines showing the magnitude of coefficient that is to be considered 'significant' from zero. These lines define 95% confidence limits for individual coefficients, under assumption that the observations are not correlated sequence value drawn from probability distributions with common mean and variance (Chatfield, 2003).

2.4.1 Indices of extreme rainfall event

Flood and Drought are two major climatic events that poses serious threat to the environment. Increasing flood risk is now being recognized as the most important sectorial threat from climate change in most parts of the region which has prompted public debate on the apparent increased frequency of extreme, and in particular, on perceived increase in rainfall intensities Oriola (1994). Flood and Drought incidences and occurrences have been reported as natural and environmental disasters.



Plate I: Flood in Kogi State farm, (<https://thisdaylive.com> > kogi) 17/08/2018)

The pattern of flood across the globe have been changing, with increasing frequency and unpredictable for local communities especially as issues of development and poverty have led more people into areas susceptible to flooding. Studies have attributed extreme rainfall to be one major reason for flooding. Flash and River flooding usually result from high rainfall within a short duration. Flash flooding takes place within hours

while river flooding takes days. Heavy rainfall during tropical raining season can lead to monsoon flooding. Many studies by Ologunorisa (2004); Odekunle (2001) have attributed extreme rainfall as a major cause of flood.

Drought is a temporary aberration and it is known to cause extensive damage and affects a significant number of people. Drought being the one that causes most damages (Obasi GOP, 1994). Drought is considered as a major natural hazard, affecting several sectors of the economy and the environment worldwide. It affects almost all the determinants of the hydrological cycle starting from precipitation and ending with stream flow in the surface water systems or the recharge and storage in the groundwater aquifers. Droughts produce a complex web of impacts that span many sectors of the society. In Nigeria drought have been reported at different scale: Adefolalu (1986) reported in the North as result of drought in the country.

2.4.2 Rainfall indices

Indices are moderate extremes which occur several times each year (often counts of days exceeding fixed or certain percentile thresholds). Indices describe frequency, amplitude and persistence of extreme which can be used for observations and models. Climate index is calculated value that can describe the state and changes in the climate system Semazzi (2011). Calculated value of rainfall indices is used in describing the state, patterns and trend of rainfall over a period of time.

Indices for climate variability and extremes have been used for a long time, by accessing days with precipitation observations above or below specific physically based thresholds (Zhang *et al.*, 2011). Indices of rainfall are derived from monthly or daily weather data. Indices from daily data attempt to objectively extract information from daily weather observations that answers questions concerning that affect humans and

natural systems (Zhang *et al.*, 2011). Extreme climate data indices are characterised in two categories: (1) The probability of occurrence (i.e., distribution that occurs frequently) and (2) the severity of occurrence (i.e., the extent of extreme event). Severity tends to be more relevant to natural system and to society. Extreme weather event lies within the “probability distribution” limit of climate-meteorological variable, revealing the unexpected aspect of the known distribution patterns for the location.

2.4.3 Importance of rainfall indices

Rainfall indices provide information on the occurrence of climate extremes in terms of frequency and intensity. Climate extreme is usually large when referring to intensity. Indices help in determining significant change over time in the heaviest daily precipitation event in a year; the change in length and intensity of heat waves or reduction in the number of days below freezing (Zhang *et al.*, 2011). The impact on socio-economic activities arising from extreme events is of importance. This is due to the fact that knowledge of patterns and change over time lend to understanding of their nature and causes, their adaptation and mitigation to damages. Agricultural water resources planning and management cannot be effective and efficiently managed without rainfall indices. (Tarhule *et al.*, 1998) analysis of monthly rainfall provide insight into the variability of dry spell for each month during wet season at inter-annual and decadal time scales (Umar *et al.*, 2014). Knowledge of trend and variation of current and historical hydro-climatological indices is pertinent to the development and sustainable management of water resource of a given region I the context of competing demand for water due to population increase and economic growth (Oguntunde *et al.*, 2006).

The impact of humans on the environment and the interactions between the various components of climate, there is need for understanding of atmospheric and environmental changes. Rainfall indices help in determining distribution of rainfall over a geographical region, which defines the flora, fauna, hydrology, and the type of agriculture and ecology of the region (Adefolalu, 2007). The type of crop grown is dependent on the rainfall amount and determining the onset and cessation of planting. Extreme weather event (flood and drought can lead to great socio-economic consequences which can be analyzed statistically to determine regime. Prediction of global, regional climate variations which determines the extent of human impacts on climate and make sound prognosis of human induced climate change.

2.4.4 Characterization of extreme rainfall indices

Several indices had been developed to detect changes in extreme climate events (Zhang *et al.*, 2011). Rainfall extreme indices with daily data can be grouped into two different aspects; Depth or intensity (amount and rate) and the other dealing with frequency (number of occurrences). Rainfall extreme indices that measure the precipitation depth (mm) or intensity (mm/day) include: Annual total wet-day precipitation (PRCPTOT), simple daily intensity index (SDII), Very wet days (R95P), Extreme wet days (R99P), Max 1-day precipitation amount (RX1day) and Max 5-day precipitation amount (RX5day) and the other that calculate the frequency (number of cases) of the index exceeding or not exceeding the defined threshold and these are Consecutive dry days (CDD), Consecutive wet days (CWD), Number of heavy precipitation days (R10 mm), and the number of heavy precipitation days (R20 mm). These indices sample a wide variety of climates and included indicators such as the total number of days annually with frost and the maximum number of consecutive dry days in a year (Zhang *et al.*, 2011).

2.4.4.1 Precipitation total

This is the most important index reflecting rainfall variation over the entire year. It is the precipitation amount on day 1 in period j. If i represent the number of days in j, as shown in equation 2.1

$$PRCPTOT_j = \sum_{n=1}^l RR_{ij} \quad (2.1)$$

Where RR_{ij} is the amount of rainfall i in j period

2.4.4.2 Simple daily intensity index (SDII)

One index that takes into account not only the total amount of precipitation throughout the year but also reflects changes in daily rainfall is the Simple Daily Intensity Index (SDII). SDII combines the total amount of annual precipitation and the number of days when rainfall (greater than 0.1 mm) actually occurs. It is the annual total precipitation divided by the number of wet days (defined as $PRCP \geq 1.0$ mm) in the year. It is measured in mm/day.

Let RR_{wi} be the daily precipitation amount on wet days, $RR \geq 1$ mm in period j. If w represents the number of wet days in j, then as in equation 2.2

$$SDII_j = \frac{\sum_{w=1}^w RR_{wj}}{w} \quad (2.2)$$

2.4.4.3 Precipitation above 95-percentile (R95P)

Index is used to measure heavy precipitation that exceeds the 99-percentile threshold. It calculates the 95th percentile of wet days only (5% wettest ‘wet days’ i.e., days > 1 mm) in baseline the average amount of rain per year that occurs in ‘heavy’ events.

Let RR_{wj} be the daily precipitation amount on a wet day w ($RR \geq 1$ mm) in period j and let RR_{wn95} be the 95th percentile of precipitation on wet days in the base period n (1996-1990). If w represents the number of wet days in the period as in equation 2.3

$$R95P_j = \sum_{w=1}^W PR_{wj} \quad (2.3)$$

Where $RR_{wj} > RR_{wn} 95$

2.4.4.4 Precipitation above 99-percentile (R99P)

Index is used for measuring heavy precipitation that exceeds the 99-percentile threshold. This is calculated as annual total precipitation when $RR > 99p$. Let RR_{wj} be the daily precipitation amount on a wet day w ($RR \geq 1.0$ mm) in period I and let $RR_{wn} 99$ be the 99th percentile of precipitation on wet days in the base period n (1961-2000). If W represents the number of wet days in the period as in equation 2.4

$$R99P_j = \sum_{w=1}^W PR_{wj} \quad (2.4)$$

Where $RR_{wj} > RR_{wn} 99$.

2.4.4.5 Precipitation in one day (RX1day)

Heavy rainfall is measured using the RX1day. Let RR_{ij} be daily precipitation amount on day 1 in period j . the maximum 1-day value for period j is in equation 2.5

$$RX1day_j = \max (RR_{ij}) \quad (2.5)$$

2.4.4.6 Precipitation on consecutive five days (RX5day)

This is used in measuring intense rainfall on consecutive 5-day precipitation. Let RR_{kj} be the precipitation amount of 5-day interval ending k , period j . Then maximum 5-day values for period j is shown in equation 2.6

$$RX5day_j = \text{Max} (RR_{kj}) \quad (2.6)$$

2.4.4.7 Consecutive dry days (CDD)

Consecutive Dry Days (CDD) index can be used to determine a change in drier conditions. It is the maximum length of dry spell which simplifies the longest period of

days with no or less than 1mm precipitation. Let RR_{ij} be the daily precipitation amount per day I during time period j in equation 2.7

$$RR_{ij} < 1 \text{ mm} \quad (2.7)$$

2.4.4.8 Consecutive wet days (CWD)

Consecutive wet day (CWD) is the maximum length of wet spell i.e., the consecutive period of wet spell with at least 1mm of precipitation. CWD gives the real time-series variation that can lead to wetter conditions. Let RR_{ij} be the daily precipitation amount on day I in period j is given in equation 2.8

$$RR_{ij} \geq 1 \text{ mm} \quad (2.8)$$

2.4.4.9 Intense precipitation above 10 mm (R10 mm)

This index is to measure the persistence of intense precipitation by the number of cases of daily rainfall exceeding 10 mm. This indicates the number of days with at least 10 mm of precipitation. Let RR_{ij} be the daily precipitation amount per day I during time period j is given in equation 2.9

$$RR_{ij} \geq 10 \text{ mm} \quad (2.9)$$

2.4.4.10 Intense precipitation above 20 mm (R20 mm)

This indicates the number of days with at least 20mm of precipitation. Let RR_{ij} be the daily precipitation amount per day I during time period j. The number of days is given in equation 2.10

$$RR_{ij} \geq 20 \text{ mm} \quad (2.10)$$

2.4.4.11 Days with NN mm of rainfall (RNN mm)

This indicates the number of days with at least NN mm of precipitation. The user threshold is NN. Let RR_{ij} be the daily precipitation amount per day I during time period j. The number of days is given in equation 2.11

$$RR_{ij} \geq NN \text{ mm} \quad (2.11)$$

2.5 Quality of Rainfall Data

2.5.1 Consistency of rainfall data

Consistency of rainfall data from individual station within the River Basin was checked using a double mass curve analysis. This contains consistency check option within each of the program that are available for processing these data types. Consistency checks involve plotting the accumulated data of the base station against the average accumulated data of the index stations. Changes between base and the index can be seen through the deviation of the accumulated base station average from the accumulated index average. The group average is computed based on all station in the group divided by the number of index station computed. Thus, the deviation can now be corrected and used to determine the accurate data of the base station.

2.5.1.1 Correlation

Correlation is a measure of association between two variables. The variables are not designated as dependent or independent variables. Spearman's correlation coefficient rho and Pearson's product-moment correlation coefficient. Spearman's techniques are selected in calculating an ordinal data. For ratio type or interval data, use Pearson's techniques. A perfect negative correlation is indicated through minus one, while a plus one indicates positive correlation. When the correlation is zero, it means there is no relationship between the two variables. When a negative correlation between two

variables, as the value of one increase, the value of the other decreases and vice versa. The standard error of a correlation coefficient is used to determine the confidence intervals around a correlation of zero.

When it is significantly outside zero, then the correlation coefficient falls outside range. The standard error can be calculated for interval or ratio-type data (used only for Pearson's product-moment correlation). The significance of the correlation coefficient is used to determine the t-statistics. The probability of the t-statistics shows whether the observed correlation coefficient occurred by chance if the correlation is zero. i.e., determine if the correlation is significantly different than zero. When the t-statistics is calculated using Spearman's rank-difference correlation coefficient, at least 30 cases before the t-distribution can be employ to determine probability. When less than 30 cases, a special table is required to find the probability of the correlation coefficient. Two basic method for homogeneity testing are basically direct and the indirect method are;

2.5.2 Direct method for homogeneity testing

2.5.2.1 Use of metadata

Among the homogeneity tools available, the most commonly used information comes from station history metadata files. Station moves, changes in instrumentation, problems with instrumentation, new formulae used to calculate mean temperature, changes in the nearby environment such as buildings and vegetation, new observers, changes in the time of observations and documentation from comparison measurement studies that might have taken place when instruments changed are all relevant information in carrying out homogeneity. Metadata are always found in station records, meteorological books, original observation forms, station inspection reports and correspondence and

other technical manuscripts. This information could be gotten from interviews from managers of stations. The quality of history metadata varies with time and so the best may not be newest. The old descriptive reports with evaluations of station locations and observer's skills by meteorologist are often more important than modern objective reports. The photograph of station in recent years have become much more common. Examining a series of pictures may reveal changes not mentioned in the inspection reports. Changes that have affected large fraction of the network is important to note.

These systematic types of changes may need to be addressed differently than changes involving only individual stations. Metadata information are specific information that are relevant to researchers and can provide precise knowledge of when discontinuity occurred and what caused it. Metadata sometimes are not complete, missing or contain errors. For instant, when the author of metadata completes the form from memory several years after the change occurred. Some important changes are discovered that are not reported in the right way in the inspection reports, Forland (1994). Interpretation of metadata sometimes creates problems. The biggest with station history metadata is how to obtain relevant information for determining discontinuities in a useable form. Some sources of metadata contained unnecessary information, making extraction of relevant information difficult and time consuming. Some countries have digitalized their metadata selection systems. Metadata offer researchers access to station history information without the expensive burden of searching through paper archives.

2.5.2.2 Side by side comparison of instruments

Instrument type changes are usually accompanied by comparison measurements. The comparison is conducted at each station so that overlapping time series between the old and new instrumentation. Comparison is only performed at limited number of stations.

2.5.3 Indirect methodologies for homogeneity testing

2.5.3.1 Use of single station data

Station data used in homogeneity testing technique are always in conjunction with metadata or comparing other stations. Data from single station is problematic due to change or lack of change may be caused by real changes in climate. There are some stations without adequate neighbours where more reliance must be given to individual station data. Station can be used to change a date when a metadata is imprecise. This is particularly true when multiple elements are available. (Zurbenko *et al.* (1996) describes a filter that has been applied to single data to date a discontinuity. The moving average filter approaches a region of the time series where there may be discontinuity as indicated by increase variability or magnitude of the slope, the half-length on the moving average on the potential discontinuity side is smaller than the half length of the other side of the data point. The process which is iterative can help to smooth out noise of the time series while retaining discontinuities as distinct breaks. Rhoades and Salinger, (1993) have derived a number of statistical procedures for homogenizing isolated station data. Adjustment for discontinuities is necessarily subjective, a variety of graphical and analytical techniques were found useful in deciding homogeneity adjustments. These involve graphical analysis, simple statistical test using annual and sub-annual differences over symmetrical intervals and a mathematical procedure to identify the most prominent change point in the time series independently of discontinuities identify by metadata.

2.6 Spatial-Temporal Variation of Rainfall

Rainfall variation pattern occurs in spatial and temporal scale which can have several benefits for hydrological studies.

2.6.1 Spatial variation

Spatial variability is in scale and magnitude within an area where long-term mean precipitation is relatively constant. In semi-arid environment which is often characterized by vast expanses of flat to gently undulating topography, where orographic features have minimum influence on rainfall distribution patterns. Spatial variability in rainfall input can be a consequence of local variation in intensity and path of convective thunderstorm within these landscapes. An understanding of spatial variation in precipitation input in this region can provide insight in historic patterns of ecosystem function and potentially guide future approaches to ecosystem management and conservation. In the grassland of North America, MAP decreases from east to west while intra-annual variation increases, (Wiens 1994). Several factors contributing to spatial variation in precipitation comprises intense spring thunderstorms influenced by sharp temperature contrast air masses and convective thunderstorm that brings high-intensive rainfall over small areas for short period of time (Peike and Doesken, 2008). Despite the control role of moisture limitation in semiarid region. Spatial variation in precipitation can influence and interact with many aspects of ecosystem structure and function, but the influence could limit movement of organization in response to spatial variation.

2.6.1.1 Temporal variation

Recent studies revealed that the climate variability in the 20th century was characterized by apparent precipitation variability in time and space (Rakib, 2012). Temporal variability in precipitation is a key factor influencing the structure and function of semiarid ecosystem (Austen *et al.*, 2004) temporal variation in precipitation at scales days to years on plants and fauna. The rocky-mountains that lie to the west of the short grass steppe influence climate and weather patterns due to the rain shadow they create

(Peike and Doesken, 2008). Topography is characterized by gently undulating plains with slopes typically 0-3%. For example, at the central plains experiment range in North Eastern Colorado vary by 6-21 meters in elevation over 1.6 kilometer.

2.6.2 Assessment of spatial-temporal rainfall variation

2.6.2.1 Spatial distribution

Rainfall spatial pattern identification can have several benefits for hydrological studies. As an example, we can mention an easier analysis for hydrological design, study of climate change effects, forecast issues, alert system or information for ungauged basins. The applied methods (convective features, dimensionless rainfall patterns, gridded daily rainfall, hydrological & ecological modelling; Principal Component Analysis are the most of all variable upon which these methods operate is varied. Evaluating rainfall distribution is more complicated in mountain environment because rainfall pattern is influence by topographical relief over short distances. Through the network of gauges, variable rainfall patterns can be characterized. Hydrologist are often required to estimate point rainfall at unrecorded locations from measurement at surrounding sites. Commonly employed method for determining spatial distribution of climate data is; topographical, graphical and numerical. Topographical method includes; contour mapping, slopes, wind speed and elevations. Graphical method includes isohyets mapping, Thiessen's polygon analysis. Numerical method includes smoothing splines, optimal interpolation and kriging and it's variant.

2.6.2.2 Spatial interpolation

This is done by estimating regionalized value of un-sampled point based on a weight of observed regionalized values. The formula for spatial interpolation is given in equation 2.12

$$Z_g = \sum_{i=1}^{n_s} \lambda_i Z_{si} \quad (2.12)$$

Where Z_g is the interpolation value at the required points Z_{si} is the observed value at point i , n_s is the total number of observed $\lambda = \lambda_i$ is the weight contributing to the interpolation.

2.6.2.3 Thiessen polygon

Thiessen Polygon and Inverse Distance Method (US Weather Service) are deterministic method based on location of the measured stations. The forecast of the regionalized value takes into account the weighted average of the observed values. Using Simple average number of stations are employed in determining spatial interpolation in the table land. Because most times, it does not provide representative measurement of rainfall use is limited.

This method assumes that the estimated values can take on the observed values closest station. The method uses nearest neighbor (NN) method (Nalder *et al.*, 1998). Under this method, construction of Thiessen polygon network is required. The polygon is formed by joining the nearby stations to others related stations and a straight-line crossing adjoining line perpendicular. The surface of each of each polygon is determined and used to balance the rain quantity of the station at the center. One limitation of this is that the polygon must be changed whenever the station is added or removed from network (Chow 1994). When a station is deleted, it is called “missing rainfall”. It is equally not suitable to mountain environment due to orographic influence of the rain Goovaerts (2000).

2.6.2.4 Smoothing splines

This is based on mathematical model for surface estimation that fits minimum curvature surface through the input points. This method fits a mathematical function to a specified

number of the nearest input while passing through the sample points. Large changes in the surface within short distances makes the method inappropriate as it can overshoot estimated value.

The Moving Window Regression (MWR) is a linear method which is conducted only in areas where a relationship between the primary and secondary variables is taught to exist. For example, in applying the MWR method to rainfall. The primary variable is rainfall while the secondary variable is the elevation. The rainfall estimation is based on modelled relationship between rainfall and elevation data closest to the estimation location.

2.6.2.5 Kriging method

In kriging method, the value of the interest variable is estimated for a particular point using weight sum of the available point observations. Usually, the data weight is chosen in order that the interpolation becomes unbiased and variance minimized. Kriging method must be linear, unsmoothed, unbiased and optimal (LAUO). Kriging is the first method of interpolation that consider the spatial dependence structure of data. The various types of kriging are which differ according to the form applied to the mean of interest variable;

- a) When it is assumed that the mean is constant and known, simple kriging is applied.
- b) Where the mean is constant but unknown, this is ordinary kriging (ORK) is applied.
- c) Where the mean is assumed to show polynomial function of spatial coordinates. This is known as universal kriging (UNK).

The last kriging is not stationary with mean. Stationarity defines itself here by the consistency of the mean, but by the covariance or more generally, semi variogram. This function which represent spatial dependence structure of the data must be half of the squared difference between pair value to the distance by which they are separated.

- d) Ordinary Cokriging (OCK) This involves estimating the variable of interest using a weighted linear combination of its observations of the auxiliary variable

2.6.2.6 Principal component analysis

Principal Component Analysis is traditionally known as empirical Orthogonal Function (EOFs) in studies of atmospheric sciences to the seasonal precipitation time series. Closely related is the principal factor analysis (PFA) of multivariate techniques which have been widely used in meteorology and climatology Wilks, (1995). Interpreting data is one of the problems encountered in statistics with more than two variables. This problem is solved by replacing a group of variables with a single new variable. This is because more variable is measuring the same driving principle governing the behavior of the system. Through the principal component variable are reduced.

The PCA creates a set of variables called principal component. According to (Tatli *et al.*, 2005) all matrices are organized such that the rows represent simultaneous observations and columns indicates observed variables at different sites. The first and second- order statistics of a multivariate x (observation matrix) is known or can be estimated from sample. In PC transform, the matrix of the variables (x) is centered by subtracting its mean and the covariance matrix of x is shown in equation 2.13

$$s_{xx} = E(x^T x) \quad (2.13)$$

Where E is the expectation operator. The PC are not invariant under scaling. The Orthogonal decomposition of s_{xx} is given in equation 2.4

$$S_{xx} = U_x D_x U_x^T \quad (2.14)$$

Where U_x is the matrix that contains the Orthogonal Eigenvector S_{xx} and $D_x = \text{diag.} (\lambda_1, \dots, \lambda_k)$ is the diagonal matrix of the eigenvalues of S_{xx} in decreasing magnitude (Tatli, 2005). The first Principal Component has the maximum variance among all choices. The PCA is used for the purposes of finding interrelations between variables in the data; interpreting and visualising data; reducing the number of variables thereby making analysis simpler. The CFs must be rotated (Richman, 1986). The varimax method (Kaiser, 1959) could be used for simplifying evaluation of the PCs patterns. The signs of the PC pattern have no meaning to interpreting them as traditional linear correlation analysis. They show the different system might affect the station over the regions. PCA is a black-box computation method that the signs or scaling brings no physical descriptions of the local climate system (Tatli *et al.*, 2005).

2.6.2.7 Temporal distribution

The use of empirical approach to quantify and express changes in a system over a period of time is known as trend analysis (Chandler and Scott, 2011). Trend analysis can help us determine if the random variable generally increase or decrease over a period in statistical terms (Helsel and Hirsch, 1992). The generally known methods are parametric (Distribution –dependent) and non-parametric (Distribution-free). These two methods can be used to determine whether a trend is significant. Parametric distribution is when the change evaluated by test can be specified in terms of one or more parameter. For instance, linear regression. Parametric testing procedures are widely used in statistics. In parametric procedure you can assume that the distribution for the data (normal distribution) and make assumptions that observations are independent of one another. The following are necessary in parametric distribution;

- i. Transform data so that its distribution is normal

- ii. You can restrict analysis to annual series for which independent assumptions are acceptable rather than using more detailed monthly, hourly and daily data. The test designed for normal distribution are sensitive to outliers and may be difficult to apply to records with large number if “less than” values. Non parametric distribution allows for few assumptions about the data (Kundzewicz and Robson, 2004). This method makes it difficult for assumption, though these methods still rely on assumption of independence. Statistics based on the rank of observations are example and play important role in non-parametric approaches. Non-parametric test are as follows;

2.7 Regression Analysis

Regression coefficient is the test statistics for linear regression. The common and simplest test for trend in its basic form assumes that data are roughly normally distributed (symmetrical & unimodal). If plot of data against time suggests a simple linear increase or decrease over a time, a linear regression Y against time T may be used to fit the data. Data are normally or serially correlated and can be misleading if seasonal cycle are present. The normality assumptions are violated but other independent assumptions hold. Data can be transform using linear regression (Helsel and Hirsch, 1992) is shown in equation 2.15

$$Y = bT + a + \varepsilon_t \quad (2.15)$$

Where, a represent the intercept, b is the slope and T are the random errors. The errors are assumed to be independent and evenly distributed. T represent the year which is taken as year 1. Response variable is likely to satisfy if the yearly average is assumed. The regression coefficient is estimated using the method of Least Square (OLS). The slope and the intercept are estimated as follows (Montgomery *et al.*, 2001) in equation 2.16 and 2.17

$$b = \frac{\sum(x-\bar{x})(y-\bar{y})}{\sum(x-\bar{x})^2} \quad (2.16)$$

$$a = \hat{y} - bT \quad (2.17)$$

The standard error is given in equation 2.18

$$SE(b) = \sqrt{\frac{\sum(Y-a-bT)^2}{(n-2)\sum(x-\bar{x})^2}} \quad (2.18)$$

\hat{y} is the mean of y, \hat{T} is the mean of T

The standard error of the slope is OLS estimations of the slope b and the standard error, if the slope can be obtained using statistical computing software. A test may be used to test that the true slope is not different from zero is given in equation 2.21

$$tb = \frac{b}{SE(b)} \quad (2.19)$$

The test statistics follows a standard distribution with df= n-2 using null hypothesis. If p-value of tb statistics is less than α . A positive (negative) of b indicates an upward (downward) linear trend and b is the magnitude of that trend. 100(1- α) % two-sided confidence interval for b is t (1- α , df= n-2) x SE (b). The strength of the trend can be imported as a percentage change over time dividing the slope of the regression line by the mean value of the quality parameter of the interest over time. To determine the percentage variability in the water quality of interest is explained by the variability of time, we look at the coefficient of determination. The coefficient of determination R^2 is the proportion of the variance in the independent variable that is predicted from the independent variable. $R^2 = 0.20$ means 20% of the variance in Y is predictable from X; After the model is fit, test for autocorrelation in the residual using the Durbin-Watson statistics can be performed (Montgomery *et al.*, 2001). The Durbin-Watson test is a test for first-order serial correlation in the residuals of a time series regression. The test statistics as shown in equation 2.20

$$d = \frac{\sum_{i=1}^n (\theta_{i+1} - \theta_i)^2}{\sum_{i=1}^n \theta_i^2} \quad (2.20)$$

Where, $e_i = y_i - \hat{y}_i$, y_i and \hat{y}_i respectively the observed and predicted values of the response variable for individual.

y_i = observed value

\hat{y}_i = predicted value of the response variable for the individual.

The i value is between 0 and 4 and reduces as the serial correlation increase. The residual is auto-correlated if the p - value for the statistics is less than a selected level of significance. The simple regression model of the equation above can be modified to account for the seasonality in the observations.

2.7.1 Spearman's rank correlation coefficient

The spearman's rank-based correlation can be used to test for the time correlation of data series (Gauthier, 2001). It can be used for trend detection. The spearman's rank correlation coefficient (ρ) which is denoted by the Greek ρ (rho) is a non-parametric measure of statistical dependence between two variables. Rank correlation help to access how well the relationship between two variables using a function known as monotonic function. The sign of the spearman correlation indicates the direction of association between X (independence variable) and Y the (dependence variable).

If the independence increases as dependent increases, the spearman correlation coefficient is positive. If Y tend to decrease when the dependence (X) increases, the spearman's coefficient is negative. When the spearman's is zero, it indicates that Y is constant when x increases. The Spearman's correlation increases in magnitude as X and Y becomes closest to being perfectly monotonic functions of each other. When X and Y are perfectly monotonically related, the spearman correlation coefficient variable is

ranked from lowest to the highest separately, for instant, 1,2,3,4. The difference between ranks of each data pair is calculated. Equal values are assigned a rank value equal to the average of their positions in the ascending order of the values. The Spearman correlation coefficient is defined between the ranked variable RX and RY as shown in equation 2.21, 2.22, 2.23 and 2.24

$$r_s = \frac{S_{RX.RY}}{\sqrt{S_{RX}S_{RY}}} \quad (2.21)$$

$$S_{RX.RY} = \sum_{i=1}^n (RX_i - \overline{RX})(RY_i - \overline{RY}) \quad (2.22)$$

$$S_{RX} = \sum_{i=1}^n (RX_i - \overline{RX})^2 \quad (2.23)$$

$$S_{RY} = \sum_{i=1}^n (RY_i - \overline{RY})^2 \quad (2.24)$$

Where, RX_i , RY_i , \overline{RX} , \overline{RY} are the ranks.

n =the number of data pairs

When there are no equal ranks, simpler expression may be used to obtain the spearman correlation coefficient is shown in equation 2.25

$$r_s = \frac{1 - 6 \sum_{i=1}^n d_i^2}{n^2 - n} \quad (2.25)$$

d_i = is the difference between ranks.

When the value of n is small, the significance level of the r_s test statistics can be looked using special tables (Helsel & Hirsch, 1992). When more than 20 values a test statistic can be solved using equation 2.26

$$t = r_s \sqrt{\frac{n-2}{1-r_s^2}} \quad (2.26)$$

This is distributed approximately as student t distribution with n -2 degree of freedom (df). The p –value associated with the positive statistics is less than α , null hypothesis is rejected which means no trend in data. If the r_s is positive, it shows an increasing trend and when negative, we conclude a decreasing trend.

Spearman correlation coefficient is used to detect trend in the time series data with no seasonal effects. If the cyclicity present in data, the test can be used after removing seasonal variation.

2.7.2 Mann-kendall test

This test is often for trend detection in hydrological time series (Dinpashoh *et al.*, 2011; Oguntunde *et al.*, 2011). This is used to test for trend in rainfall data in the study. Mann-Kendall known as M-K rank correlation is applicable when the data value of a time series can be assumed to obey the model in equation 2.27

$$X=f(t) + \epsilon_t \quad (2.27)$$

Where $f(t)$ is a monotonic increasing or decreasing function of time. The ϵ_t is assumed to be from the same distribution with zero mean. Variance is considered to be constant in time. Mann-Kendall test statistics S is given in equation 2.28

$$S = \sum_{k=1}^{n-1} \sum_{j=k+1}^{n-1} \text{sgn}(X_j - X_k) \quad (2.28)$$

Where n is the length of the time series X_1 — X_n and $\text{sgn}(\cdot)$ is the sign function, X_j and X_k are values in year's in j and k respectively over time t . Each data value is compared to all subsequent data values. The initial value of the Mann- Kendall statistics S assumed to be zero (0) showing no trend. If a data value from a later time period is higher than the previous data value, S increases by +1 or if the data value of previous is higher than later then, S decremented 1. The net result of the increment or decrement yield the final value of S . When the value of S is positive then trend becomes upward and when negative it shows decreasing trend. When S is high and positive, it shows increasing trend but when low and negative, trend is decreasing. There is no assumption to the underlying distribution of the data when it is non-parametric.

2.7.3 The Sen's estimator of slope

This is another non-parametric test used to determine the magnitude of change in the rainfall record (Shahid, 2011). To estimate the true slope of an existing trend, Sen's non-parametric method is used. Sen's method can be used in cases where trend can be assumed to be linear (Tabari and Talaei, 2011; Sen's 1968). The method of calculating Sen's slope estimator requires a time series of equally spaced data. Sen's method proceeds by calculating the slope as a change in measurement per change in time as shown in equation 2.29.

$$Q = \frac{X_j - X_k}{j - k} \quad (2.29)$$

Where, Q is the slope between data point X_i and X_k

X_i = data measurement in time j

X_k = data measurement at time k

j= time k, X_i and X_k constitute the pairs of observation identified by place in the series. The median of these estimates is Sen's estimator of slope. The approach involves computing slopes for all the pairs of time points and then using the median of these slopes as an estimate of the overall slope Q. As such, it is insensitive to outlier and can handle a moderate number value below the detection limit and missing values.

2.8 Standardised Anomaly Index (SAI)

Standardized Anomaly Index Estimation Model for each of the stations, rainfall series were analyzed for fluctuation using Standardized Anomaly Index (SAI) which is a commonly used index for regional climate change studies (Babatolu *et al.*, 2013). Station rainfall is expressed as a standardized departure i x from the long-term mean (i.e., the mean of the base period),

Standardised Anomaly Index was calculated as the difference between the annual total of a particular year and the long term (first moment) average rainfall divided by second moment (standard deviation) of the long-term data. This characteristic of SAI has contributed to its popularity for application in drought monitoring and also makes possible the determination of wet/dry spell years in the record (WMO, 2012).

The standardised formula is given by equation 2.30

$$Z = \left(\frac{x - \mu}{\sigma} \right) \quad (2.30)$$

Where,

Z is the standardized anomaly index

x_i = the annual rainfall of a particular year

μ = first moment (mean annual)

σ = second moment (standard deviation)

Hayes *et al.*, 1999) gave a classification of the category of anomaly based on the severity of drought as shown in the Table 2.1.

Table 2.1: Standardised anomaly index value classification

SAI Value	Category
2.0+	Extremely Wet
1.5 to 1.99	Very Wet
1.0 to 1.49	Moderately Wet
-0.99 to 0.99	Near Normal
-1.0 to -1.49	Moderately Dry
-1.5 to -1.99	Severely Dry
-2 and less	Extremely Dry

Source: (Hayes *et al.*, 1999)

2.9 Regionalisation of Rainfall

Regionalisation of rainfall refers to delineation of rainfall in an area into homogeneous groups (regions or clusters). Regionalisation of rainfall is very necessary in hydro-climatic analysis such as (i) meteorological drought analysis, agricultural planning for effective water management that may arise as a result of low rainfall, (ii) forecasting

and downscaling of precipitation, (iii) design of water control systems (e.g. dams and levees) and conveyance structures to mitigate damages. When spatial and temporal variability is complex, regionalization becomes a challenging task. Regions are often delineated many purposes by analyzing rainfall patterns (e.g. extreme, long term aggregated through the daily, monthly and annual). Homogeneous regions delineated for different purposes may not be identical and may not be unique.

2.9.1 Approaches to rainfall regionalisation

The conventional practice was to delineate regions based on physiography and or political/administrative boundaries. Srinivas (2013) opined such delineated region may not have definite relationship to causal/exploratory variables influence on rainfall. To delineate effective homogeneous zones, a well regionalisation approaches have been developed over the past decades. This includes those based on

2.9.1.1 Correlation analysis

The time series corresponding to all pairs of rain gauges in the study area. The first step is to pair gauges that have the highest correlation in rainfall as identical. The second are those greater than certain specified threshold and this is repeated until all gauges are assigned to the tentative groups. These approach to regionalisation found application in countries like Nigeria, United Kingdom, Tanzania and Sierra-Leone. The major challenge of regionalizing based on correlation approach is that the delineated regions are sensitive to the choice of threshold value employed.

2.9.1.2 Principal component analysis: (PCA)

Often referred as eigenvector or Empirical Orthogonal Function or Singular Decomposition Principal Components (PC) are orthogonal to each other which are derived through correlation and /or covariance matrix of rainfall in the study area. This

approach involves plotting the un-rotated PC. The first PCs that accounted for significant percentage of the total variance loading on the map of the study area, or representing stations at point in two-dimensional space leading PCs. In regionalizing extreme rainfall, regions at frequency (growth) curves of rainfall extremes are constructed for each of the delineated regions using pooled information from the region. Srinivas (2013) by fitting regional regression relationship between PCs and the parameters of the distribution. This approach had been applied to precipitation data from various parts of the world including Africa, United Kingdom, Mexico, Austria, India Switzerland, Italy and Spain. This becomes cumbersome when large PCs account for significant percentage of total variance to address this problem PCA based on sequential sieving of stations was proposed for regionalisation.

This procedure involves identification of first major sequential region by grouping sites that are highly correlated with the first significant PC. Those grouped sites are omitted and reduced dataset and subjected to PCA.

2.9.1.3 Common factor analysis (CFA)

This approach to regionalisation involves application of factor analysis to inter-site correlation matrix to arrive at a common factor and specific factors. The analysis assumes a basic model for data that allows for accounting for specific variance which is not possible with PCA. The specific variance is related to local forcing that influence rainfall variability at the individual gauges in the study area and is different from the forcing that is common to a group of gauges. In PCA, specific variance is distributed among all the loadings, indicating that the sum of localized effect is spread over the modes. In CFA, the variance is not manifested on any of the loadings. The common factor optimized to maximize variance shared by stations (Communality).

2.9.1.4 Cluster analysis procedure

Cluster analysis is used in delineating homogeneous rainfall groups owing to their effectiveness in interpreting patterns in data of explanatory influencing rainfall or loading PCs result from PCA. Each gauge is represented by a vector that comprises of explanatory variables which are referred to as attributes. The practice is to consider attributes as statistics computed from rainfall records. The statistic includes mean annual/seasonal/monthly and daily rainfall. When such statistics (attributes) form the basis for regionalisation, adequate number of sites with sufficiently long period of contemporaneous observations observation is necessary to form meaningful region and cannot be delineated in ungauged area that are not necessarily contiguous in geographical space. This approach find application in United States of America, Spain, Australia, South Africa, Lesotho, India and China.

2.9.1.5 Spectra analysis

Gauges that show significantly low spectra variability that are group to form a region. Monte-Carlo procedure was employed to assess spectral homogeneity of a region which was proposed and its utility in delineating a spectrally homogeneous region was demonstrated. The procedure involves examining whether spectra variability of the region differs significantly from that expected in realization of white noise process whose number is equal to that of sites in the region. Spectra variability refers to variation among Power Spectra Density (PSD) of standardized anomaly rainfall time series. Forming homogeneous rainfall sub-regions in India by grouping Monsoon Spectra Density (MSD) whose spectra variability is less than the expected in realization of white noise process at specified confidence level. An alternative option is to form groups (regions) through application of agglomerative hierarchical clustering procedures

2.9.1.6 Hierarchical regionalisation approach

This explicitly account for spatial variability in moment of predictand (extreme rainfall). It is based on the hypothesis of higher order moment (e.g., skewness and kurtosis) of extreme rainfall data that do not display significant spatial variability over a larger area than relatively lower order moment (coefficient of variation) which in turn is assumed to vary more slowly over space than the first-order moment. Frequency of analysis at the target sites is used to estimate distribution parameters controlling the higher (lower) order moment. This approach may not be appropriate for larger geographical areas.

2.9.1.7 Region of influence approach

This consider each large site to have its own region consisting of those whose distance to the target site in a weighted multi-dimensional space of predictors does not exceed a chosen threshold distance value. Pool information from all sites in a region form basis for constructing a regional frequency curve, and in the process each site could be weighted according to its proximity to the target site. This approach contradicts with the notion of forming geographically contiguous regions and has subjectively in the selection of weight and threshold value.

Regions delineated using the conventional regionalization procedure may not be reliable when the study area is sparsely gauged and period of contemporaneous records for the gauges considered inadequate to account for sampling variability. Areas that are ungauged cannot be delineated.

CHAPTER THREE

3.0 MATERIALS AND METHODS

3.1 Materials

3.1.1 Dataset

The meteorological station (data) use to analysis of study were selected to represent the extent of spread and based on availability of records of data. The data consist of daily rainfall and temperature (minimum and maximum) obtained from Lower Niger River Basin Development Authority Ilorin, Kwara State. Six stations had records for thirty-five (35) years between 1979 and 2013. Consistency test were carried out to produced quality data and homogeneity check to detect days with missing data and outliers which may have been introduced through human error or instrument fault.

3.1.2 Location of the study area

Lower Niger River Basin (LNRB) of Nigeria comprises majorly of two states namely Kwara and Kogi. The Lower Niger River Basin is located in the middle belt of Nigeria between latitude 7°N and 12°N and longitude 3°E and 9°E as shown in the study area map (Figure 3.1). The latitude and longitude of the various stations where the secondary data was used to analyse spatiol-temporal analysis is shown in Table 3.1. The LNRB is on the downstream side of while the Upper Niger River Basin is on the Upstream of River Niger. The study area is characterised by rainfall which varies in amount from 100 mm in the North and 1300 mm in the south. Its source is in the Guinea highland in South Eastern Guinea. River Niger has a length of 4200 km. The river passes through four countries of which Niger and Nigeria are named. Nigeria is in West Africa between latitude 40°N and longitude 20°E and 150°E having a total land mass of 923.8×10^6 km boarded on the East by Chad and Cameroon, on the North by Niger, on the West by Benin Republic and on the South by Gulf of Guinea. Two seasons exist predominantly

in Nigeria (Wet and Dry) annually. Raining season begins by April and ends in October. Temperature within the basin ranges from 11 to 27 °C minimum and 20 to 43 °C maximum. Figure 3.1 shows the study map of LNRB and Table 3.1 shows the elevation of stations

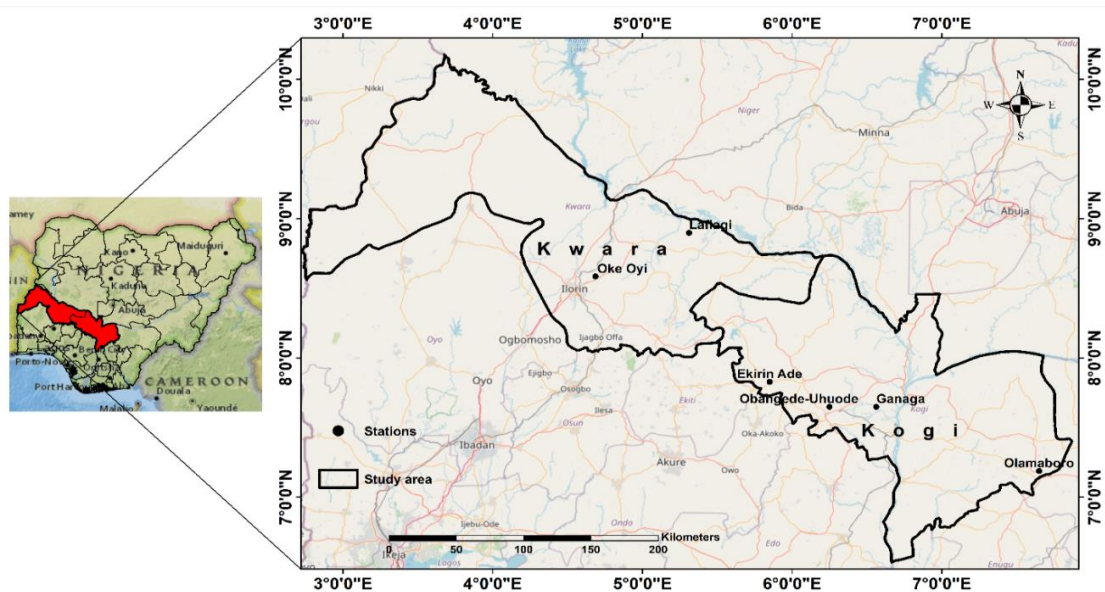


Figure 3.1: Map of Lower Niger River Basin. Source: (Modified after OSGF, 2010)

Table 3.1: Study Area Stations with Latitude and Longitude

Station	LATITUDE	LONGITUDE	Elevation	Data (Years)
Olamaboro	7° 11' 15" 0N	7° 38' 58" 6° E	411m	35
Ganaga	7° 38' 58" 6' N	6° 15' 00" 0° E	88.67m	35
Obangede	7° 38' 56" 9' N	6° 20' 05" 0° E	201m	35
Ekirin Ade	7° 49' 40" 7' N	5° 51' 00" 0° E	497.12m	35
Lafiagi	8° 53' 54" 7' N	5° 18' 45" 0° E	116m	35
Oke Oyi	8° 35' 10" 6' N	4° 41' 15" 0° E	388.21m	35

3.1.3 Hydrometeorology of the study area

The rainfall within the LNRB authority usually of three weather conditions annually; the warm, humid rainy season and very dry season. Within dry and wet is a harmattan period caused by the North East Trade winds accompanied by dust haze. The LNRB are located in the middle belt region of Nigeria between latitude 9 °N and 12 °N and between longitude 3 °E and 9 °E. The Kwara state region is drained by Awon,

tributaries. The annual rainfall ranges between 1000 -1500 mm with an average temperature of 27 °C. The annual rainfall is between 800 - 1300 mm with average temperature of 26.8 °C.

3.2 Methods

3.2.1 Data collection

The daily temperature (maximum & minimum) and daily rainfall data across the Lower Niger River Basin which covers six meteorological stations for a period of 35 years (1979 - 2013) was collected from LNRBDA. Daily rainfall and temperature data were computed up to form monthly, annual and decadal series of LNRBDA from the representative gauging stations within the river basin. These stations were chosen because of availability of data that covers 35-years.

3.2.2 Data quality analysis (preliminary)

Based on the understanding of the specific nature of the problems that drives the motivation for the study, there is the need to ensure that the available data (rainfall and Temperature) are of high quality; i.e., reduce the possibilities of severe perturbations by considering stochastic characteristics like statistical moments. To address this effectively, years with more than 30% of missing data after (Peralta-Hernandez *et al.*, 2009) or missing gaps extending up to 3 or more years were discarded. On the other hand, for shorter periods, interpolation was employed to fill in the gaps so as to ensure consistency in data length. Specifically, to this end, the following approaches were employed, namely:

- i. Homogeneity Tests,
- ii. Persistence analysis via autocorrelation.

3.2.2.1 Homogeneity tests

The essence here was to account for potential systematic stochastic persistence biases (noise) that might mask climate change signals; in order to determine the variability that exist in the data for instances, long-term variations, trends so as to avert wrong conclusions about climate change which may compromise the reliability and quality of any assessment. Thus, the Kruskal-Wallis homogeneity test and Wald-Wolfowitz runs test were adopted.

3.2.2.2 Kruskal-Wallis homogeneity test

Kruskal-Wallis test was employed to carry out homogeneity test assessment. This is used to determine if the time series are homogeneous or not. Non parametric Kruskal-Wallis (k-w) Turkes (1996) was used in calculating the k-w test statistics (X_k), observations of each sub-period (or each series) are replaced by the rank r_{ij} as occupied in the total ordered sample series. If k is the number of sub-periods for the independent series); n_j , $j= 1, 2, \dots, k$ represents the sample size of the sub-periods j.

The test statistics X_k is computed as in equation 3.1, 3.2 and 3.3

$$X_k = \left[\frac{12}{n(n+1)} \sum_{j=1}^k \frac{k_j^2}{n_j} \right] - 3(n+1) \quad (3.1)$$

Where,

$$R_j = \sum_{i=1}^{n_j} r_{ij} \quad (3.2)$$

and

$$n = \sum_{i=1}^n n_j \quad (3.3)$$

Null hypothesis of the homogeneity of the means, X_k is distributed approximately as χ^2 with (k-1) degree of freedom. Homogeneity of variance using the sample test can be verified. By applying same test to the series obtained, the homogeneity of variance can

be realized. Replacing each rank r_{ij} with the absolute value to the deviation from average (Turkes, 1996). Sample size of the sub-period and significance level of the test were taken as $n_j = 5$, $\alpha = 0.05$. Assessment for each statistically significant result with the help of additional information available with plotted time series graph.

3.2.2.3 Wald-Wolfowitz runs test

The test statistic as reported in Turkes (1996), the quantity $R = \sum$ number of sign changes in the series, $i = 1, 2, \dots, n$ where x_i is replaced by +1, if $x_i > \text{median}$ or -1, if $x_i < \text{median}$.

The statistic has an approximately normal distribution of mean and variance in equation 3.4 and 3.5

$$E(R) = \frac{2n_1n_2}{n+1} \quad (3.4)$$

$$\text{Var } R = \frac{2n_1n_2(2n_1n_2 - n)}{n^2(n-1)} \quad (3.5)$$

And n_1, n_2 , respectively denote the number +1 and -1 element, in the series and $n = n_1 + n_2$

3.2.2.4 Persistence analysis

The persistence analysis basically, is to examine the available data for serial dependence. The presence or otherwise of serial dependence in the data time series was evaluated via the instrumentality of autocorrelation.

3.3 Spatial Variation

3.3.1 Kriging method for producing spatial map of LNRB

The map of LNRB was prepared using a topographical sheet on a scale of 1:250,000 covering Kwara and Kogi states within the basin region. Arc.GIS10.2 on scale of 1:250,000 was used to extract the file shapes. The six meteorological station were not

evenly distributed over the study area. The station does not represent the entire basin well selected station had data gaps as shown by the distance wide apart. The mean annual and inter-seasonal rainfall and temperature formed the data. Microsoft Excel would be used to arranged and calculate the mean. Spatial analysis map plotted on ArcGIS 10.2 using kriging method of interpolation. Annual values and inter-seasonal (AMJ, JAS and ON) mean over each station were calculated. Annual mean determined from the equation 3.6

$$\bar{X} = \frac{1}{n} \sum_{i=1}^n X_j \quad (3.6)$$

\bar{X} = Annual mean data

X_i = Data point (stations)

N = Number of stations within a state

The mean equation is used to obtain annual rainfall and temperature from the total estimates. Value for monthly, inter-seasonal and annual were derived for analysis. This kriging method has the advantage of smoothing extreme irregularity thereby making it easy to detect underlying rainfall and temperature patterns.

3.3.2 Temporal variation

3.3.2.1 Analysis of serial dependence (autocorrelations)

Analysis of Serial Dependence was done to establish serial correlation of rainfall and temperature series. Any positive or negative autocorrelation in the time series data can cause a large effect on trend detection. Durbin-Watson (DW) standard test was applied. The test of null hypothesis (H_0) shows no existence of serial correlation or alternative hypothesis (H_a) shows existence of serial correlation. DW statistics boundary condition lie between 0-4 ranges with a value near 2, indicating no first order serial correlation. Positive serial correlation is associated with DW value below 2 and negative serial

correlation with DW value above 2. This was evaluated using the equation 3.7, 3.8 and 3.9

$$DW = \sum_{t=2}^T (\hat{E}_{t-1} - \hat{E}_{t-2})^2 / (\sum_{t=1}^T \hat{E}_t^2) \quad (3.7)$$

$$\hat{\rho} = (\sum_{t=2}^n e_t e_{t-1}) / (\sum_{t=1}^n e_t^2) \quad (3.8)$$

$$d = 2(1-\hat{\rho}) \quad (3.9)$$

where \hat{E}_t and e_t are time series at time t , $\hat{\rho}$ is the usual first order autocorrelation coefficient of the time series. N is the length of data

3.3.3 Temporal resolution for trend analysis (trend test)

3.3.3.1 Mann-Kendall test

This test is often for trend detection in hydrological time series (Dinpashoh *et al.*, 2011; Oguntunde, *et al.*, 2011). This is used to test for trend in rainfall and temperature data in the study to confirm the significance of observed trend. Time series of rainfall and temperature data were inputted into Excel template for the purpose of determining M-K test. Z statistics of rainfall and temperature time series with level of significance was calculated. Trend along with significant level records in temperature and rainfall was used to get z statistics. Mann-Kendall known as M-K rank correlation and is applicable when the data value of a time series can be assumed to obey the model as in equation 3.10

$$X = f(t) + \epsilon_t \quad (3.10)$$

Where $f(t)$ is a monotonic increasing or decreasing function of time. The ϵ_t is assumed to be from the same distribution with zero mean. Variance is considered to be constant in time. Mann-Kendall test statistics S is given in equation 3.11

$$S = \sum_{k=1}^{n-1} \sum_{j=k+1}^{n-1} \text{sgn}(X_j - X_k) \quad (3.11)$$

Where n is the length of the time series $X_i \dots X_n$ and $\text{sgn}(\cdot)$ is the sign function, X_j and X_k are values in year's j and k respectively over time t . The variance is given in equation 3.12

$$\text{VAR}(S) = \frac{1}{18} \left[n(n-1)(2n+5) - \sum_{p=1}^q (t_p - 1)(2t_p + 5) \right] \quad (3.12)$$

Where q is the number of tied groups, t_p is data value in the number of data point in group k , in cases where the sample size $n > 10$, the test statistics $Z(S)$ is calculated from equation 3.13

$$Z(S) = \begin{cases} \frac{S-1}{\sqrt{V(S)}}, & \text{If } S > 0 \\ 0 & \text{If } S = 0 \\ \frac{S+1}{\sqrt{V(S)}}, & \text{If } S < 0 \end{cases} \quad (3.13)$$

Positive value of $Z(S)$ indicates increasing trend, while negative $Z(S)$ value shows decreasing trends. Trends are considered significant if $Z(S)$ are greater than the standard normal deviate.

$Z_{1-\alpha/2}$ for the desired value of α . Each data value is compared to all subsequent data values. The initial value of the Mann-Kendall statistics S assumed to be zero (0) showing no trend.

3.3.3.2 Mann - Kendall test for monthly or seasonal series

In line with Hirsch *et al.* (1992), the Kendall test in this regard that allows for seasonality in the observations collected over a time period was employed; to do this, the Mann-Kendall test was computed on each season.

Thus, let the monthly or seasonal series be represented by the matrix

$$\mathbf{X} = \begin{pmatrix} x_{11} & \cdots & x_{1p} \\ \vdots & \ddots & \vdots \\ x_{n1} & \cdots & x_{np} \end{pmatrix}$$

Here, p is the number of seasons for n years under consideration; similarly, let the matrix

$$\mathbf{R} = \begin{pmatrix} R_{11} & R_{12} & \cdots & R_{1p} \\ R_{21} & R_{22} & \cdots & R_{2p} \\ \vdots & \vdots & & \vdots \\ R_{n1} & R_{n2} & \cdots & R_{np} \end{pmatrix}$$

denote the ranks corresponding to the observations in \mathbf{x} where the n observations for each season are ranked among themselves. Thus, each column of \mathbf{R} is a permutation of $(1, 2, \dots, n)$. Specifically, the rank matrix R_{ij} was computed as in equation 3.14

$$R_{ij} = \frac{1}{2} \left[n + 1 + \sum_{k=1}^n \text{sgn}(x_{ij} - x_{kj}) \right] \quad (3.14)$$

The Mann-Kendall test statistic for each season is shown in equation 3.15 and 3.16

$$S_i = \sum_{k=1}^{n-1} \sum_{j=k+1}^n \text{sgn}(x_{ji} - x_{ki}) \quad (3.15)$$

where, n is water years, i = number of seasons and a season here is defined as one calendar month, and S_i , the S-statistic in the Mann - Kendall test for season i ($i = 1, 2, \dots, 12$)

$$S' = \sum_{i=1}^p S_i, \quad p = \text{seasons}; \quad \sigma_{s'}^2 = \sum_{i=1}^p \text{Var}(S_i) \quad (3.16)$$

To account for serial correlation, as in monthly flow or discharge processes, the variance of S' is defined as in equation 3.17

$$\sigma_{s'}^2 = \sum_{i=1}^p \text{Var}(S_i) + \sum_{g=1}^{p-1} \sum_{h=g+1}^p \sigma_{gh} \quad (3.17)$$

Where the covariance matrix σ_{gh} is expressed as follows is shown in equation 3.18 and 3.19

$$\hat{\sigma}_{gh} = \frac{1}{3} \left[K_{gh} + 4 \sum_{i=1}^n R_{ig} R_{ih} - n(n+1)^2 \right] \quad (3.18)$$

$$K_{gh} = \sum_{i=1}^{n-1} \sum_{j=i+1}^n \text{sgn} \left[(x_{jg} - x_{ig})(x_{jh} - x_{ih}) \right] \quad (3.19)$$

This is for a “no missing” data situation, and g and h are different seasons, respectively.

The test statistic Z' which is standard normally distributed, is evaluated in equation 3.20

$$z' = \begin{cases} (S' - 1)/\sigma_s & S' > 0 \\ 0 & S' = 0 \\ (S' + 1)/\sigma_s & S' < 0 \end{cases} \quad (3.20)$$

3.3.3.3 Determination of the magnitude of change of trend (Sen's Slope)

This is another non-parametric test used to determine the magnitude of change in the rainfall record and temperature. To estimate the true slope of an existing trend, Sen's non-parametric method is used. Sen's method can be used in cases where trend can be assumed to be linear (Sen's 1968). The method of calculating Sen's slope estimator requires a time series of equally spaced data. Sen's method proceeds by calculating the slope as a change in measurement per change in time as shown in 3.21

$$Q = \frac{X_j - X_k}{J - k} \quad (3.21)$$

Where Q is the slope between data point X_j and X_k

X_j = data measurement in time j

X_k = data measurement at time k

j=time k, X_j and X_k constitute the pairs of observation identified by place in the series

For a time series x having n observations, there are a possible $N = n(n-1)/2$ values of Q that can be calculated. According to Sen's method, the overall estimator of the slope is the median of these N values and Q . The overall slope estimator Q^* is given by equation 3.22 and 3.23

$$Q^* = \begin{cases} Q_{(N+1)/2} & \text{if } N \text{ is odd} \\ \frac{Q_{\frac{N}{2}} + Q_{(n+2)/2}}{2} & \text{if } N \text{ is even} \end{cases} \quad (3.22)$$

$$\frac{Q_{\frac{N}{2}} + Q_{(n+2)/2}}{2} \text{ if } N \text{ is even} \quad (3.23)$$

The confidence interval of the slope is calculated from the same array of ordered slopes Q_i using indexes M_1 and M_2 . The lower and upper limits of the confidence interval, Q_{min} and Q_{max} , are the M_1^{th} largest and the $(M_2+1)^{th}$ largest of the N ordered slope estimates Q_i as shown in the equation (3.24 and 3.25)

$$Q_{lower} = Q_{M_1} \quad (3.24)$$

$$Q_{upper} = Q_{M_2+1} \quad (3.25)$$

Where $M_1 = (N - C_\alpha)/2$

$$M_2 = (N + \alpha/2) * \sqrt{Var(S)} \quad (3.26)$$

Where S is the Mann-Kendall test statistics, and C_α is the confidence interval using tabulated Z . as shown in equation 3.27

$$Z_{1-0.05/2} = 1.96 \quad (3.27)$$

Values for cumulative normal distribution, the 95% confidence interval is calculated using the median of these estimates is Sen's estimator of slope. The approach involves computing slopes for all the pairs of time points and then using the median of these slope to estimate the overall slope Q . This is because Sen's is sensitive to outliers and can handle limited number of values below the detection limit and missing values. The slope magnitude in the overall was computed by using the statistic β given in equation

3.3.3.4 Statistical change point (SCP) or mutation detection

The change point or mutation detection was done by employing the Pettit's test and Sequential Mann-Kendall test (SQ-MK test).

(i) Pettit's test

The approach after Pettit (1979) is commonly applied to detect change point in hydrological time series or climatic series with continuous data. It Test the Null H_0 ; the T variables follows one or more distribution that have the same location parameters (no change) against the alternative a change exists. The non-parametric statistics is defined as in equation in equation 3.28 and 3.29

$$K_T = \text{Max}|U_{t,n}| \quad (3.28)$$

$$U_{t,n} = \sum_{i=1}^t \sum_{j=t+1}^n \text{sgn}(x_i - x_j) \quad (3.29)$$

The change point of the series is located K_T provided that statistics is significance. The significant probability of K_T is approximated for ≤ 0.05 .

This method is ranked based test and the null hypothesis of the observations is that the observations for the test are independent and identically distributed

Suppose R_1, \dots, R_t are the ranks of the t observations, y_1, \dots, y_t in the complete sample of n observations for the two-sided test (i.e., one in which the alternative hypothesis does not specify the direction of change)

. The process for the implementation of the test is shown in equation 3.30

➤ Compute U_k statistic using the following formula

$$U_k = 2 \sum_{i=0}^n m_i - k(n + 1) \quad (3.30)$$

Where, m_i is the rank of the i^{th} observation when the values x_1, x_2, \dots, x_n in the series are arranged in ascending order and k takes values from 1, 2, . . . , n.

Define the statistical change point test (SCP) is shown in equation 3.31

$$K = \max_{1 \leq k \leq n} |U_k| \quad (3.31)$$

When, U_k attains maximum value of k in a series, then a change point will occur in the series. The critical value is shown in equation 3.32

$$K_\alpha = [- \ln \alpha (n^3 + n^2) / 6]^{1/2} \quad (3.32)$$

Where, n is number of observation and α is level of significance which determines the critical value.

(ii) Sequential Mann – Kendall test (SQ – MK test)

The SQ-MK test developed by Sneyer (1990) was used for determining the year of significant change in trend. The test set up a progressive series, a progressive one $U(t)$ and a backward (lag) $u'(t)$. If they cross each other and diverge beyond specific threshold value, then, there is a statistically significant trend. The point where they cross each other indicate the approximate year at which trend begun.

The $U(t)$ is the standardized variable that has a zero mean and the unit standard deviation. The SQ behavior fluctuate around the zero level. The magnitude of x_j annual mean time series.

$$(j=1, \dots, n)$$

$$X_k = (k=1, \dots, j-1)$$

Note: Let $U(t)$ be a standardised variable that has zero mean and unit deviation such that its sequential behaviour revolves around zero level. $u(t)$ is the same as the z values that are found from the first to last data point. It considers the relative values of the terms in the time series (x_1, x_2, \dots, x_n) .

The process is computed as follows:

1. Compute the magnitudes of x_j annual mean series ($j = 1, \dots, n$) with x_k , ($k = 1, \dots, j-1$).

At each comparison, count the number of cases $x_j > x_k$ and denote same as n_j .

- (a) The test statistic t is given by the equation 3.33

$$t_j = \sum_1^j n_j \quad (3.33)$$

- (b) The mean and variance of the statistic are shown in equation 3.34 and 3.35

$$e(t) = \frac{n(n-1)}{4} \quad (3.34)$$

$$\text{Var } t_j = \frac{j(j-1)(2j+5)}{72} \quad (3.35)$$

2. Compute the sequential values of u as in equation 3.36

$$U(t) = \frac{t_j - e(t)}{\sqrt{\text{var}(t)}} \quad (3.36)$$

3. Similarly, compute the values of $u'(t)$ in a backward manner. In doing so, start from the end of the series.

4. Determine the point of intersection of the curves. The intersection of the curves showing the forward (u) and backward (u') represents the time when a trend or change starts; the critical value for 95% level is ± 1.96 .

3.3.3.5 Coefficient of variation

The coefficient of variation indicates the amount of fluctuation in rainfall and temperature recorded over a long period of time from the mean values as shown in equation 3.37

$$\text{CV} (\%) = \frac{\sigma}{\mu} \times 100 \quad (3.37)$$

Where CV is the coefficient of variation in percentage

σ = represent standard deviation

μ = represent mean

3.4 Standardised Anomaly Index (SAI)

Standardized Anomaly Index Estimation Model for each of the stations, rainfall series were analyzed for fluctuation using Standardized Anomaly Index (SAI) which is a

commonly used index for regional climate change studies (Babatolu *et al.*, 2013). Station rainfall is expressed as a standardized departure from the long-term mean (i.e., the mean of the base period), Standardised Anomaly Index was calculated as the difference between the annual total of a particular year and the long term (first moment) average rainfall divided by second moment (standard deviation) of the long-term data. This characteristic of SAI has contributed to its popularity for application in drought monitoring and also makes possible the determination of wet/dry spell years in the record (WMO, 2012). Employing the theory of runs, using a threshold of value (0); which states that any value above zero is wetter than normal (flood) and any value below zero is less than normal (dry spell) as shown in equation 3.38

The formula is given

$$Z = \left(\frac{x_i - \mu}{\sigma} \right) \quad (3.38)$$

Where,

Z is the standardized anomaly index

x_i = the annual rainfall of a particular year

μ = first moment (mean annual)

σ = second moment (standard deviation)

3.5 Principal Component Analysis

Principal Component Analysis (PCA) can be used in the study of climatology and meteorology to further analyze data into monthly, annual, decadal and seasonal segment. Variability that exists between variability (Richman, 1996; Jolliffe, 1990) and can reduce a large number of interrelated variables from a multivariate data table to few variables (principal components). These variables correspond to a linear combination of the originals. The number of principal components is less than or equal to the original variables. The information in a given data set corresponds to the total variation it

contains. The goal of PCA is to identify directions (or principal components) along which the variation in the data is maxima. It reduces the dimensionality of a multivariate data to two or three components that can be visualized graphically with minimal loss of information.

PC transform, the matrix of the variables (X) is centered by subtracting its mean, and then the covariance matrix of x is obtained as shown in equation 3.39

$$S_{XX} = E(X^T X) \quad (3.39)$$

Where E is operator's expectation. Knowing that the principal component is not invariant under scaling. Orthogonal decomposition of S_{XX} is given without loss of generality in equation 3.40.

$$S_{XX} = X_X D_X U_X^T \quad (3.40)$$

Where U_x is the matrix having the orthogonal eigenvectors of S_{XX} and $D_x = \text{diag}(\lambda_1, \dots, \lambda_k)$ represent the diagonal matrix of the eigenvalues of S_{XX} in decreasing order of magnitude. (Tatli *et al.*, 2005). The principal component is given in equation 3.41

$$V_X = X D_X \quad (3.41)$$

Where, V_X of columns represent individual PC

CHAPTER FOUR

4.0 RESULT AND DISCUSSION

4.1 Preliminary Analysis of Result

The essence here was to account for potential systematic stochastic persistence biases (noise) that might mask climate change signals; in order to determine the variability that exist in the data for instance, long-term variations, trends so as to avert wrong conclusions about climate change which may compromise the reliability and quality of any assessment. Thus, 3 models of homogeneity namely; Pettit's test, Standardised normal homogeneity test (SNHT) and Buishand test (BRT) was adopted.

The rainfall data from the time series (1979 - 2013), as the computed p-values for the stations are greater than the alpha (α) significance level of (0.05) except at Oke Oyi where the Pettit's is less than level of significance, one cannot reject the null hypothesis. Therefore, there is no significant difference between the data series. The coefficient of variation between the data series is insignificant, the data series is homogeneous. The Table 4.1 below showed the computed P-value and Figure 4.1 shows the graph of rainfall from 1979-2013. The homogeneous test for Figure 4.1 shows linear variability in trend.

Table 4.1: Rainfall Homogeneity test result for the LNRB at 95% significance level

S/N	Stations	Pettit	SNHT	BRT
1	Ekirin Ade	0.226	0.351	0.157
2	Ganaga	0.590	0.281	0.567
3	Lafiagi	0.100	0.150	0.038
4	Obangede	0.714	0.400	0.369
5	Oke Oyi	0.017	0.092	0.009
6	Olamaboro	0.317	0.330	0.102

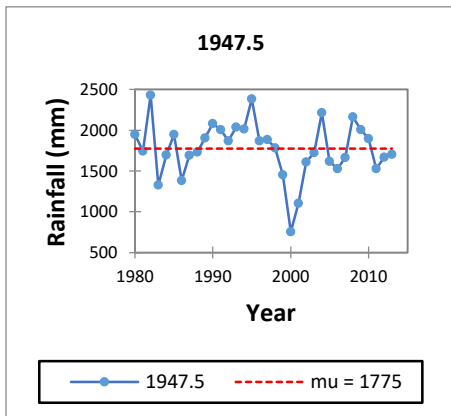


Figure 4.1a: Rainfall Pettit's Test

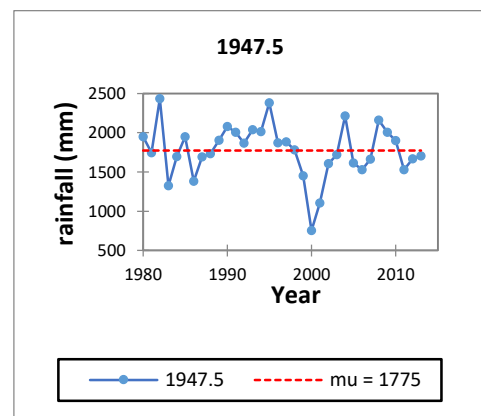


Figure 4.1b: Rainfall SNHT Test

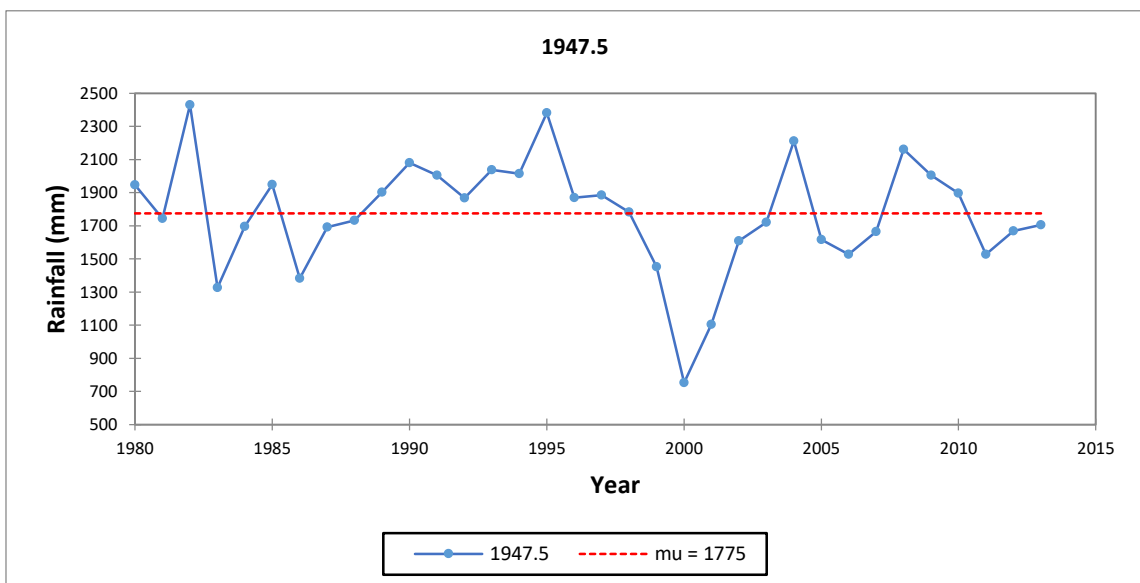


Figure 4.1c: Buishand Test (BRT)

Maximum temperature homogeneity result shows that the p-value is less than the significance level, therefore the null hypothesis should be rejected and alternative hypothesis accepted. All station displayed inhomogeneity. The shift in trend suggests an upsurge in temperature rise. This portends increase evaporation, increase in heat-related mortality and extreme climate effect such as drought. The Table 4.2 shows maximum temperature for homogeneity result and Figure 4.2 depicting the change in trend.

Table 4.2: Maximum Temperature Homogeneity Test Result for the LNRB at 95% Significance Level

S/N	Stations	Pettit	SNHT	BRT
1	Ekirin Ade	0.0001	0.0001	0.0001
2	Ganaga	0.0001	0.0001	0.0001
3	Lafiagi	0.0001	0.0001	0.0001
4	Obangede	0.0001	0.0001	0.0001
5	Oke Oyi	0.000	0.000	0.001
6	Olamaboro	0.0001	0.0001	0.0001

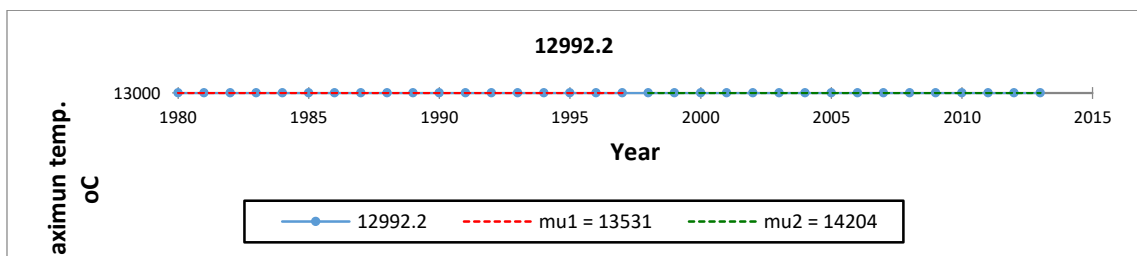


Figure 4.2a: Pettit's Test

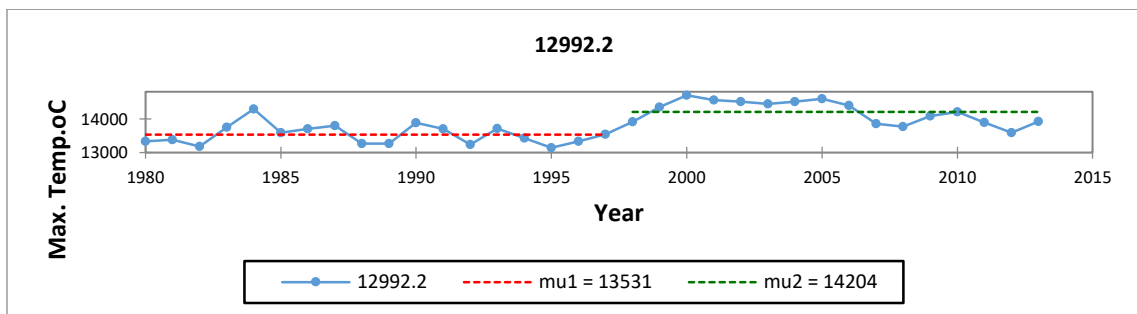


Figure 4.2b: Maximum Temperature SNHT Test

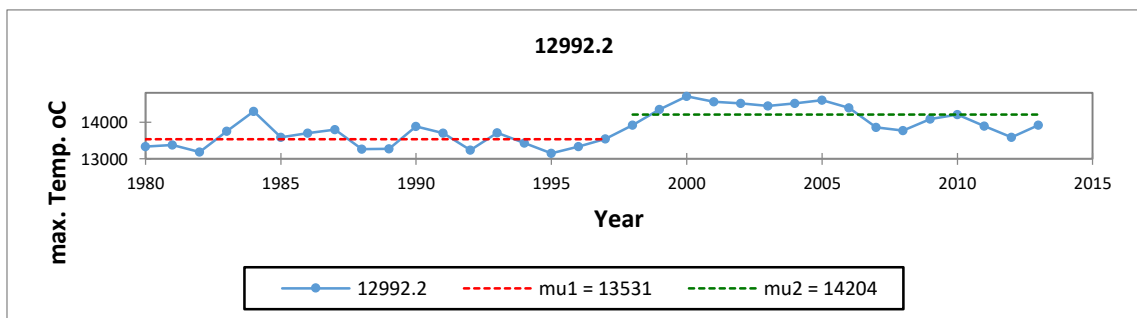


Figure 4.2c: Maximum Temperature BRT Test

The minimum temperature showed that p-value is less than the significance level for all station except, Oke Oyi. The null hypothesis for Ekirin Ade, Ganaga, Obangede, and

Olamaboro is rejected and alternative hypothesis accepted. Contrarily, the null hypothesis cannot be rejected for Oke Oyi station, because the p-value was greater than the significance level. The Table 4.3 shows minimum temperature homogeneity result.

Table 4.3: Minimum Temperature Homogeneity test result for the LNRB at 95% significance level

S/N	Stations	Pettit	SNHT	BRT
1	Ekirin Ade	0.0001	0.0001	0.0001
2	Ganaga	0.004	0.002	0.001
3	Lafiagi	0.0001	0.0001	0.0001
4	Obangede	0.013	0.008	0.004
5	Oke Oyi	0.153	0.259	0.099
6	Olamaboro	0.0001	0.0001	0.0001

4.1.1 Geographical autocorrelation

An autocorrelation test was carried out to investigate the measure of association among the gauging stations for the rainfall, maximum temperature and minimum temperature data. The result in the annual data rainfall, maximum temperature and minimum temperature. From the Table 4.4 a large positive autocorrelation was found in all stations at lag 1= $\phi < 2$

Table 4.4: Minimum Temperature Homogeneity Test Result for LNRB at 95% Significance

Station	Rainfall ϕ	Maximum Temperature ϕ	Minimum Temperature ϕ
Ekirin Ade	0.345657	0.757411	0.368532
Ganaga	0.301153	0.763490	0.379082
Lafiagi	0.411265	0.707729	0.144613
Obangede	0.338421	0.791615	0.391997
Oke Oyi	0.373406	0.666220	0.020806
Olamaboro	0.346612	0.766397	0.222925

4.2 Descriptive Statistics of Time Series Characterization of Rainfall

4.2.1 Annual and seasonal time series Plot for the stations and their statistics

From Table 4.5, the mean annual maximum temperature within the Basin ranged from 32.48 at Ekirin Ade station to a highest of 37.91 at Lafiagi from 1979-2013. The coefficient variation showed partial deviation within the Basin. This may account for the variability that contributed to the anomalies in the pattern of temperature. The Higher the mean annual temperature, the higher the coefficient of variation 11.66%. The skewness showed partial deviation from negative to positive. Similarly, from Table 4.6 annual minimum temperature (1979-2013) shows Ekirin Ade having the least of 20.85⁰C to a highest value of 22.11⁰C. Oke Oyi shows the highest deviation of 2.49. The coefficient of variation shows marked variability within the Basin from 7.17 at Ekirin Ade to 11.72 at Oke Oyi. The skewness also showed deviation of the distribution towards left side of symmetry.

Table 4.7 Rainfall result of the descriptive statistics reveals that annual rainfall over the LNRB from 1979 to 2013 rose from 3.20 mm/day at Lafiagi to a high of 4.05 mm/day at Ekirin Ade. Partial variability of annual rainfall shows deviation from 3.34 at Ganaga to 4.86 at Ekirin Ade. Coefficient of variation for annual rainfall within the Basin ranges from 89.58 at Ekirin Ade to 120.99% at Lafiagi. The skewness revealed deviation in the positive side of the symmetry.

Table 4.5: Descriptive Statistics for Maximum Temperature

Name	μ	σ	CV	Min.	Max	C_{xx}
Ekirin Ade	32.48	4.25	13.10	24.44	40.88	0.00
Ganaga	34.71	4.65	13.40	25.49	44.43	0.02
Lafiagi	37.91	4.42	11.66	27.19	46.47	-0.29
Obangede	32.96	4.22	12.80	24.76	41.89	0.02
Oke Oyi	35.72	4.55	12.73	25.82	44.80	-0.10
Olamaboro	34.68	4.83	13.91	25.83	45.32	0.11

Mean (μ); Standard deviation (σ); Coefficient of Variation (CV); Minimum (mi); Maximum (max) and Skewness (C_{xx})

Table 4.6: Descriptive Statistics for Minimum Temperature

Name	μ	σ	CV	Min.	Max	C_{xx}
Ekirin Ade	20.85	1.49	7.17	14.13	24.20	-0.76
Ganaga	22.15	1.78	7.94	15.47	26.12	-0.32
Lafiagi	22.11	2.43	10.98	15.15	26.96	-0.54
Obangede	21.46	1.60	7.46	14.70	25.15	-0.51
Oke Oyi	21.25	2.49	11.72	11.63	25.20	-1.30
Olamaboro	21.97	1.99	9.19	14.06	25.94	-0.86

Mean (μ); Standard deviation (σ); Coefficient of variation (CV); Minimum (mi); Maximum (max) and Skewness (C_{xx})

Table 4.7: Descriptive Statistics for Rainfall

Name	μ	σ	CV	Min.	Max	C_{xx}
Ekirin Ade	4.86	4.86	89.58	0.00	19.91	0.61
Ganaga	3.27	3.34	102.38	0.00	17.99	0.98
Lafiagi	3.20	3.87	120.99	0.00	15.93	1.09
Obangede	4.05	3.83	94.74	0.00	20.07	0.75
Oke Oyi	3.05	3.57	116.85	0.00	16.06	1.12
Olamaboro	3.63	3.61	99.48	0.00	15.57	0.79

Mean (μ); Standard Deviation (σ); Coefficient of Variation (CV); Minimum (mi); Maximum (max) and Skewness (C_{xx})

4.3 Characterisation of Extreme Rainfall Indices

4.3.1 Trend and magnitude of rainfall and temperature

Table 4.7 gives a vivid summary of Mann-Kendall and Sen's Slope estimator for all the gauging station at 95% significance alpha level. The Non-Parametric Mann-Kendall test, Z statistics shows the trend of the series for 35 years for each gauging station. The trend analysis in all the substations were not statistically significant. For maximum temperature, (Table 4.8) only Ganaga showed decreasing trend of -0.07 while the other stations showed increasing trend but statistically insignificant. The minimum temperature analysis (Table 4.9) shows four stations namely; Ekirin Ade, Ganaga, Obangede and Oke Oyi depicting decreasing trend while Lafiagi and Olamaboro showed increasing trend. The trend analysis for minimum temperature is not significant statistically. Annual rainfall trend showed that statistically, at 95% confidence interval,

three stations namely; Ekirin Ade, Obangede and Ganaga showed decreasing insignificant trend. From Table 4.10 Olamaboro depicted increasing trend.

Table 4.8: Maximum Temperature Trend Result of the LNRB

S/N	Station	Times Series (n)	Test Z	Sen's Slope Q (mm/yr.)	Trend (95% confidence interval)	SQ-MK Change Point
1	Ekirin Ade	34	0.35	26.8	No sig. trend	1979
2	Ganaga	34	-0.07	-33.2	No sig. trend	1981
3	Lafiagi	34	0.41	12.7	No sig. trend	1981
4	Obangede	34	0.19	26.4	No sig. trend	1988
5	Oke Oyi	34	0.40	13.1	No sig. trend	1988
6	Olamaboro	34	0.24	28.6	No sig. trend	1994

Table 4.9: Minimum Temperature Trend Result of the LNRB

S/N	Station	Times Series (n)	Test Z	Sen's Slope Q (mm/yr.)	Trend (95% confidence interval)	SQ-MK Change Point
1	Ekirin Ade	34	-0.40	4.5	No sig. trend	1981
2	Ganaga	34	-0.51	5.2	No sig. trend	1988
3	Lafiagi	34	0.02	5.0	No sig. trend	1985
4	Obangede	34	-0.46	4.2	No sig. trend	1980
5	Oke Oyi	34	-0.22	-7.2	No sig. trend	1987
6	Olamaboro	34	0.31	1.9	No sig. trend	1987

Table 4.10: Annual Rainfall Trend Result in the LNRB

S/N	Station	Times Series (n)	Test Z	Sen's Slope Q (mm/yr.)	Trend (95% confidence interval)	SQ-MK Change Point
1	Ekirin Ade	34	-0.46	3.6	No sig. trend	1984
2	Ganaga	34	-0.15	2.9	No sig. trend	1984
3	Lafiagi	34	0.00	-0.7	No sig. trend	1985
4	Obangede	34	-0.15	2.7	No sig. trend	1987
5	Oke Oyi	34	0.11	-4.5	No sig. trend	1988
6	Olamaboro	34	0.31	5.1	No sig. trend	1983

The monthly Mann-Kendall trend analysis Table 4.11(a-f) is summarised for Rainfall, maximum temperature and minimum temperature in all the stations.

Ekirin Ade: The monthly trend revealed decreasing insignificant in February, April and October. This could be as result of little rainfall in these months. Maximum temperature; there was positive significant trend in the months except for January and April. Minimum temperature was highest in July (7,5 mm/yr.) as shown in Table 4.11a.

Table 4.11a: Monthly Rainfall, Maximum Temperature and Minimum Temperature Trend Result Ekirin Ade

Months	Rainfall		Max. Temperature		Min. Temperature	
	MK Test Z	Significance Level (%)	MK Test Z	Significance Level (%)	MK Test Z	Significance Level (%)
Jan.	0.62	95	1.28	95	2.16	95
Feb.	0.74	95	3.75	95	1.72	95
March	4.54	95	4.85	95	4.76	95
April	1.01	95	1.81	95	2.49	95
May	3.79	95	3.75	95	3.13	95
June	2.64	95	5.40	95	4.50	95
July	2.05	95	5.77	95	7.05	95
Aug.	2.36	95	4.36	95	5.03	95
Sept.	0.44	95	4.28	95	5.95	95
Oct.	0.08	95	2.18	95	3.88	95
Nov.	0.44	95	2.14	95	1.98	95
Dec.	0.04	95	2.87	95	0.26	95

Ganaga: Rainfall trend showed decreasing significant trend. Maximum temperature depict positive significant trend. Minimum trend also revealed significant positive trend except in January and December as shown in Table 4.11b.

Table 4.11b: Monthly Rainfall, Maximum Temperature and Minimum Temperature Trend Result at Ganaga

Months	Rainfall		Max. Temperature		Min. Temperature	
	MK Test Z	Significance Level (%)	MK Test Z	Significance Level (%)	MK Test Z	Significance Level (%)
Jan.	0.33	95	1.61	95	-1.52	95
Feb.	-0.44	95	4.85	95	2.31	95
March	-4.96	95	6.44	95	5.97	95
April	0.93	95	2.34	95	4.08	95
May	-2.64	95	4.72	95	4.61	95
June	-2.16	95	6.08	95	6.50	95
July	1.87	95	5.93	95	7.43	95
Aug.	1.63	95	5.16	95	5.95	95
Sept.	-2.73	95	4.94	95	6.02	95
Oct.	-0.88	95	4.63	95	3.68	95
Nov.	-1.43	95	4.72	95	2.16	95
Dec.	-0.97	95	4.19	95	-0.09	95

Lafiagi: rainfall trend showed decreasing trend. There was significant positive trend in maximum temperature. Minimum temperature also revealed positive trend except in Jan. and Dec. as shown in Table 4.11c.

Table 4.11c: Monthly Rainfall, Maximum Temperature, Minimum Temperature, and Trend Result at Lafiagi

Months	Rainfall		Max. Temperature		Min. Temperature	
	MK Test Z	Significance Level (%)	MK Test Z	Significance Level (%)	MK Test Z	Significance Level (%)
Jan.	1.74	95	2.89	95	-0.71	95
Feb.	-2.49	95	3.04	95	0.51	95
March	-4.06	95	4.89	95	0.02	95
April	1.94	95	1.90	95	3.09	95
May	-2.64	95	2.76	95	4.14	95
June	-4.81	95	4.10	95	5.07	95
July	-2.25	95	4.21	95	6.37	95
Aug.	1.63	95	3.39	95	5.25	95
Sept.	-1.94	95	3.70	95	5.53	95
Oct.	-0.35	95	3.44	95	2.76	95
Nov.	-1.26	95	3.26	95	0.79	95
Dec.	-2.09	95	3.26	95	-1.61	95

Obangede: rainfall showed highest decreasing trend in March. Maximum Trend showed significant positive trend except January and April. Minimum temperature trend depicted positive trend as shown in Table 4.11d

Table 4.11d: Monthly Rainfall, Maximum Temperature and Minimum Temperature Trend Result at Obangede

Months	Rainfall		Max. Temperature		Min. Temperature	
	MK Test Z	Significance- Level (%)	MK Test Z	Significance- Level (%)	MK Test Z	Significance- Level (%)
Jan.	0.02	95	1.32	95	-1.85	95
Feb.	-0.71	95	3.55	95	1.94	95
March	-4.85	95	5.25	95	5.25	95
April	0.09	95	1.87	95	3.00	95
May	-3.48	95	4.23	95	3.84	95
June	-2.49	95	5.14	95	5.51	95
July	1.54	95	6.22	95	7.14	95
Aug.	2.07	95	4.98	95	5.93	95
Sept.	-1.08	95	4.98	95	6.55	95
Oct.	-0.44	95	3.35	95	4.01	95
Nov.	-0.84	95	3.53	95	2.03	95
Dec.	-0.88	95	3.00	95	0.02	95

Oke Oyi: Rainfall showed decreasing significant trend. Maximum temperature revealed increasing positive trend except in January. Minimum temperature trend depicted significant positive trend as shown in Table 4.11e.

Table 4.11e: Monthly Rainfall, Maximum Temperature and Minimum Temperature Trend Result at Oke Oyi

Months	Rainfall		Maximum Temperature		Minimum Temperature	
	MK Test Z	Significance Level (%)	MK Test Z	Significance Level (%)	MK Test Z	Significance Level (%)
Jan.	-2.91	95	1.21	95	1.68	95
Feb.	-2.67	95	3.33	95	0.22	95
March	-5.14	95	5.51	95	0.31	95
April	-3.44	95	3.57	95	3.17	95
May	-3.57	95	3.00	95	4.32	95
June	-5.03	95	5.25	95	5.69	95
July	-1.90	95	5.16	95	8.13	95
Aug.	2.69	95	3.79	95	5.97	95
Sept.	-0.48	95	2.78	95	7.03	95
Oct.	-0.22	95	1.81	95	4.74	95
Nov.	-2.78	95	1.76	95	0.40	95
Dec.	-1.39	95	1.56	95	1.06	95

Olamaboro: Monthly rainfall trend depicted significant decreasing trend in March, May, June and September. The Maximum temperature revealed significant positive trend except in January. Minimum temperature also revealed significant positive trend except in January and December as shown in Table 4.11f

Table 4.11f: Rainfall, Maximum Temperature and Minimum Temperature Trend Result at Olamaboro

Months	Rainfall		Maximum Temperature		Minimum Temperature	
	MK Test Z	Significance Level (%)	MK Test Z	Significance Level (%)	MK Test Z	Significance Level (%)
Jan.	0.09	95	1.28	95	-1.15	95
Feb.	1.43	95	3.75	95	1.23	95
March	-2.91	95	4.85	95	3.04	95
April	1.06	95	3.75	95	3.26	95
May	-3.13	95	5.40	95	3.44	95
June	-3.04	95	5.77	95	4.83	95
July	1.21	95	4.36	95	6.41	95
Aug.	0.77	95	4.28	95	4.28	95
Sept.	-3.26	95	4.28	95	6.57	95
Oct.	-0.24	95	2.18	95	4.32	95
Nov.	-0.09	95	2.14	95	1.37	95
Dec.	0.02	95	2.87	95	-0.06	95

The Sen's slope estimator was employed to determine the change per unit time of trend in rainfall, maximum temperature and minimum temperature. Table 4.7, 4.8 and 4.9 paint a vivid picture of the magnitude of slope in the time series. Positive and negative sign indicate an upward and downward slope respectively. For rainfall, Sen's slope shows increasing trend with Olamaboro having the highest slope of (5.1 mm/year). Oke Oyi and Lafiagi shows negative slope of (-4.5 mm/year and -0.7 mm/year) respectively. The Sen's slope for maximum temperature for all stations shows positive change per unit time except Ganaga with least negative trend of -33.2 mm/year.

Similarly, the Sen's slope for minimum temperature shows upward slope except for Oke Oyi that depicted downward slope of -7.2 mm/year. The magnitude of the slope is shown in figure 4.3

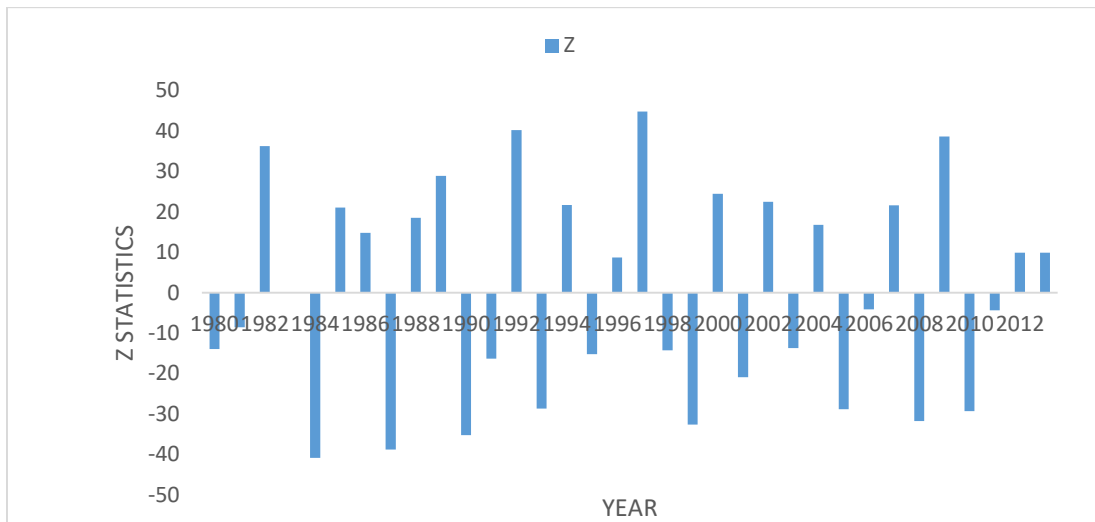


Figure 4.3: Sen's slope of Ekirin Ade maximum temperature from 1979-2013

The sequential trend was used to detect change point of trend. Table 4.7, 4.8 and 4.9 shows the result change point per unit time of rainfall, maximum temperature and minimum temperature respectively. The figure below shows the sequential trend of Ekirin Ade Minimum temperature. The progressive series $U(t)$ and the Lag1 $U'(t)$ series interceded each other at one point which showed the years of change (time).

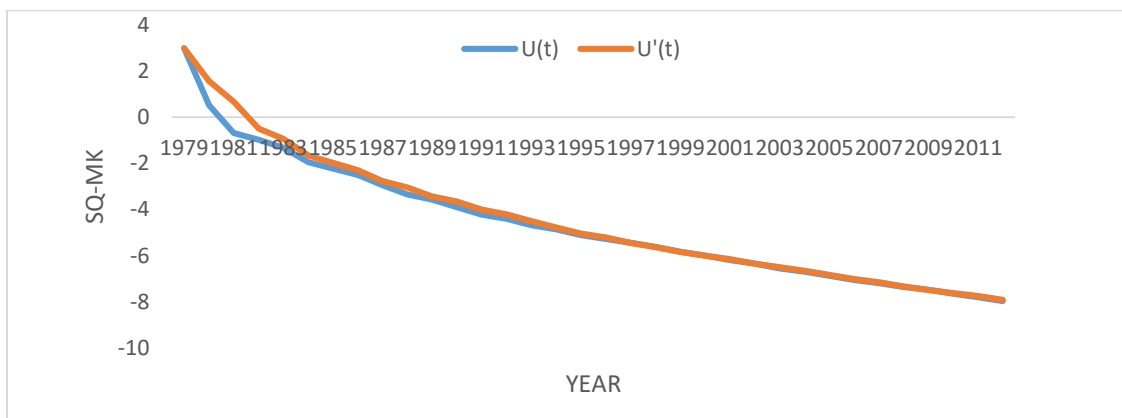


Figure 4.4: Sequential Mann-Kendall change per unit time of Ekirin Ade from 1979-2013

4.3.2 Spatial distribution of the mean annual and seasonal rainfall

The results of the annual rainfall of the stations showed that Ekirin Ade and Obangede recorded highest mean annual rainfall amount ($R_r \geq 1780$ mm) for a period of 1979-2013. Areas of lowest rainfall amount are found around Oke Oyi and Lafiagi with mean annual ranging from 1120.5 mm to 1200 mm.

Analysis performed on inter-seasonal variability Figure 4.5 (a-d) of rainfall for the area shows similar behavior with that of the annual analysis. Ekirin Ade records the highest in rainfall values for the April-June (AMJ), July-Sept (JAS) and Oct.-Nov. (ON) seasons with 301 mm, 510 mm and 224 mm respectively. Kriging interpolation method has helped to examine and estimate inter-seasonal rainfall variability and mean rainfall across the Basin. Generally, rainfall pattern within the Basin depicts trend of peak and low from 1979-2013 as shown in Figure 4.5(a-d).

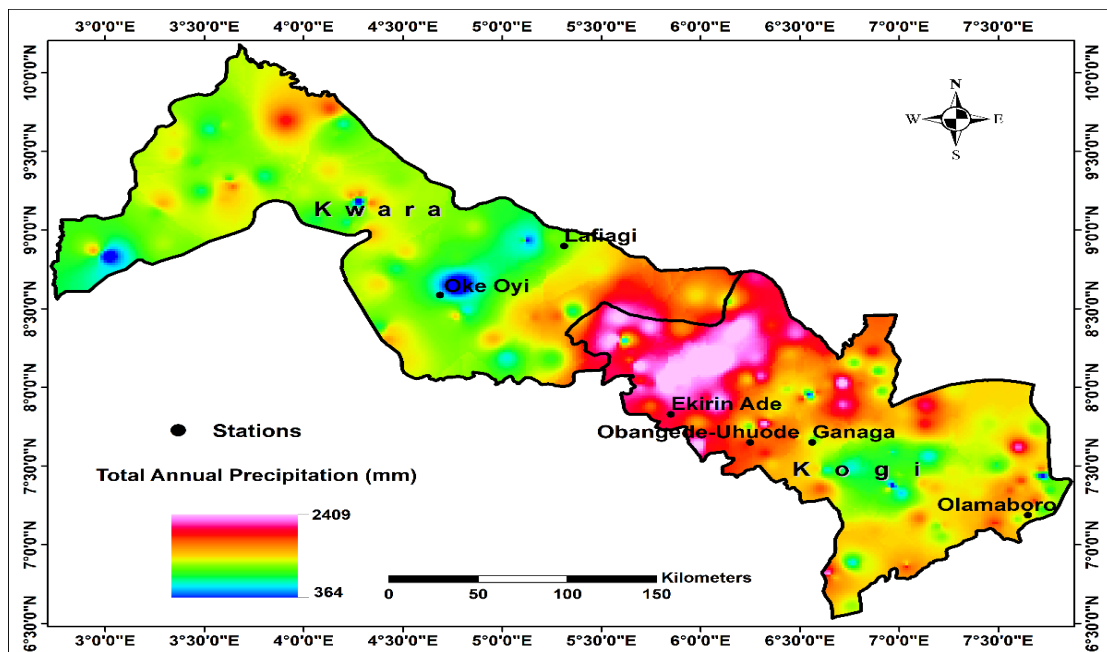
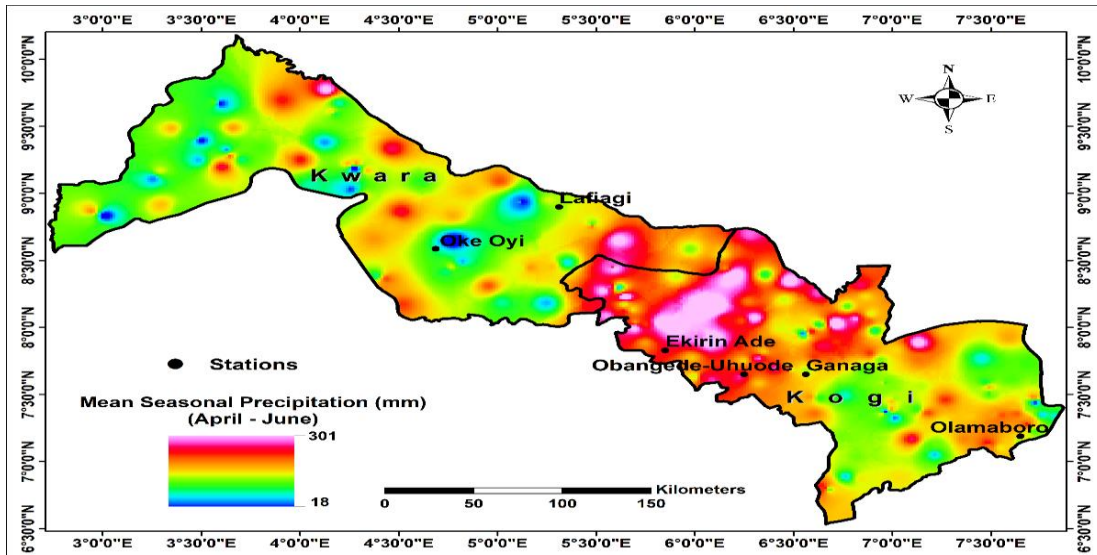


Figure 4.5a: Total Annual Spatial Rainfall (Mar-Nov)



4.5b: Seasonal Spatial Rainfall (April –June)

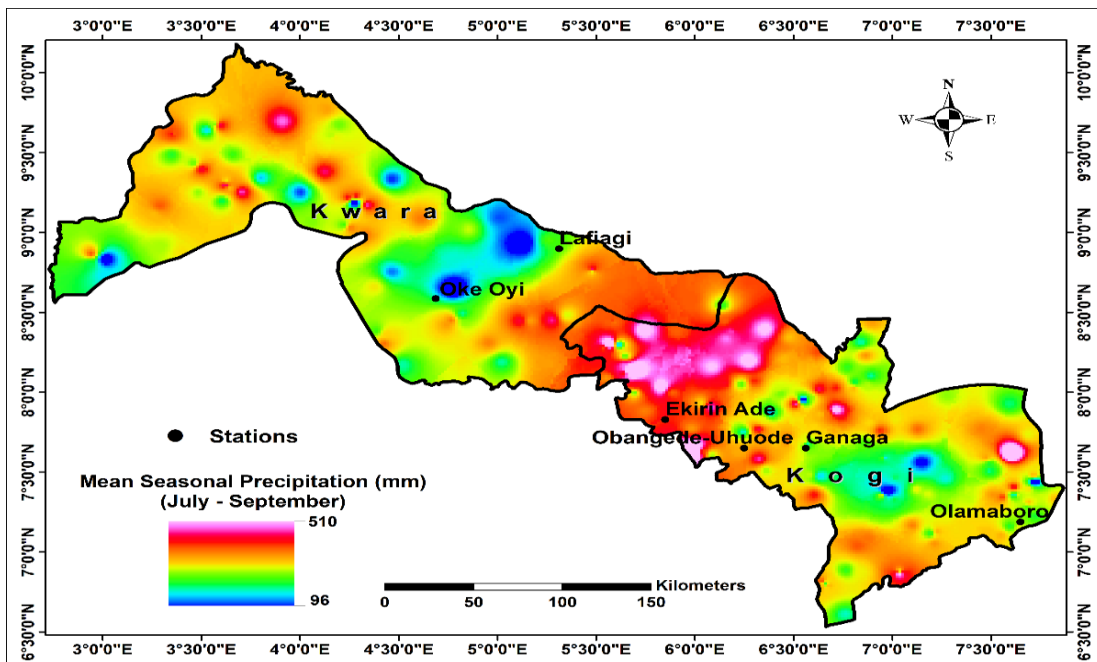


Figure 4.5c: Seasonal Spatial Rainfall (July –Sept)

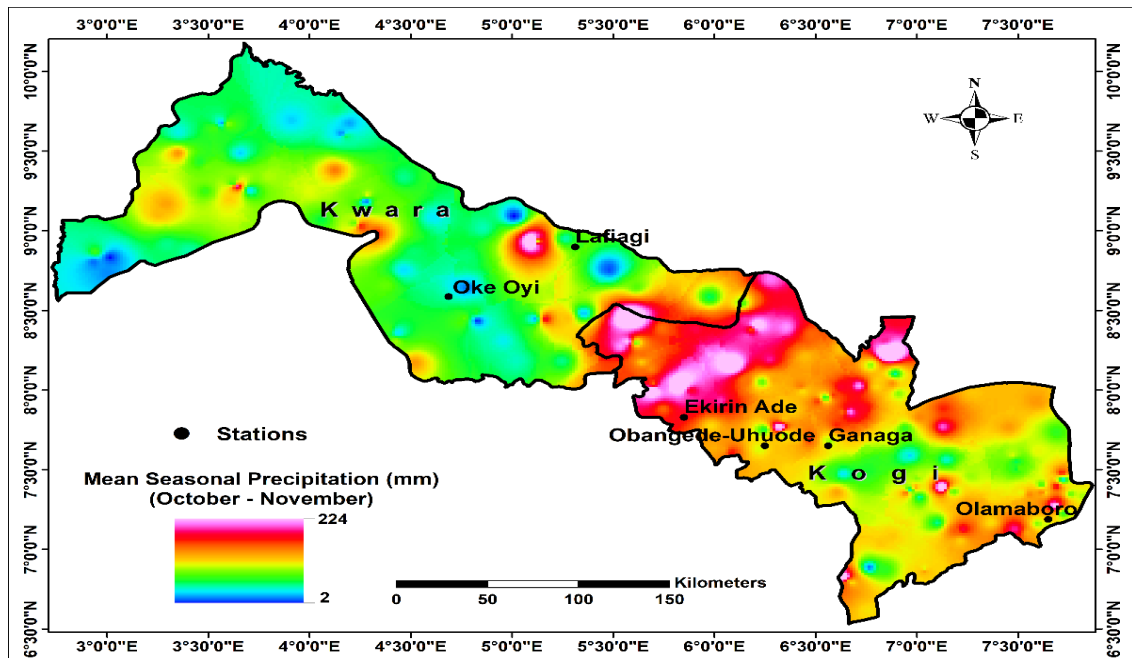


Figure 4.5d: Seasonal Spatial Rainfall (Oct-Nov)

4.4 Determination of Flood and Dry Spell using Standardised Anomaly Index

Standardized anomaly index estimation Model was employed in rainfall series to determine rainfall above normal (flood) and rainfall below normal (dry spell or drought). Station rainfall is expressed as a standardized departure i_x from the long-term mean (i.e., the mean of the base period).

Standardised anomaly index was calculated as the difference between the annual total of a particular year and the long term (first moment) average rainfall divided by second moment (standard deviation) of the long-term data. This characteristic of SAI has contributed to its popularity for application in drought monitoring and also makes possible the determination of anomalies in hydro-climatic variables. The maximum temperature standardised anomaly values is shown in Table 4.12.

Table 4.12 revealed the anomalies in maximum temperature trajectory where the positive values showed warmer than normal and negative value colder than normal. The result shows that the last fifteen (15) years have been the hottest ever. This is also in line

with World-wide temperature report which has showed global temperature increase. The implication of having warmer than normal temperature is increase in evaporation and transpiration activities which directly affect water resources over time. This may result in little dry spell and affect the growth of crops and animal production level which decreases with increase in temperature. Increase in temperature affect the distribution of rainfall spatially. Heat related hazard may manifest with increase in temperature.

Table 4.12: Maximum Temperature Standardised Anomalies for LNRB

Year	STANDARD ANOMALIES EKIRIN ADE	STANDARD ANOMALIES GANAGA	STANDARD ANOMALIES LAFIAGI	STANDARD ANOMALIES OBANGEDE	STANDARD ANOMALY OKE OYI	STANDARD ANOMALIES OLAMABORO
1979	-1.30	-1.30	-1.75	-1.26	-2.07	-1.44
1980	-0.85	-1.00	-1.03	-0.87	-0.97	-0.81
1981	-1.01	-1.08	-0.94	-1.00	-1.13	-0.81
1982	-1.44	-1.69	-1.34	-1.51	-1.23	-1.48
1983	-0.44	-0.99	-0.15	-0.78	0.34	-0.67
1984	0.31	-0.04	0.99	0.21	1.21	0.06
1985	-0.60	-0.48	-0.49	-0.45	-0.56	-0.45
1986	-0.53	-0.40	-0.26	-0.32	-0.45	-0.29
1987	0.07	-0.24	-0.05	-0.11	0.24	0.00
1988	-0.89	-1.12	-1.17	-0.95	-1.02	-0.87
1989	-0.95	-1.32	-1.17	-1.11	-1.25	-0.93
1990	0.06	0.05	0.13	0.14	0.15	0.18
1991	-0.45	-0.49	-0.25	-0.32	-0.56	-0.58
1992	-1.43	-1.62	-1.23	-1.41	-1.13	-1.47
1993	-0.72	-1.15	-0.24	-0.86	-0.24	-0.82
1994	-1.21	-1.12	-0.83	-1.26	-1.02	-0.98
1995	-0.80	-1.10	-1.43	-0.88	-1.09	-0.90
1996	-1.04	0.44	-1.03	-1.00	-0.76	-0.84
1997	-0.91	1.34	-0.60	-0.83	-0.78	-1.21
1998	0.82	0.44	0.20	0.72	0.19	0.62
1999	1.62	1.34	1.10	1.62	0.77	1.69
2000	1.03	0.71	1.85	0.94	2.11	1.13
2001	1.48	1.03	1.54	1.30	1.75	1.06
2002	1.06	1.09	1.45	1.34	1.48	1.33
2003	1.56	1.38	1.30	1.60	1.16	1.35
2004	1.44	1.63	1.45	1.74	1.01	1.93
2005	1.96	1.77	1.63	1.99	1.51	2.13
2006	1.31	0.81	1.20	1.15	1.37	1.05
2007	0.67	-0.04	0.06	0.32	0.08	0.33

Table 4.12: Cont'd

2008	0.97	0.24	-0.12	0.60	0.11	0.46
2009	0.04	0.08	0.56	0.07	0.25	0.26
2010	0.74	0.51	0.81	0.61	0.34	0.88
2011	0.21	0.85	0.14	0.37	0.09	0.34
2012	-0.35	0.64	-0.49	0.04	-0.17	-0.06
2013	-0.42	0.82	0.21	0.15	0.27	-0.18

Table 4.13 below shows a summary of 6 gauging stations depicting warmer than normal. The result is same for the entire Basin where the last 15 years have been attested to be hottest. Similarly, the result revealed that 1979-1998 have been colder than normal for most years across stations within the Basin. Temperature at less than normal affect can affect animal and crop production. At higher temperature, the rate of chemical reaction increases with temperature. More minerals can be dissolved into water from surrounding rocks which increases electrical conductivity. Warm water resources may not hold less dissolved oxygen than cool water which may affect living organism in surrounding water resource.

Table 4.13: Warmer than normal maximum Temperature Standardized Anomaly.

Ekirin Ade		Olamaboro		Lafiagi		Obangede		Oke Oyi		Ganaga	
Year	σ	Year	σ	Year	σ	Year	σ	Year	σ	Year	σ
2005	1.96	2005	2.18	2006	1.20	2005	1.99	2006	1.37	2005	1.77
2004	1.44	2004	1.25	2005	1.62	2004	1.74	2005	1.51	2004	1.63
2003	1.56	2003	1.35	2004	1.45	2003	1.60	2004	1.01	2003	1.38
2002	1.31	2002	1.33	2003	1.29	2002	1.34	2003	1.16	2002	1.09
2001	1.43	2001	1.05	2002	1.45	2001	1.30	2002	1.48	2001	1.03
2000	1.66	2000	1.12	2001	1.54	2000	0.94	2001	1.75	2000	0.71

σ = warmer than normal

Table 4.14: Colder than Normal maximum Temperature Standardized Anomaly

Ekirin Ade		Olamaboro		Lafiagi		Obangede		Oke Oyi		Ganaga	
Year	β	Year	β	Year	β	Year	β	Year	β	Year	β
1994	-1.21	1995	-1.43	1997	-1.21	1989	-1.11	1989	-1.25	1989	-1.32
1992	-1.43	1992	-1.23	1994	-0.98	1988	-0.95	1988	-1.02	1988	-1.12
1988	-0.89	1989	-1.17	1992	-1.47	1983	-0.78	1985	-0.56	1983	-0.90
1982	-1.43	1988	-1.17	1989	-0.93	1982	-1.51	1982	-1.23	1982	-1.69
1981	-1.01	1980	-1.03	1982	-1.48	1981	-1.00	1981	-1.13	1981	-1.08
1979	-1.30	1979	-1.75	1979	-1.44	1980	-0.87	1980	-0.97	1980	-1.00

β = colder than normal

The standardised anomaly for minimum temperature showed positive and negative values. The positive is warmer than normal and the negative colder than normal in the night time temperature. The Table 4.15 revealed a shift in temperature from colder than normal to warmer than normal.

Table 4.15: Minimum Temperature Standardised Anomalies for LNRB

Year	STANDARD ANOMALIES EKIRIN ADE	STANDARD ANOMALIES GANAGA	STANDARD ANOMALIES LAFIAGI	STANDARD ANOMALIES OBANGEDE	STANDARD ANOMALIES OKE OYI	STANDARD ANOMALIES OLAMABORO
1979	0.15	-0.14	-0.05	0.00	0.51	0.17
1980	-0.14	-0.16	0.19	-0.18	0.39	0.21
1981	-0.45	-0.58	-0.74	-0.50	-0.22	-0.66
1982	-0.77	-0.66	-0.52	-0.75	-0.58	-0.23
1983	-1.09	-1.23	-1.05	-1.17	-1.17	-1.47
1984	-0.97	-1.06	-0.49	-1.01	-0.80	-0.97
1985	-1.00	-0.91	-0.73	-0.94	-0.78	-1.02
1986	-0.92	-0.75	-0.57	-0.82	-0.50	-0.39
1987	0.81	0.75	1.15	0.74	1.60	1.02
1988	0.67	0.67	0.81	0.63	1.04	1.19
1989	-2.25	-2.35	-2.26	-2.32	-2.44	-2.23
1990	0.60	0.61	0.73	0.60	0.62	0.68
1991	0.37	0.16	0.55	0.23	0.87	0.55
1992	-1.91	-2.17	-2.28	-2.05	-2.44	-1.92
1993	-0.60	-0.78	-0.23	-0.73	-0.33	-0.57
1994	-0.70	-0.77	-0.47	-0.74	-0.52	-0.30
1995	0.10	-0.12	-0.25	-0.05	-0.16	0.03
1996	-0.16	-0.22	-0.88	-0.22	0.57	-0.19
1997	-0.21	-0.55	-0.69	-0.41	-0.60	-0.61
1998	0.40	0.36	-0.30	0.38	-0.50	-0.10
1999	0.78	0.68	0.84	0.74	0.82	0.37
2000	-0.22	-0.47	-0.80	-0.29	-1.29	-1.74
2001	0.49	0.31	-0.32	0.36	-0.56	-0.33
2002	0.59	1.53	0.90	0.67	0.45	0.03
2003	1.52	1.68	1.53	1.51	1.15	1.37
2004	1.30	1.85	0.73	1.49	0.47	1.41
2005	1.84	1.58	1.59	1.90	1.25	1.47
2006	1.59	0.22	1.63	1.62	1.02	1.64
2007	0.38	0.22	0.14	0.29	-0.25	0.10
2008	0.18	0.11	-0.58	0.14	-1.05	-0.04
2009	1.11	1.21	1.73	1.18	1.21	1.25
2010	1.53	1.52	1.23	1.52	1.37	1.64
2011	-1.57	-0.83	-1.13	-1.23	-0.50	-0.81
2012	-1.14	-0.29	-0.21	-0.74	0.07	-0.22
2013	-0.30	0.58	0.81	0.14	1.27	0.69

Minimum temperature also depicted similarity in pattern with maximum temperature. It showed colder than normal from 1979-1998 and transited to warmer than normal from 1999 to 2013. This revealed increase in temperature during the day and night could be as a result of climate change effect on the Basin. Table 4.16 shows minimum temperature standardised anomaly of 6 gauging stations from 1979 -2013. The pattern painted shows warmer period from 1999 to 2011 and colder from 1980 to 1997.

Table 4.16: Summary Six years Warmer than Normal Minimum Temperature Standardized Anomaly.

Ekirin Ade		Olamaboro		Lafiagi		Obangede		Oke Oyi		Ganaga	
Year	σ	Year	σ	Year	σ	Year	σ	Year	σ	Year	σ
2010	1.53	2013	0.69	2010	1.23	2010	1.52	2010	1.37	2010	1.52
2009	1.11	2010	1.64	2006	1.63	2009	1.18	2009	1.21	2009	1.21
2008	0.18	2009	1.24	2005	1.58	2006	1.62	2006	1.02	2005	1.58
2007	0.38	2007	0.10	2004	0.73	2005	1.90	2005	1.25	2004	1.85
2006	1.59	2005	1.64	2003	1.53	2004	1.49	2003	1.15	2003	1.68
2005	1.83	2004	1.47	1987	1.15	2003	1.51	2002	0.45	2002	1.53

σ = warmer than normal

Table 4.17: Summary of Six years Colder than Normal Minimum Temperature Standardized Anomaly.

Ekirin Ade		Lafiagi		Olamaboro		Obangede		Oke Oyi		Ganaga	
Year	β	Year	β	Year	β	Year	β	Year	β	Year	β
1997	-0.21	2011	-1.13	2000	-1.74	1989	-2.32	2008	-1.05	2012	-1.14
1994	-0.71	1992	-1.28	1997	-0.61	1986	-0.82	2000	-1.29	2011	-1.57
1992	-1.91	1989	-2.26	1993	-0.57	1985	-0.94	1989	-2.44	1992	-1.91
1989	-2.25	1987	-0.57	1992	-1.92	1984	-1.01	1986	-0.50	1989	-2.25
1986	-0.92	1986	-0.73	1989	-2.23	1983	-1.17	1985	-0.78	1986	-0.92
1985	-1.00	1983	-1.05	1985	-1.02	1982	-0.75	1984	-0.80	1985	-1.00

β = colder than normal

The standardised anomaly of rainfall within the LNRB revealed positive and negative anomaly (little dry spell or drought and wetter than normal or flood). Rainfall anomaly showed correlations in behavior across the Basin. The points at which the anomaly is positive indicates wetter than normal rainfall which is by the upward bars while negative anomalies (downward bars) shows rainfall below normal (Little Dry Spell).

Figure 4.6 show the trend of rainfall and it is evident that there were positive anomalies from 1979 to 1997 in rainfall variability within the Basin. This transition could be as a result of climate change effect on the Lower Niger River Basin.

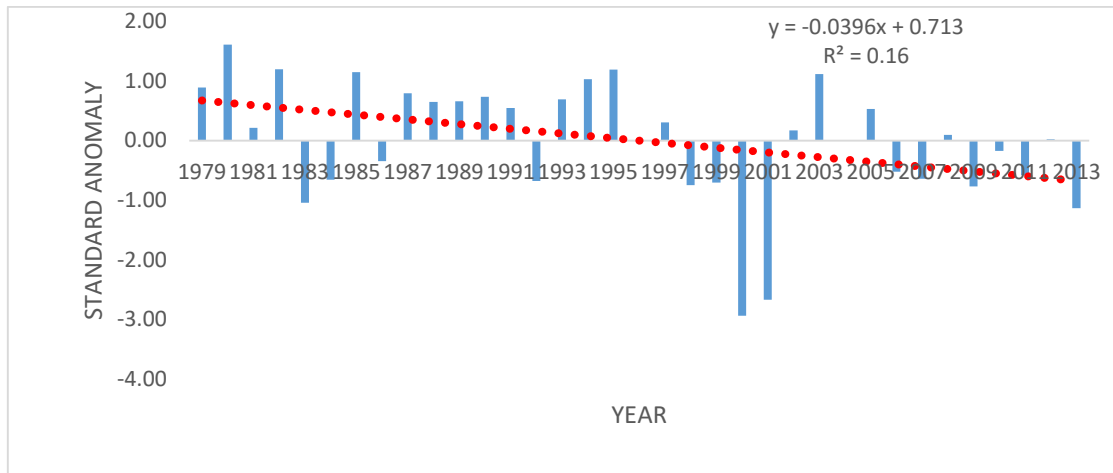


Figure 4.6: Rainfall Standardised Anomaly of Oke Oyi from 1979-2013

The standardised anomaly of rainfall also depicted positive and negative values. The positive values shows more rainfall than normal which may result in flash flooding within the Basin. The negative values depicted less rainfall which could result in little dry spell (drought). Table 4.18 shows the anomaly value of the six meteorological stations.

Table 4.18: Rainfall Standardized Anomalies values for the LNRB

Year	EKIRIN ADE	GANAGA	LAFIAGI	OBANGEDE	OKE OYI	OLAMABORO
1979	0.5	-0.19	1.44	0.89	0.89	-0.34
1980	0.5	0.53	1.09	1.61	1.61	0.05
1981	-0.11	-0.2	0.51	0.21	0.21	0.11
1982	1.95	1.68	1.25	1.2	1.2	2.21
1983	-1.36	-1.13	-0.68	-1.05	-1.05	-0.37
1984	-0.25	0.06	-0.6	-0.65	-0.65	0.67
1985	0.51	0.69	1.65	1.15	1.15	1.03
1986	-1.19	-1.2	0.06	-0.34	-0.34	-1.16
1987	-0.27	-0.32	0.37	0.8	0.8	0.04
1988	-0.14	0.17	0.72	0.65	0.65	0.39
1989	0.37	0.14	1.04	0.66	0.66	0.67
1990	0.9	0.11	-0.21	0.74	0.74	0.05
1991	0.67	0.36	0.03	0.55	0.55	1
1992	0.26	0.46	-0.56	-0.68	-0.68	0.33
1993	0.77	-0.17	-0.21	0.69	0.69	-0.33
1994	0.7	0.46	1.07	1.03	1.03	-0.14
1995	1.8	2.05	0.98	1.19	1.19	1.47
1996	0.27	0.6	0.1	0	0	0.32
1997	0.31	-0.28	-0.12	0.31	0.31	0.05
1998	0.01	0.14	-0.41	-0.75	-0.75	0.26
1999	-0.98	-0.54	-1.09	-0.71	-0.71	-0.69
2000	-3.08	-2.59	-2.95	-2.94	-2.94	-3.03
2001	-2.02	-1.57	-2.49	-2.67	-2.67	-1.83
2002	-0.52	-0.02	0.39	0.17	0.17	-0.72
2003	-0.17	0.41	1.63	1.12	1.12	0.09
2004	1.3	1.3	0.15	0	0	0.87
2005	-0.49	-0.54	0.24	0.53	0.53	-0.62
2006	-0.75	-0.24	-0.06	-0.52	-0.52	-0.76
2007	-0.34	0.34	-0.44	-0.64	-0.64	0.43
2008	1.14	2.35	-0.47	0.09	0.09	1.88
2009	0.67	0.95	-0.93	-0.77	-0.77	0.89
2010	0.35	0.05	-0.05	-0.18	-0.18	0.11
2011	-0.75	-1.39	-0.82	-0.58	-0.58	-1.26
2012	-0.33	-1.2	0.34	0.02	0.02	-0.82
2013	-0.22	-1.28	-0.95	-1.14	-1.14	-0.85

Table 4.19 shows the summary of the numbers of years with more rainfall (flooding) and less rainfall (dry spell) in percentage of years. The rainfall standardized anomalies result showed that Ekirin Ade and Lafiagi depicted similarity in rainfall. From the table

4.19 above, these two stations showed 51% rainfall above normal (flood) and 49% less than normal (dry spell). Similarly, Obangede and Oke Oyi result showed that within 35 years, rainfall above normal were 19 years, little dry spell was 14 years and 2 years of normal rainfall. Ganaga had 19 years of rainfall above normal and 16 years of less rainfall. The result showed 80% colder than normal in the first and second decades and transited to warmer than normal in the last 15years. The switch portends a disturbing situation as it comes with health-related hazards. The warmer than normal temperature will affect water resources requirement and agricultural planning.

Table 4.19: summary of wetter years and little dry spell of rainfall from 1979-2013 in the LNRB

Station	Data size (year)	Wetter years	Less rainfall years	Normal	% wetter (above normal) years	% Less rainfall than normal (years.)	% normal
Ekirin Ade	35	18	17	Nil	51	49	Nil
Ganaga	35	19	16	Nil	54	46	Nil
Lafiagi	35	18	17	Nil	51	49	Nil
Obangede	35	19	14	2	54	40	6
Oke Oyi	35	19	14	2	54	40	6
Olamaboro	35	21	14	Nil	60	40	Nil

4.5 Regionalisation of Rainfall into Coherent Zones

4.5.1 Results principal component analysis of rainfall

The entire PCs of monthly precipitation series were obtained. The result of the first six PCs Table 4.20 which are significant according to scree plot analysis (Wilks, 1995). The Eigenvalues of the six (6) locations, the results were output by validating the model developed for the PC. The six PCs explained 100% of the cumulative variance of monthly series, Considering the first three PCs is sufficient for a PC based on analysis, since the first few PCs are associated with large scale synoptic pattern over the LNRB. Moreover, the full set of principal components is as large to as the original set of

variables. The sum of the variance of the first 3 component exceed 97% of the total cumulative variance in monthly series of principal component analysis PCA as shown in Figure 4.7

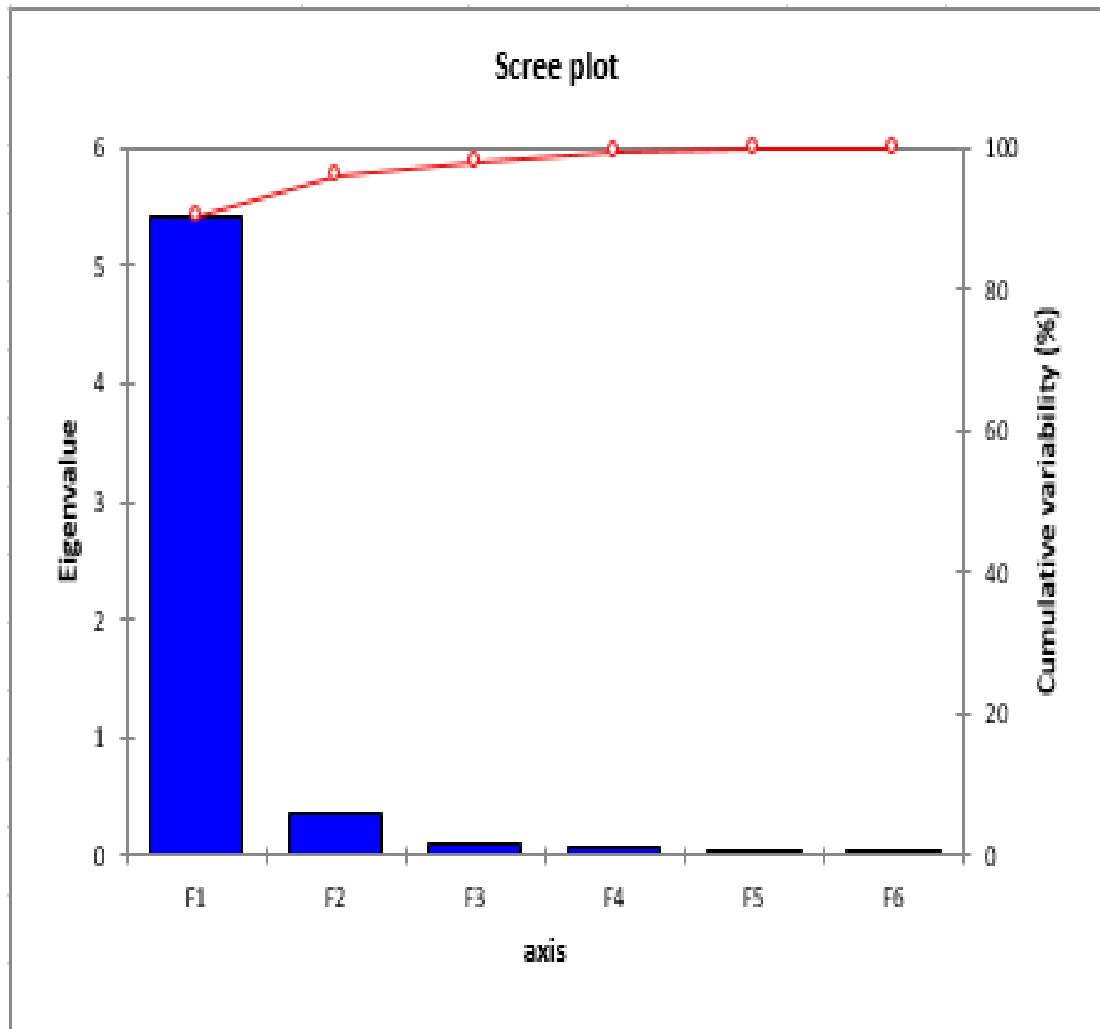


Figure 4.7: Scree Plot diagram

The principal component analysis revealed the Eigenvalue of 5.41 with a 90.3% unrotated variance explained. The varimax rotated variance of 97.98% cumulatively shows the contributions of the first three PCI's. This clearly showed that the other PCI's contribution to the variance is 2.12% and can be neglected as shown in Table 4.20

Table 4.20: Eigenvalues and Variance of the Non-Rotated first six principal components (PCs) for monthly precipitation series from 1979 - 2013

No	Unrotated Eigenvalues	Unrotated Variance Explained (VE) %	Cumulative (VE) %	Varimax rotated Eigenvalues %	Varimax rotated (VE) %	Cumulative (VE) %
1	5.4147	90.2552	-	0.5495	54.95	-
2	0.3560	5.9336	96.18	0.3865	38.65	93.60
3	0.1082	1.8034	97.98	0.0438	4.38	97.98

4.5.2 Component coefficients

The first result of the principal components function, contain the coefficients of the linear combination of the original values that generate the principal components. The coefficients are known as factor loadings. The first three PCs revealed the contributions of the PC as Table 4.21.

According to PCA, the first Empirical Orthogonal Function (EOF) explained of the total variance. The first principal component (PC1) show variation. (Table 4.21) affecting the region as a whole, with maximum loading at the center of the Basin, hence represents rainfall i.e., all places wet or all places dry. All factor exhibits positive correlation with the principal component. The correlation coefficient between the precipitation at any point and the principal component is obtained from the product of the factor loading and square root of the eigenvalue.

The second PC2 show variation (Figure. 4.21b) west and east of a zero-line extending from the northern part of the Basin to the southern part. The second PC2, (EOF) explained 5.93% and component coefficient show positive and negative

The 3rd PC3 explained only 1.80% of variance.

Table 4.21: Principal Components Coefficients of the LNRB Rainfall Series.

Station	PC1	PC2	PC3
Obangede	0.4196	-0.2992	-0.2643
Oke Oyi	0.3997	0.4881	-0.3739
Olamaboro	0.4091	-0.2662	0.6948
Ganaga	0.4189	-0.2706	0.1181
Lafiagi	0.3852	0.6783	0.2982
Ekirin Ade	0.4160	-0.2610	-0.4525
Cumulative Variance			
%	90.25	5.93	1.8034

The geographical distribution pattern of loading of the first three principal component (PC1) computed for monthly rainfall total series of the six stations within the LNRB are shown in Figure 4.8

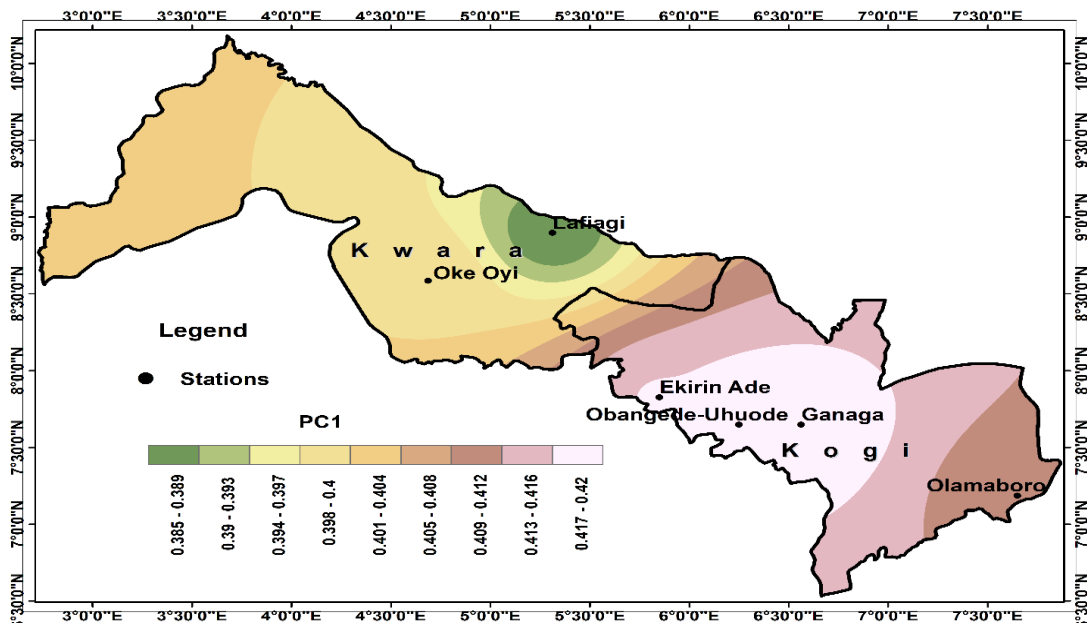


Figure 4.8 Principal Component 1

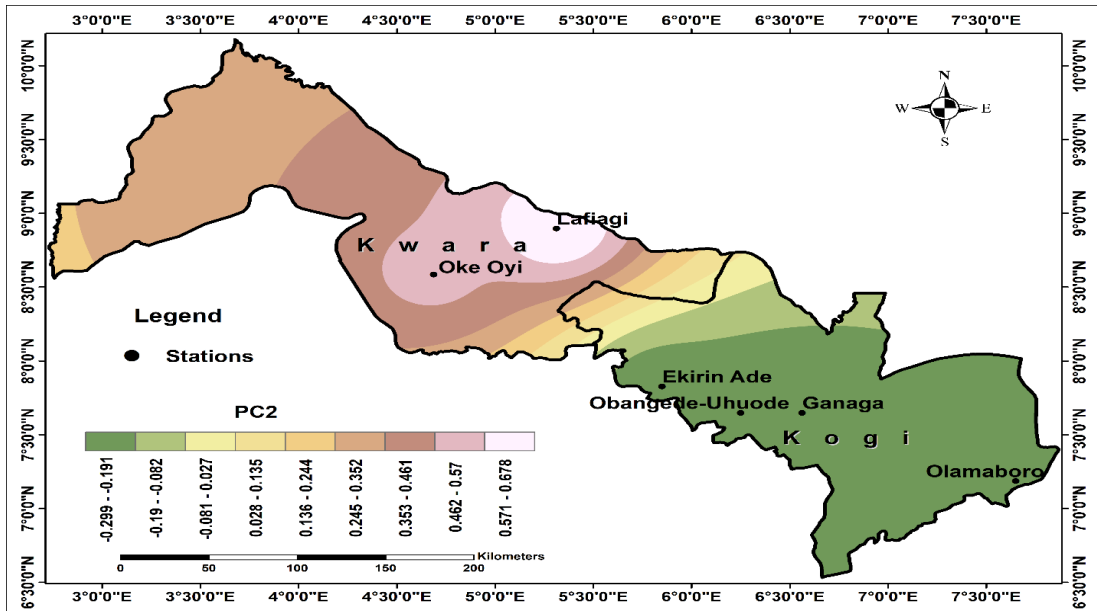


Figure 4.9: Principal Component 2

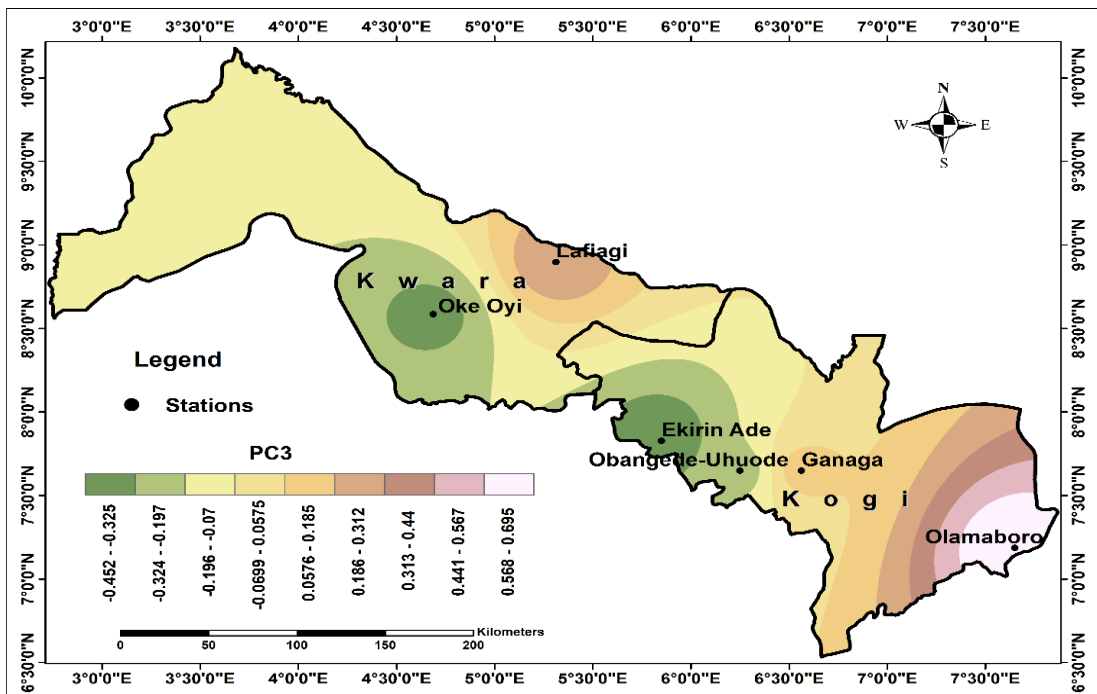


Figure 4.10: Principal Component 3

To investigate the relationship among variables as shown in Figure 4.7 each variable (station) can be represented by the factor loadings for two principal components (dimensions). All variables are plotted with respect to the PC1 and PC2 and shows positive correlation with the PC1 and PC2. From the figure, Lafiagi and Oke Oyi are

correlated with 38.65% of variance, while Ekirin Ade, Ganaga, Obangede and Olamaboro are strongly correlated with 54.95% of variance as shown in Table 4.22.

Table 4.22:Factor loading

	D1	D2	D3
Obangede	0.8713	0.4744	0.0913
Oke Oyi	0.5493	0.8140	0.0203
Olamaboro	0.7870	0.4553	0.3964
Ganaga	0.8381	0.4790	0.2138
Lafiagi	0.4154	0.8681	0.2253
Ekirin Ade	0.8613	0.4908	0.0277

The factor loading map D1 and D2 shows the relationship among variables. Factor loading D3 was not consider in the cluster analysis because it magnitude was less than 0.400. The loading map after varimax rotation are shown in Figure 4.11and 4.12 respectively.

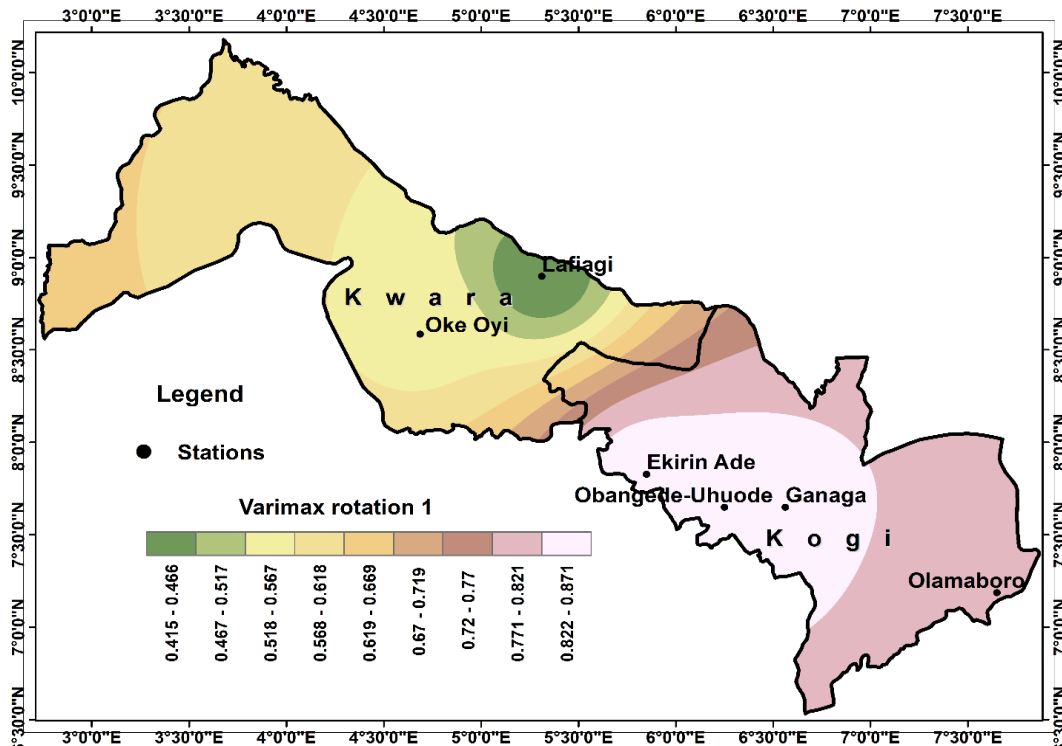


Figure 4.11: Factor Loading D1

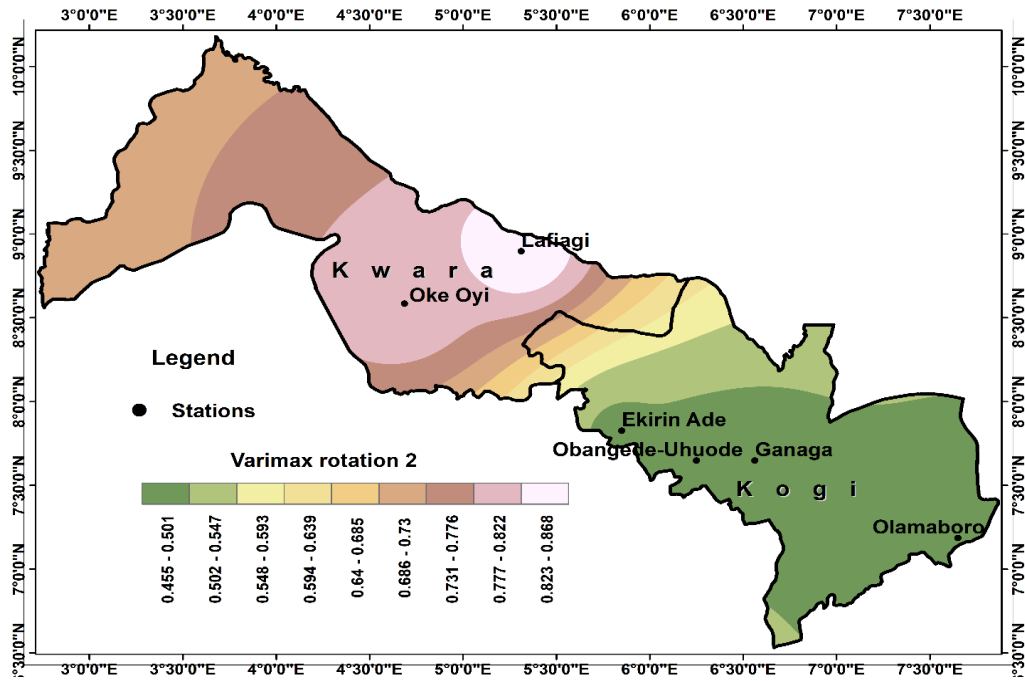


Figure 4.12: Factor Loading D2

The biplot map shows how data are clustered after varimax rotation. Factor loading D1 shows 54.95% contribution and D2 38.65% as shown in Figure 4.13. Variable axes D1 and D2 contributing 93.60% after varimax rotation. From Figure 4.14 four clusters namely; Obangede, Ganaga, Olamaboro and Ekirin Ade depicts stronger relationship than Lafiagi and Oke Oyi. The six stations cluster are within the 1st quadrant as shown in Figure 4.15

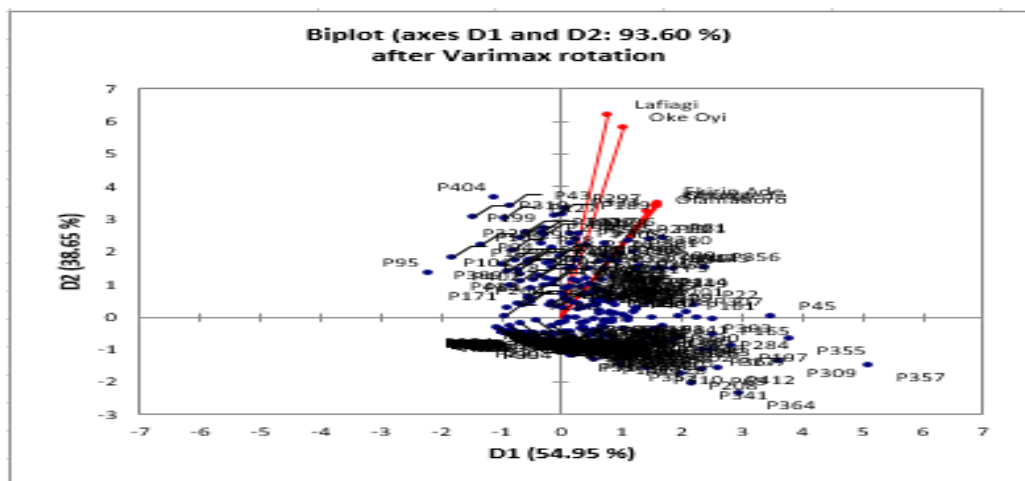


Figure 4.13: Biplot Map

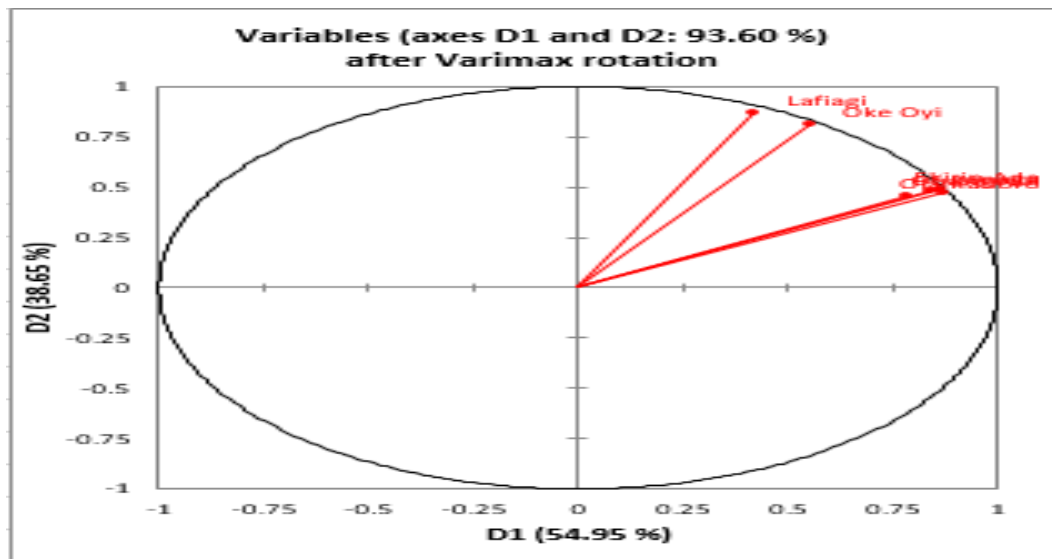


Figure 4.14: Correlation of stations

4.6 Regionalisation of Coherent Rainfall

The characteristics of rotated PCs is used to delineate coherent homogeneous region of rainfall variation over the study area. By selecting a loading magnitude for which sharp gradient on different rotated PC. A loading Magnitude of 0.4 was used for delineation of homogeneous zones.

The factor loading D1 and D2 was analysed using the K-means Cluster analysis. D3 was not consider because it has less than 0.4000 in magnitude. K-means cluster analysis showed 2 clusters; cluster 1 has four stations or observations while cluster 2 has two stations/observations as shown in Table 4.23 and cluster centroid of D1 and D2 in Table 4.24 and Table 4.25

Table 4.23: Cluster Analysis

Variables	No of Stations	Cluster sum of Squares	Average (mm) distance from centroid	Maximum (mm) distance from centroid
D1	4	0.084	0.127	0.221
D2	2	0.031	0.125	0.125

Table 4.24: Cluster Centroid (mm)

Variable	Cluster 1	Cluster 2	Grand Centroid
D1	0.8394	0.4824	0.7204
D2	0.4749	0.811	0.5969

Table 4.25: Distance between Cluster Centroids (mm)

Cluster 1	0.0000	0.5149
Cluster 2	0.5149	0.0000

The final partition of k-means clustering analysis of D1 and D2 revealed that the LNRB is categorised as one coherent homogeneous zone as shown in Table 4.26

Table 4.26: Final Partition

Cluster	No of observations/stations	Within Cluster sum of squares	Average distance from centroid (mm)	Maximum distance from centroid (mm)
1	6	0.469	0.268	0.413

CHAPTER FIVE

5.0 CONCLUSION AND RECOMMENDATIONS

5.1 Conclusion

Analysis of distribution, variability, trend of maximum & minimum temperature and rainfall of over 35-years data from the LNRB revealed the following;

The Standard Normal Homogeneity Test was employed for homogeneity, from the result, statistical homogeneity was found among the gauging station for rainfall. Maximum temperature depicted Inhomogeneity. Similarly, minimum temperature depicted inhomogeneity except at Oke Oyi where the computed p-value was > 0.05 significance level.

Geographical Autocorrelation test was used to test for relationship among the stations in rainfall and temperature (maximum & minimum). A positive correlation was found in all stations for maximum temperature, minimum temperature and rainfall.

The result of Mann- Kendall MK trend analysis showed statistically insignificant (increasing or decreasing) in annual data for maximum, minimum and rainfall respectively. However, the monthly Mann-Kendall (Z) trend analysis showed increasing or decreasing trend in rainfall, maximum temperature and minimum temperature.

The Sen's slope estimator was employed to determine the change per unit time of trend in rainfall, maximum temperature and minimum temperature. The results showed a change in magnitude of slope in the time series.

The spatial variability of the annual rainfall of the stations showed spatial variability of rainfall across the stations within the Basin. Ekirin Ade and Obangede recorded highest mean annual rainfall amount ($R_r \geq 1780$ mm) for a period of 1979-2013. Areas of

lowest rainfall amount are found around Oke Oyi and Lafiagi with annual ranging from 1120.5 mm to 1200 mm. respectively.

It could be concluded that standardised anomaly showed a shift in temperature from colder than normal for the last 2 decades to warmer than normal. This shift provides a disturbing trend in climate parameters trajectory which could result in heat related hazards, water resources management and agricultural planning. From discussion in anomaly of rainfall, it was discovered that the last 15-years has experience more rain than normal. The results depicted more flood within the Basin.

The varimax rotation of PCs simplifies the loading structure which has been used to regionalise monthly rainfall of the Basin. However, the k-clustering analysis revealed that the Lower Niger River Basin is one coherent homogeneous zone.

5.2 Recommendations

The following recommendations are given below;

- i. Climate change is known to be affecting rainfall and temperature variability in space and time; therefore, using more advance statistical software, spatial temporal analysis should be conducted to reveal spatial variability anomalies and action taken to mitigate the effect.
- ii. Further research is needed in combination with advanced statistical modeling for micro or macro scale climate change risk management and adaptation planning within the LNRB.

5.3 Contribution to Knowledge

Based on the conclusion drawn, the study has contributed in the following measures;

- a) The entire LNRB has been divided into 1 coherent homogeneous rainfall zones.

- b) Temperature transition from colder to warmer conditions may result to heat related mortality/hazards and attendant water resource challenge
- c) The research of the study can be used as basis for climate change impact in LNRB.

REFERENCES

- Adefolalu, D. O. (1986). Further Aspects of Sahelian Drought as Evidenced from Rainfall Regime of Nigeria. *Arch. Meteorology. Geophysical. Bioclimatology Service*. B 36, 277–295.
- Adefolalu, D. O. (2007). Climate Change and Economic Sustainability in Nigeria, Paper Presented at the *International Conference on Climate Change and Economic Sustainability held the Nnamdi Azikiwe University, Enugu, Nigeria*. 12-14
- Adepitan, J. O., Falayi, E. O. & Ogunsanwo, F. O. (2017). Confirmation of climate change in southwestern Nigeria through analysis of rainfall and temperature variations over the region. *Covenant Journal of Physical and Life Sciences*, 5(1), 20-39
- Afangideh, I., Ekpe, A. & Offiong, A. (2013). Implications of Changing Rainfall Pattern on Building Loss in Calabar. *International Journal of Innovative Environmental Research*, 1(2), 10-18.
- Ankrah, J. (2018). Climate change impacts and coastal livelihoods; an analysis of fishers of coastal Winneba, Ghana. *Ocean Coast Management*. 161, 141-146.
- Arnell, N. W., Lowe, J. A., Challinor, A. J. & Osborn, T. J. (2019). Global and regional impacts of climate change at different levels of global temperature increase. *Climatic Change*, 1553, 377-391.
- Ati, O. F., Abaje, I. B & Ishaya, S. (2009). Nature of potable water supply and demand in Jema'a Local Government Area of Kaduna State, Nigeria. *Research Journal of Environmental and Earth Sciences*, 1(1), 16-21.
- Austin A. T; Yahdjian, L; Stark J.M.; Belnap J.; Porporato A.; Norton U.; Ravetta D.A. and Schaeffer SM (2004). Water Pulses and Biogeochemical Cycles in arid and Semiarid Ecosystems. *Oecologia* 141, 221-235
- Ayansina A. & Ogunbo, S. (2009). GIS Approach in Assessing Seasonal Rainfall Variability in Guinea Savanna Part of Nigeria, *7th FIG Regional Conference, Vietnam*, 16, 19-22
- Babatolu, J.S. & Akinnubi, R.T. (2013). Surface Temperature Anomalies in the River Niger Basin Development Authority Areas, Nigeria. *Atmospheric and Climate Sciences*, 3, 532-537. <https://doi.org/10.4236/acs.2013.34056>
- Chandler, R.E. & Scott, E. M. (2011). Statistical Methods for Trend Detection and Analysis in the Environmental Sciences, *John Wiley & Sons, Ltd*, 39-47, ISBN 978-0-470-01543
- Chatfield (2003). Climate Change or Climate fluctuation? *Journal Arid Environs* 1(1), 18-33
- Chow V. T. (1994). Engineering Analysis of Hydrological Data with special Application to Rainfall Intensity *Uni. Of Illinois Engineering. Experiment Station, Bulletin* 414, 23-42

- Collins, N., Jones, S., Nguyen, T. H. & Stanton, P. (2017). The contribution of human capital to a holistic response to climate change: learning from and for the Mekong Delta, Vietnam. *Asia Pacific Business Review*, 23(2), 230-242.
- Cronin, J., Anandarajah, G., & Dessens, O. (2018). Climate change impacts on the energy system: a review of trends and gaps. *Climatic change*, 151(2), 79-93.
- De Jesus, A. L., Thompson, H., Knibbs, L. D., Kowalski, M., Cyrus, J., Niemi, J. V., & Morawska, L. (2020). Long-term trends in PM_{2.5} mass and particle number concentrations in urban air: The impacts of mitigation measures and extreme events due to changing climates. *Environmental Pollution*, 263, 34-51
- Dinpashoh Y., Jhajharia D., Fakheri-Fard A., Singh VP., Kahya E. (2011) “Trend in Reference Crop Evapotranspiration over Iran. *Journal Hydrology*, 399, 422-433
- Easterling, D. R. (1997) Maximum and Minimum Temperature Trends for the *Global Science* 277, 364–367.
- Fan, J. & Lv, J. (2010). A selective overview of variable selection in high dimensional feature space. *Statistica Sinica*, 20(1), 101-103
- Forland, E. J. (1994). “Trends and Problems in Norwegian Snow Records”, in Heino, R. (Ed), *Climate Variations in Europe, Proceedings of the European Workshop held in Kirkkonummi (Majvik), Finland 15-18 May (1994). Publications of the Academy of Finland*, 94, 205-215.
- Funk, C., Rowland, J., Eilerts, G., Kebebe, E., Biru, N., White, L., and Galu, G., (2012). A Climate Trend Analysis of Ethiopia, U. S. Geological Survey Fact Sheet 6, 2012-3053.
- Gauthier, T. D. (2001). Detecting Trend using Spearman’s Rank Correlation Coefficient. *Environmental Forensics*, 2, 359-362, ISBN 1527-5930
- Goovaerts P. (2000). Geostatistical Approaches for Incorporating Elevation into the Spatial Interpolation of Rainfall. *Journal Hydrology*. (Amsterdam, Neth.), 228, 113-129.
- Hasanean, H. M. (2001). Fluctuations of Surface Air Temperature in the East Mediterranean. *Theoretical Applied Climatology*. 68(1), 75–87
- Hayes, M.J., Svoboda, M.D., Wihite, D.A. & Vanyarkho, O.V., (1999). Monitoring the 1996 drought using the standardized precipitation index. *Bulletin of the American meteorological society*, 80(3), 429-438
- Helsel, D. R. & Hirsch, R. M. (1992). *Statistical Methods in Water Resources*, Elsevier, ISBN 0-444-81463-9, Amsterdam.
- Hirsch, R. M., Slack, J. R. & Smith, R. A. (1982). Techniques of trend analysis for monthly water quality data. *Water resources research*, 18(1), 107-121.
- IPCC, (2005). *Climate change 2005. Physical Science basis (summary for policy makers)*, 4, 9-10

- IPCC, (2007). Climate Change and World Food Security: A New assessment, Global Environmental Change 9, S51–S67
- Jolliffe, I. T. (1990). Principal component analysis: a beginner's guide—I. Introduction and application. *Weather*, 45(10), 375-382.
- Kaiser, H. F. (1959). Computer program for varimax rotation in factor analysis. *Educational and psychological measurement*, 19(3), 413-420.
- Karl, T. R., Janes, P. D., Knight, R. W., Kukla, J., Plummer, N., Razuvayev, V., Gallo, K. P., Lindesay, J., Charlson, R. J. & Peterson, T. C. (1993). Asymmetric Trends of Daily Maximum and Minimum Temperatures: Empirical Evidence and Possible Causes. *Bull American Mathematics Society*. 74, 1007–1023.
- Kendall, M. & Ord, J.K. (1990). Time series, 3rd Edition, Edward Arnold, London
- Kundzewicz, Z., W. & Robson, A. J. (eds.) (2000). Detecting Trend and other Changes in Hydrological Data World Climate Programme-Water, World Climate Programme Data and Monitoring, WCDMP-45, WMO/TD (1013), *World Meteorological Organization, Geneva, Switzerland*
- Kunkel, K. E., Easterling, D.R. Redmond, K., & Hubbard, K., (2003). Temporal Variation of Extreme Precipitation Events in the United States; 1895-2000. *Geophysical Research letters*, 30, 17-19
- Lee, T., Son, C., Kim, M., Lee, S., & Yoon, S. (2020). Climate Change Adaptation to Extreme Rainfall Events on a Local Scale in Namyangju, South Korea. *Journal of Hydrologic Engineering*, 25(5), 5-10
- Lin, Y., Liu, Z., Luan, H., Sun, M., Rao, S., & Liu, S. (2015). Modeling relation paths for Representation learning of knowledge bases. *ArXiv preprint arXiv: 6-7, 1506.00379*.
- Meissner K, Weaver A, Matthews H, Cox P (2003). The Role of Land Surface Dynamics in Glacial Inception: A Study with the UVic Earth System Model. *Climate Dynamics*. 21, 515–537
- Montgomery, D. C., Peck, E. A. & Vining, G. G. (2001). *Introduction to Linear Regression Analysis*, 3rd Edition, John Wiley & Sons, New York.
- Mukwada, G. & Manatsa, D. (2018). Is climate change the Nemesis of rural development: An analysis of patterns and trends of Zimbabwean Drought. In *Climate change, extreme events and disaster risk reduction*, 1, 173-182). Springer, Cham.
- Nalder, I. A. & Wein, R. W. (1998). Spatial interpolation of climatic normals: test of a new method in the Canadian boreal forest. *Agricultural and forest meteorology*, 92(4), 211-225.
- Nicholson, S. E. (2013). The West African Sahel: A review of recent studies on the rainfall regime and its interannual variability. *International Scholarly Research Notices*,

- Ning, J., Liu, J., Kuang, W., Xu, X., Zhang, S., Yan, C. & Ning, J. (2012). Spatiotemporal patterns and characteristics of land-use change in China during 2010–2015. *Journal of Geographical Sciences*, 28(5), 547-562.
- Obasi GOP 1965. Atmospheric Synoptic Climatological Features over the West African Region. *Nigerian Meteorological Service Technical Note*. Number 28.
- Obot, N. I. Chendo, M.A.C., Udo S. O. & Ewona I. O. (2012). Evaluation of Rainfall Trend in Nigeria for about 30 years (1978-2007). *International journal of physical science* 5 (14), 2217-2222.
- Obot, N. I., Chendo, M. A. C., Udo S. O. & Ewona, I. O. (2010). Evaluation of Rainfall Trends in Nigeria for 30 years (1978-2007). *International Journal of the Physical Sciences* 14, 2217-2222,
- Odekunle, T. O. (2001). The magnitude – Frequency Characteristic of Rainfall in Ondo, Southwestern Nigeria. *Ife Research Publications in Geography*, 8, 36 – 41.
- Office of the Surveyor General of the Federation (2010).
- Oguntunde, P. G., Abiodun, B. J. & Lischeid, G. (2011). Rainfall trends in Nigeria, 1901–2000. *Journal of Hydrology*, 411(3-4), 207-218.
- Olaniran, O J (1983). Flood Generating Mechanism at Ilorin, Nigeria. *GeoJournal*, 7. 271 – 279.
- Ologunorisa, E. T. (2004). Rainfall Flood Prediction in the Niger Delta, Nigeria (Abstract), *International Conference in Hydrology: Science and Practice for the 21st Century*, London, U.K.
- Oriola, E. O. (1994). Strategies for Combating Urban Flooding in a Developing Nation: A Case Study of Ondo, Niger. *The Environmentalist* 14, 57-62
- Osang, J. E., Ewona, I. O., Obi, E. O., Udoimuk, A. B., & Kamgba, F. A. (2013). Analyses of radiation and rainfall pattern In Kano State Northern Nigeria (1978-2007). *International Journal of Scientific & Engineering Research*, 4(9), 10-25
- Peike R. A. & Doesken N. (2008). Climate of the Shortgrass Steppe. In: Lauenroth W, Burke I. (eds) *Ecology of the Shortgrass Steppe*. Oxford University Press, New York, 14-29
- Peralta-Hernandez, A. R., Balling Jr, R. C., & Barba-Martínez, L. R. (2009). Comparative analysis of indices of extreme rainfall events: Variations and trends from southern México. *Atmósfera*, 22(2), 219-228.
- Pettit, R. D. (1979). Effects of picloram and tebuthiuron pellets on sand shinnery oak communities. *Rangeland Ecology & Management/Journal of Range Management Archives*, 32(3), 196-200.
- Prober, S. M., Colloff, M. J., Abel, N., Crimp, S., Doherty, M. D., Dunlop, M., & Williams, K. J. (2017). Informing climate adaptation pathways in multi-use woodland landscapes using the values-rules-knowledge framework. *Agriculture, Ecosystems & Environment*, (241), 39-53.

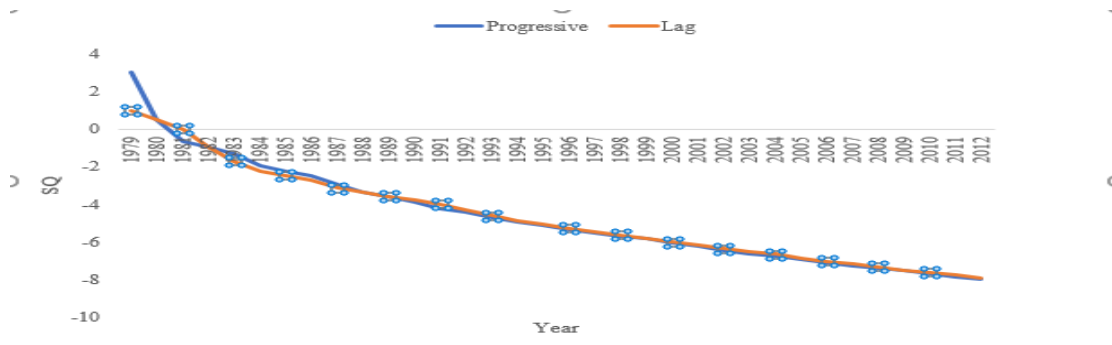
- Rakib Z. (2018). Characterisation of Climate Change in Southwestern Bangladesh: “Trend Analysis of Temperature, Humidity, Heat Index and rainfall” *Climate Research*, 1, 1-29
- Rakib Z. (2013). Extreme Temperature Climatology and Evaluation of Heat Index in Bangladesh during 1981-2010. *J. Presidency Univ.* 2(2), 84-95
- Ratnayake, U. & Herath S. (2005). Changing Rainfall and its Impact on Land Slides in Sri Lanka, *Journal Mou. Science.* 2(3), 218-224
- Rhoades, D. A. & Salinger, M. J. (1993). “Adjustment of Temperature and Rainfall Records for Site Changes” *International Journal Climatology.* 13, 899-913
- Richman M. B. (1986). Rotation of principal components. *Journal of climatology* 6, 293-335
- Sarwar Md. H., Kushal, R. & Dilip K. D. (2014). Spatial and Temporal Variability of Rainfall over the South West Coast of Bangladesh. *Journal Climate*, 2, 28-46
- Semazzi, R. T, (2010). The Magnitude of Decadal and Multidecadal Variability in North America Precipitation. *Journal Climate*, 23, 842-850
- Sen, P. K. (1968). Estimates of the regression coefficient based on Kendall's tau. *Journal of the American statistical association*, 63(324): 1379-1389.
- Shahid, S. (2011). Trends in Extreme Rainfall events of Bangladesh. *Theoretical and applied Climatology*, 104(3), 489-499
- Snyder, P.K., Delire, C. & Foley, J.A. (2004). Evaluating the Influence of Different Vegetation Biomes on the Global Climate. *Climate Dynamics.* 23, 279–302.
- Srinivas, V. (2013). Regionalization of precipitation in India—a review. *Journal of the Indian Institute of Science*, 93(2), 153-162.
- Tabari, H. & Talaei, P. H. (2011). Temporal variability of precipitation over Iran: 1966–2005. *Journal of Hydrology*, 396(3-4), 313-320.
- Tarhule, A. & Woo, M. K. (1998). Changes in Rainfall Characteristics in Northern Nigeria. *International Journal Climatol.* 18, 1261-1271.
- Tatli, H., Dalfes, H. N. & Menteş, Ş. S. (2005). Surface air temperature variability over turkey and its connection to large-scale upper air circulation via multivariate techniques. *International Climatology Journal*, 25(3), 331-350.
- Tayanc, M., Baltaci, H. & Oktay Akkoyunlu, B. (2019). Atmospheric conditions of extreme precipitation events in western Turkey for the period 2006-2015
- Tigchelaar, M., Battisti, D. S., Naylor, R. L. & Ray, D. K. (2018). Future warming increases probability of globally synchronized maize production shocks. *Proceedings of the National Academy of Sciences*, 115(26), 6644-6649.
- Turkes, M., Sumer, U.M. & Demir, I. (2002) Re-evaluation of Trends and Changes in Mean, Maximum and Minimum Temperatures of Turkey for the period 1929–1999. *International Journal Climatology.* 22, 947–977.

- Udo-Inyang & Ini. D. Edem (2012). Analysis of Rainfall Trends in Akwa Ibom State, Nigeria. *Journal of Environment and Earth Science*, 12 (8), 60-70
- Umar, D. R., Diaz, N. & Graham, E. (2014). Decadal Variability of Precipitation over Western North America. *Journal Climate*, 11, 3148-3166
- Wiens, J. (1994) Predictability of Patterns and Variability of Precipitation at IBP Grassland Biome Sites. US IBP Grassland Biome, Technical Report 168, Colorado State University, Fort Collins, CO USA
- Wilks, D. S. (1995). Statistical methods in the Atmospheric Sciences, 1995. *San Diego, CA: Academic Press*
- World Metrology Organization (2012). Standardised Precipitation Index User Guide WMO-No. 1090 7 ISBN 978-92-63-11091-6
- Zhang, Y. (2011). Analysis of impacts of Climate Variability and Human activity on Stream flow for River Basin in North East China. *Journal on Hydrology*, 410(3-4), 239-247.
- Zurbenko, I, Porter, P.S., Rao, S.T., Ku, J. Y., Gui, R., Eskridge, R.E. (1996). Detecting Discontinuities in Time Series of Upper Air data: Development and Demonstration of an Adaptive Filter Technique. *Climate Journal*, 9, 3548-3560.

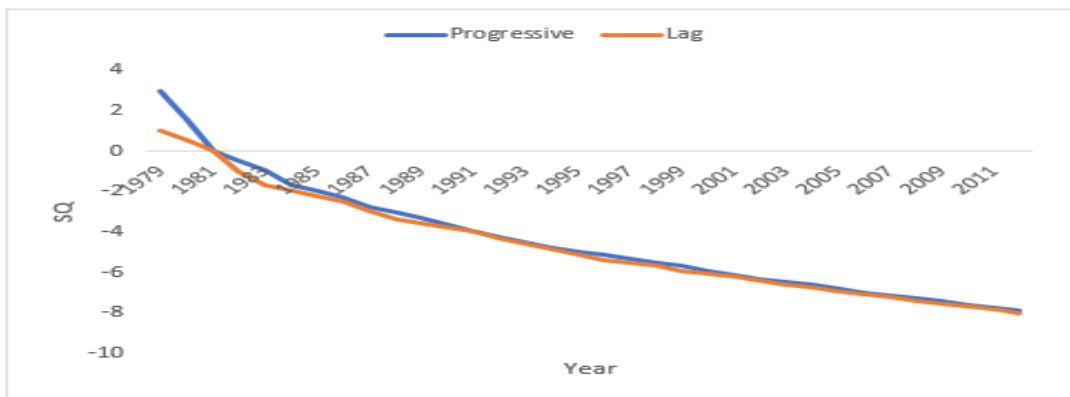
APPENDICES

APPENDIX A

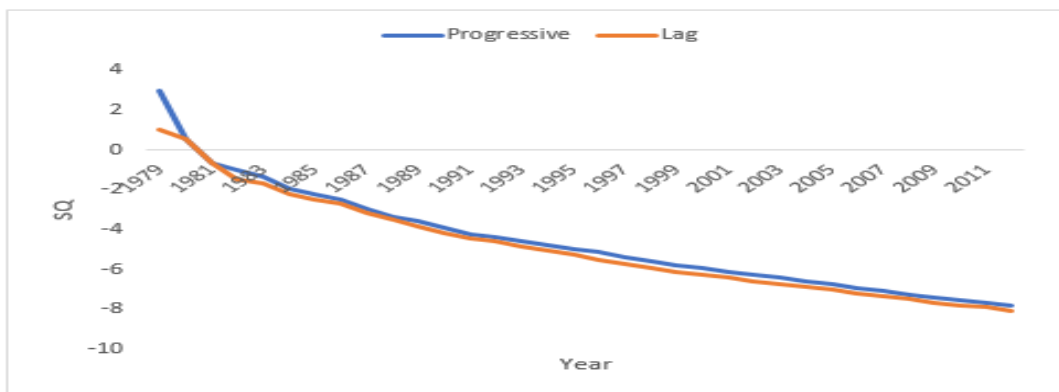
Figure of Sequential Trend in Maximum Temperature



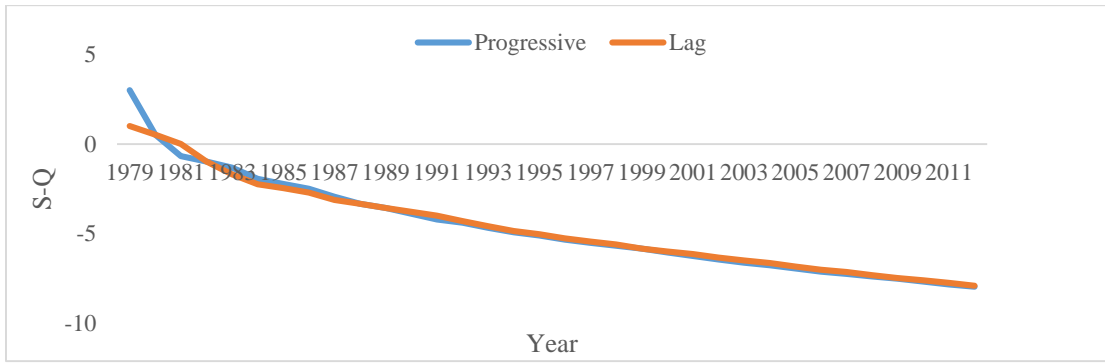
Olamaboro



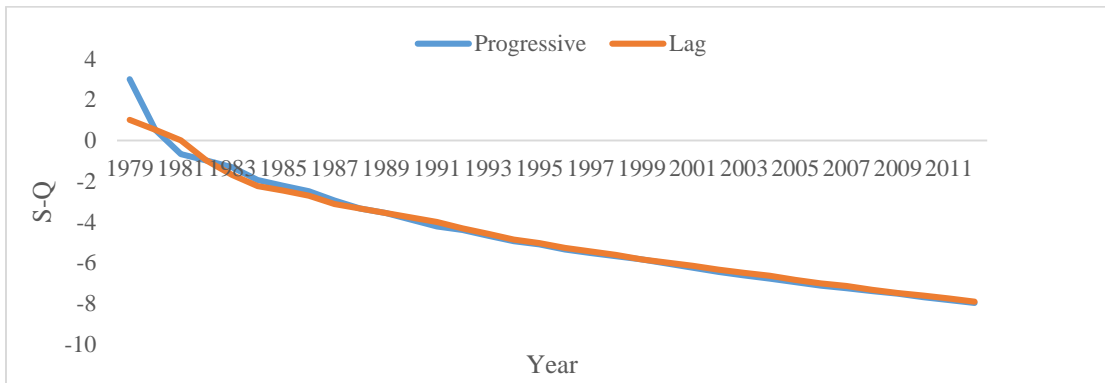
Lafiagi



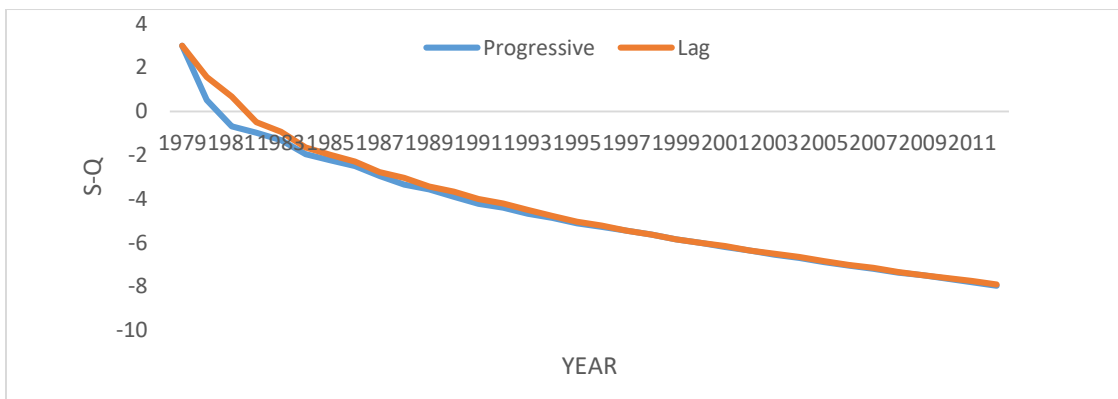
Ganaga



Obangede



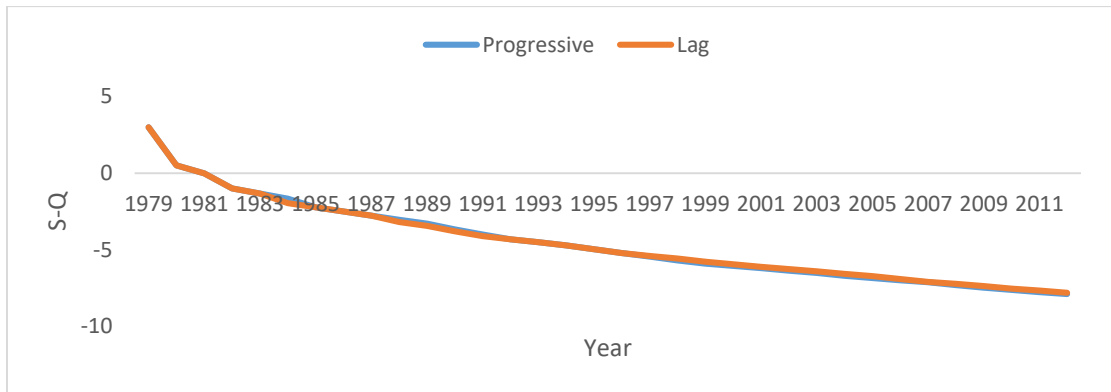
Oke Oyi



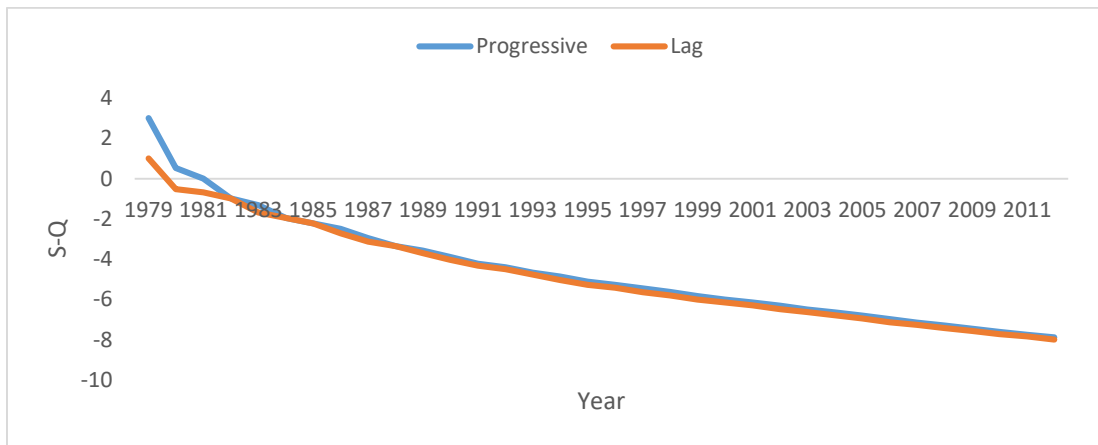
Ekirin Ade

APPENDIX B

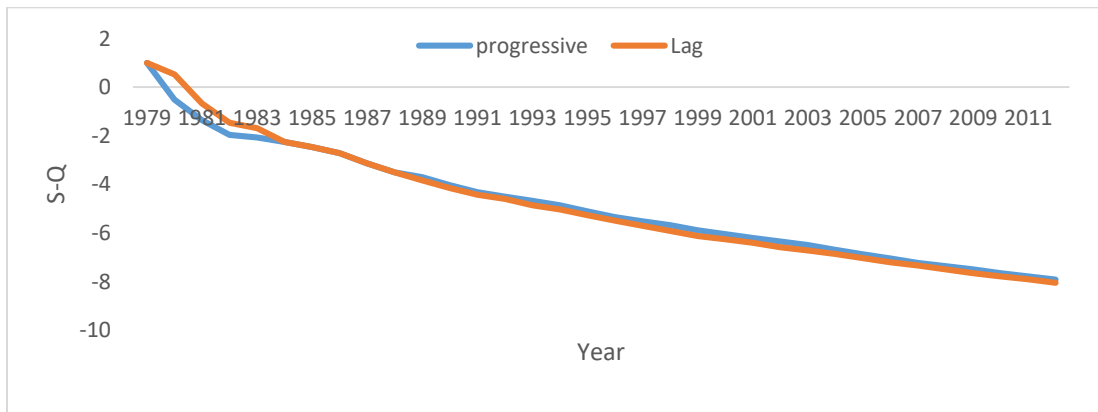
Sequential Trend for Minimum Temperature



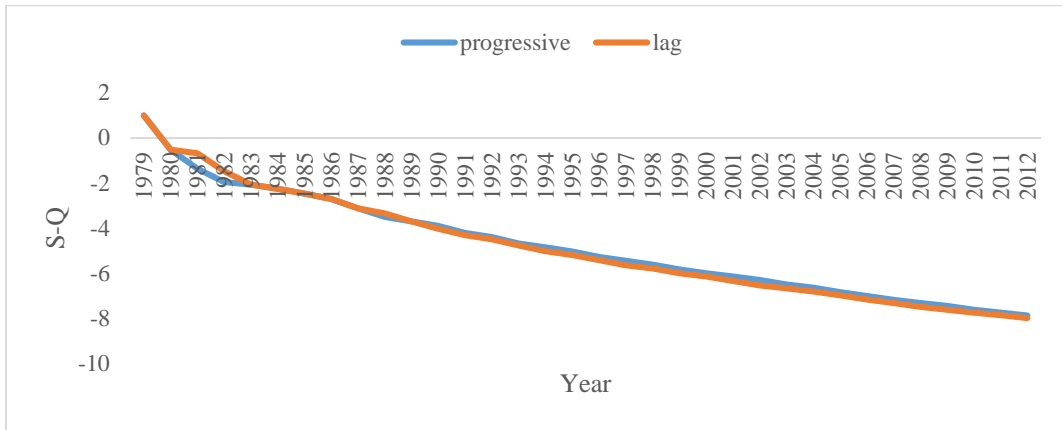
Olamaboro



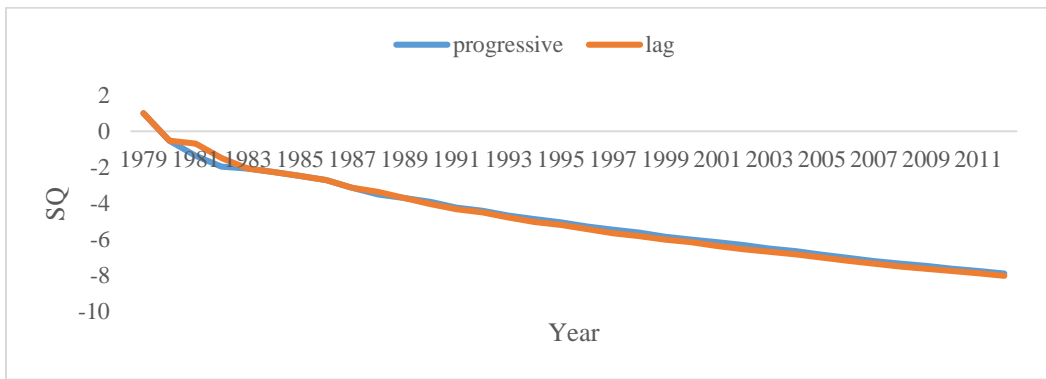
Lafiagi



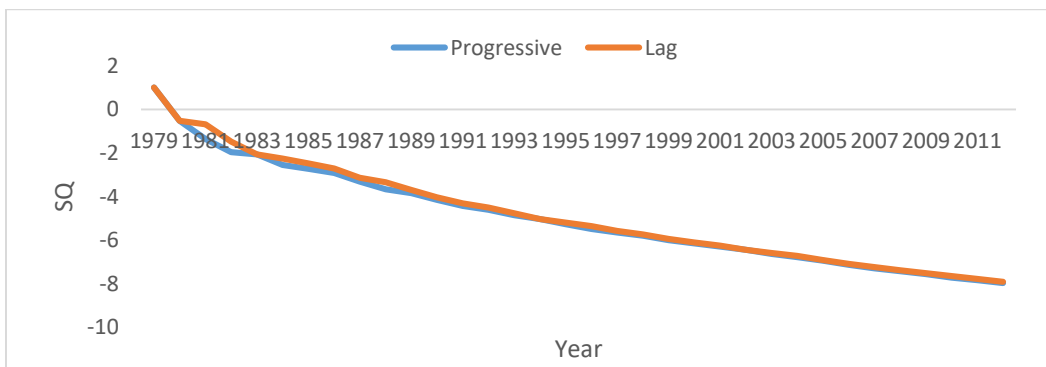
Ganaga



Obangede



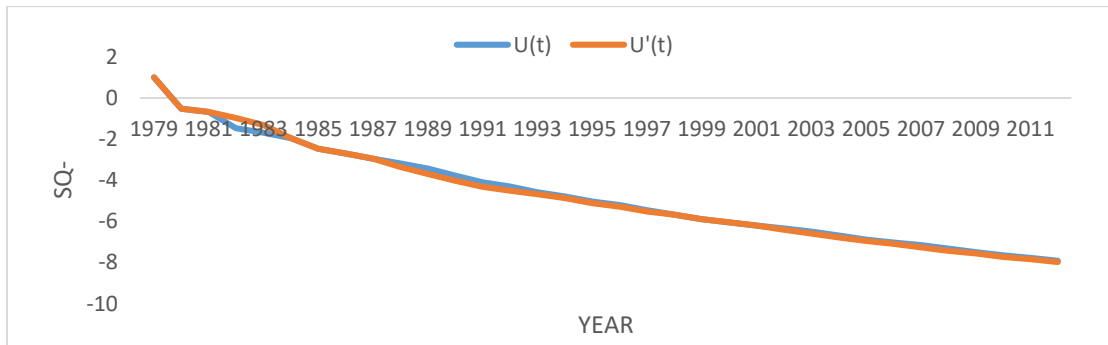
Oke Oyi



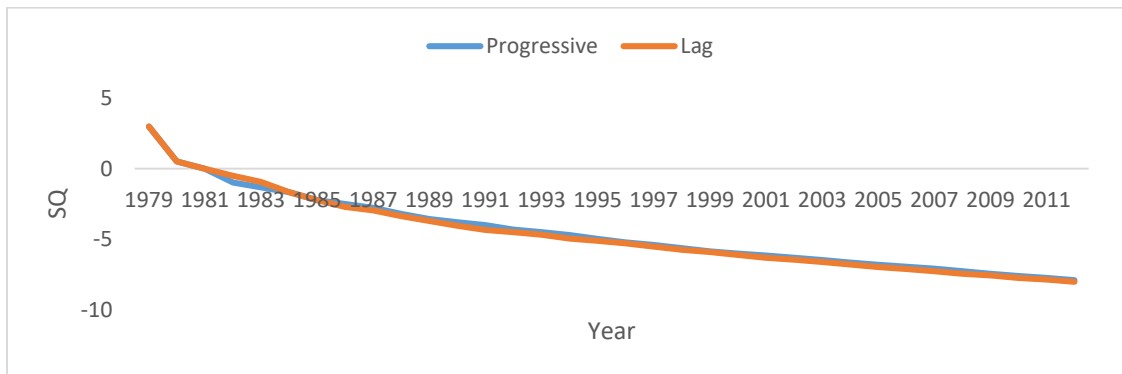
Ekirin Ade

APPENDIX C

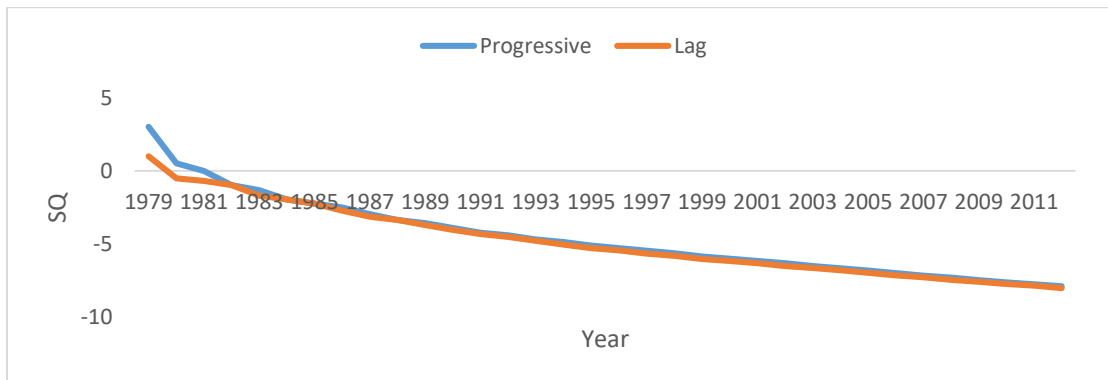
Sequential Trend of rainfall



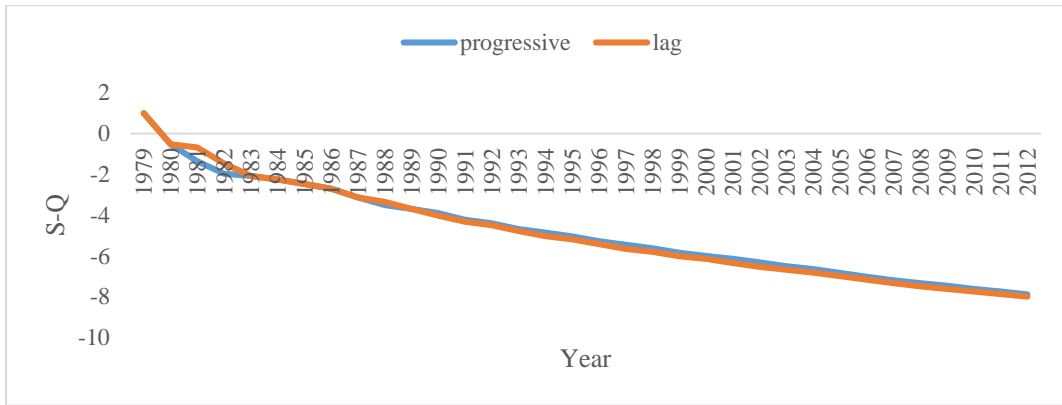
Ekirin Ade



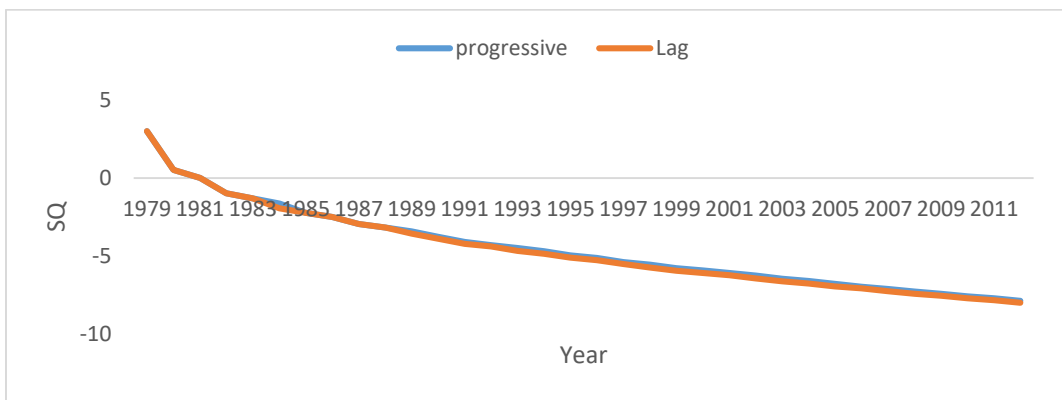
Ganaga



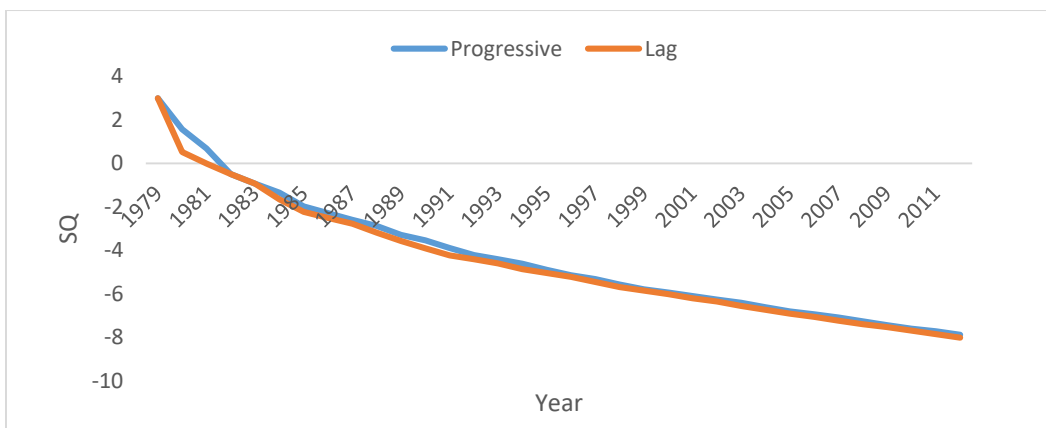
Lafiagi



Obangede



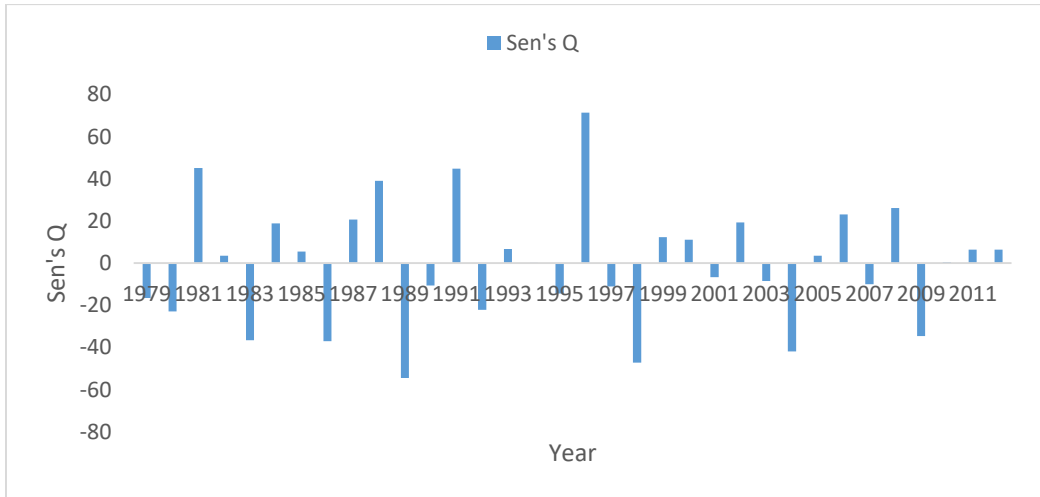
Oke Oyi



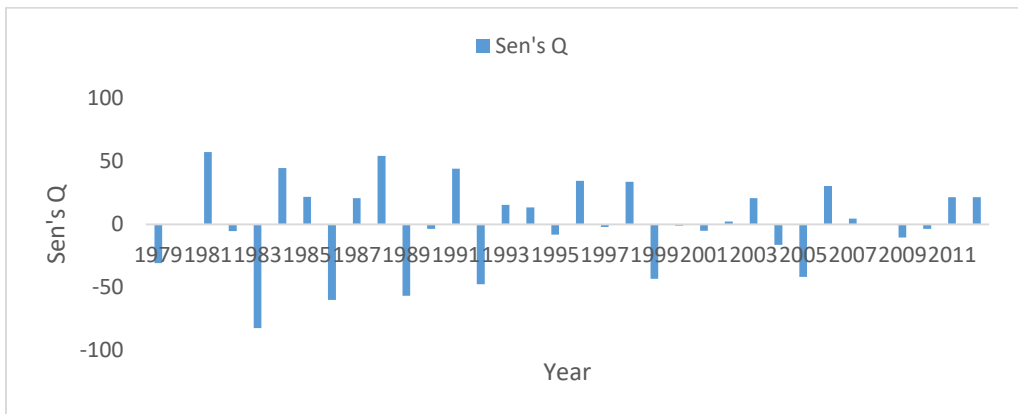
Olamaboro

APPENDIX D

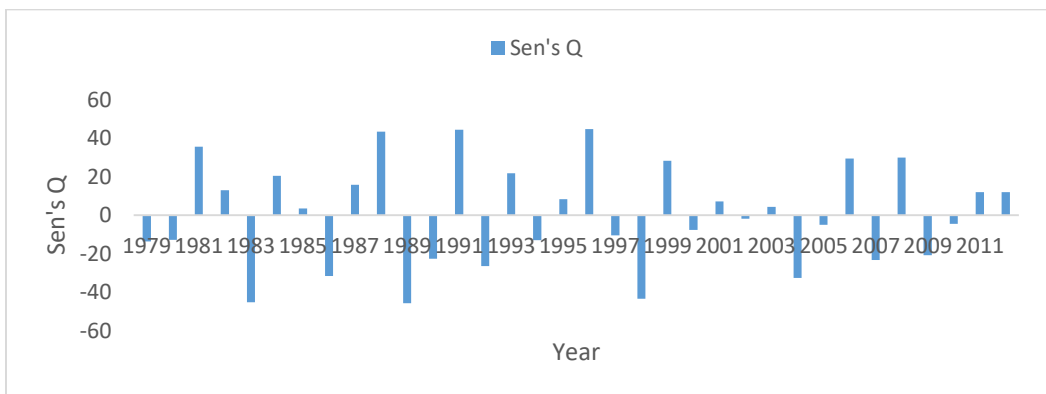
Sen's Slope Maximum Temperature



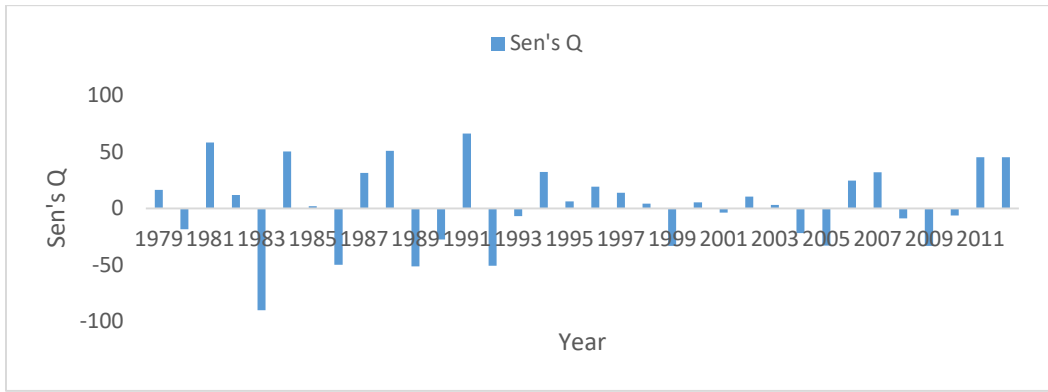
Olamaboro



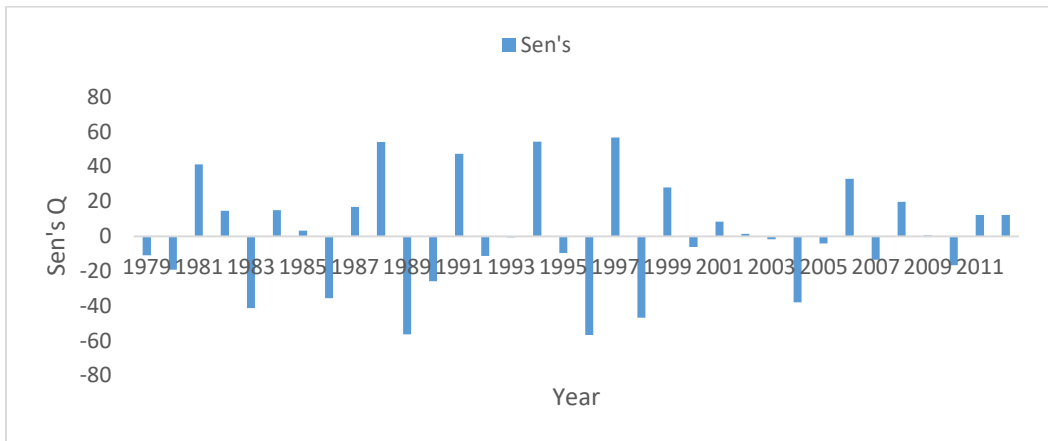
Oke Oyi



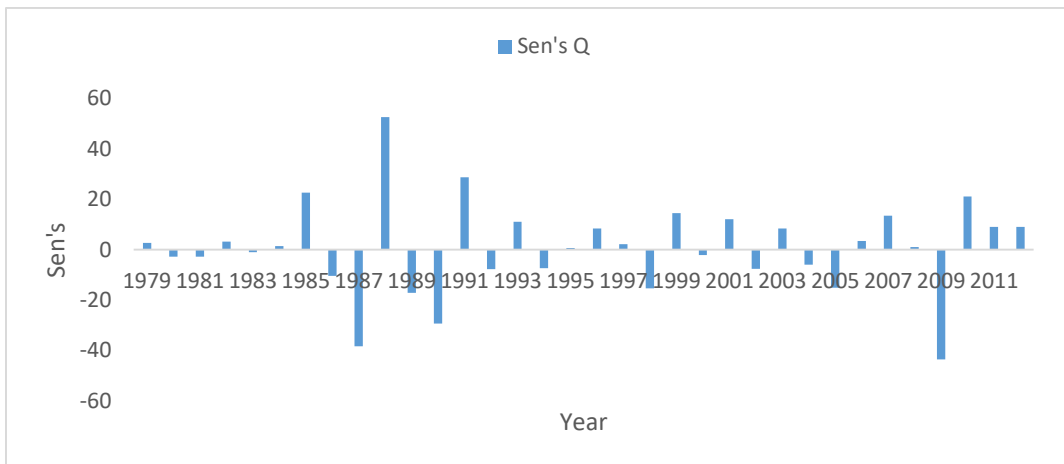
Obangede



Lafiagi



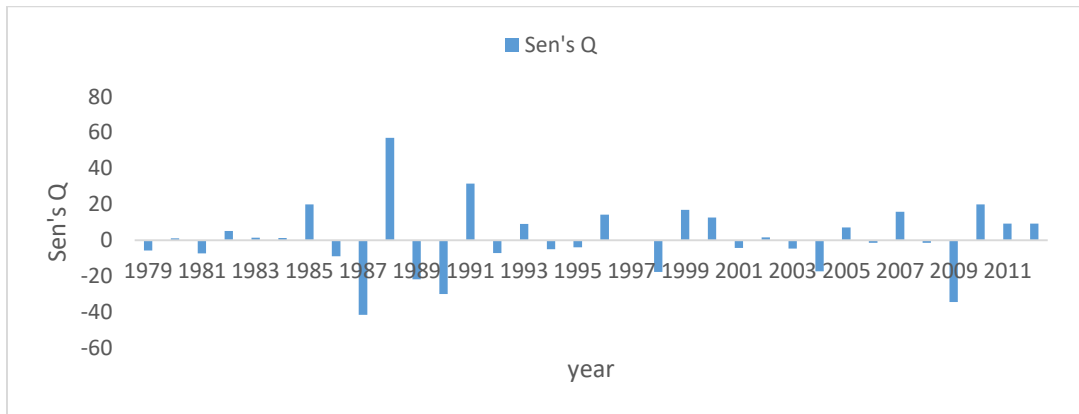
Ganaga



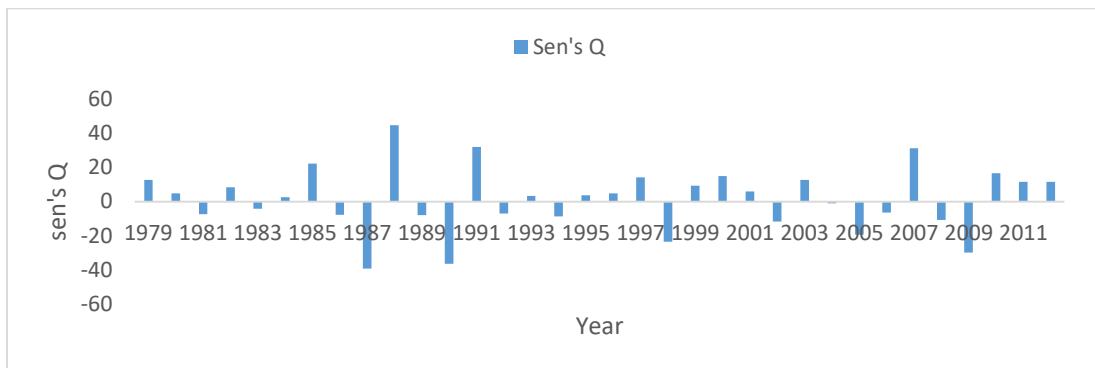
Ekirin Ade

APPENDIX E

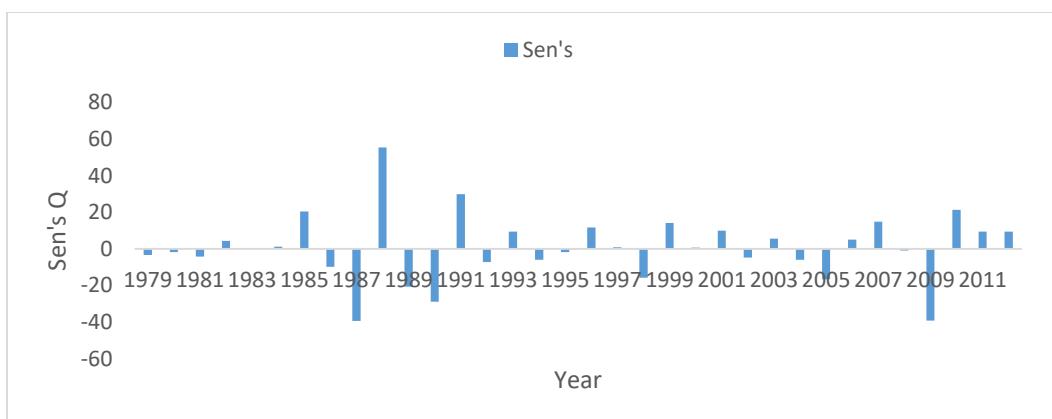
Sen's Slope for Minimum temperature



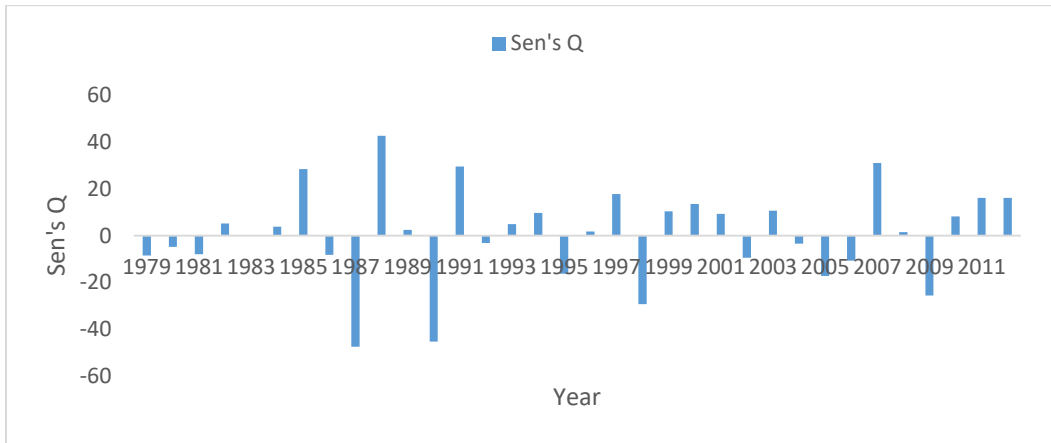
Ganaga



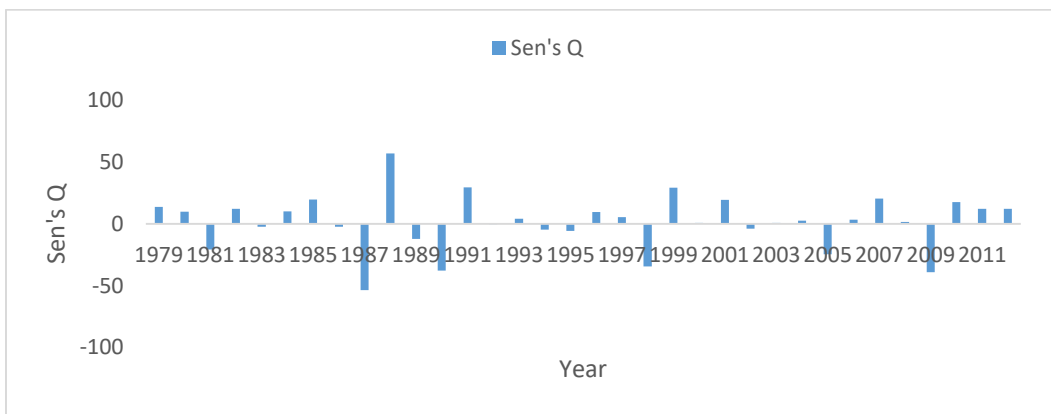
Lafiagi



Obangede



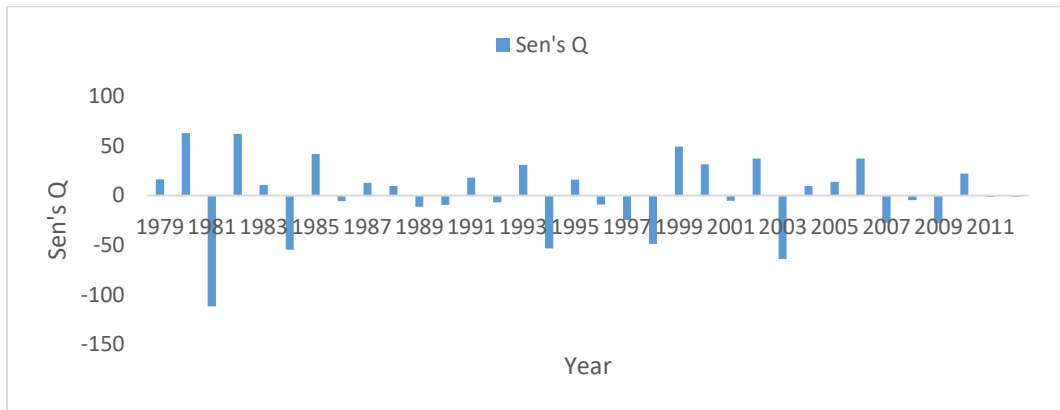
Oke Oyi



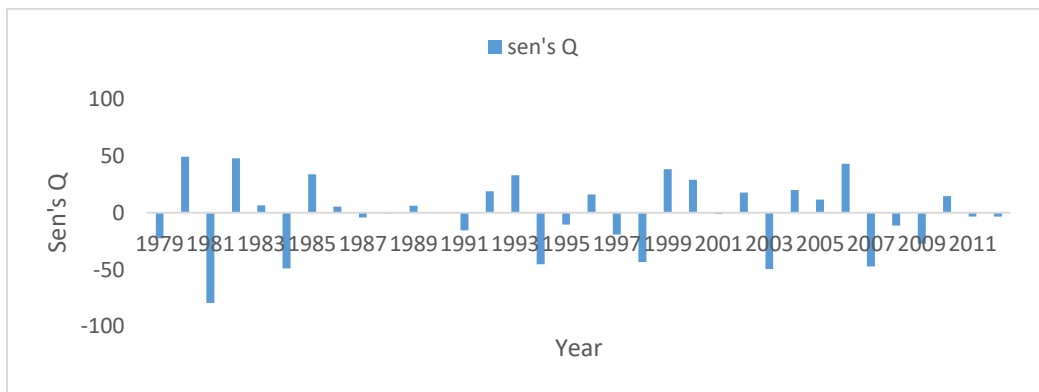
Olamaboro

APPENDIX F

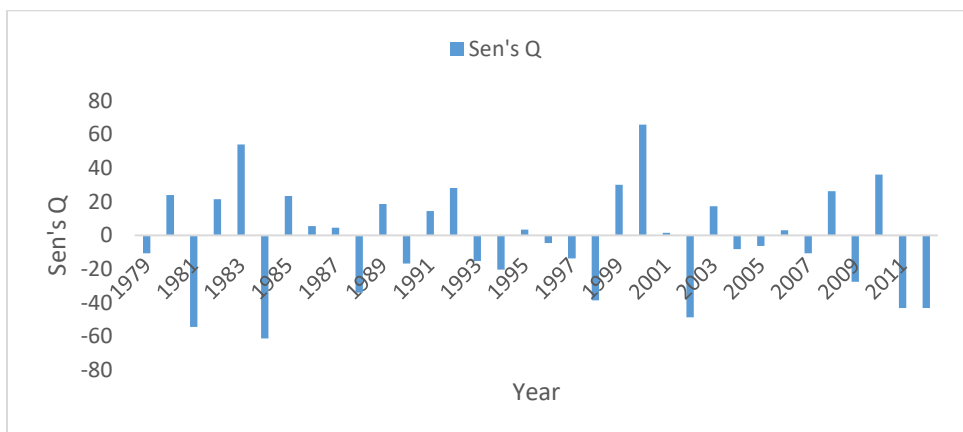
Sen's Slope Rainfall



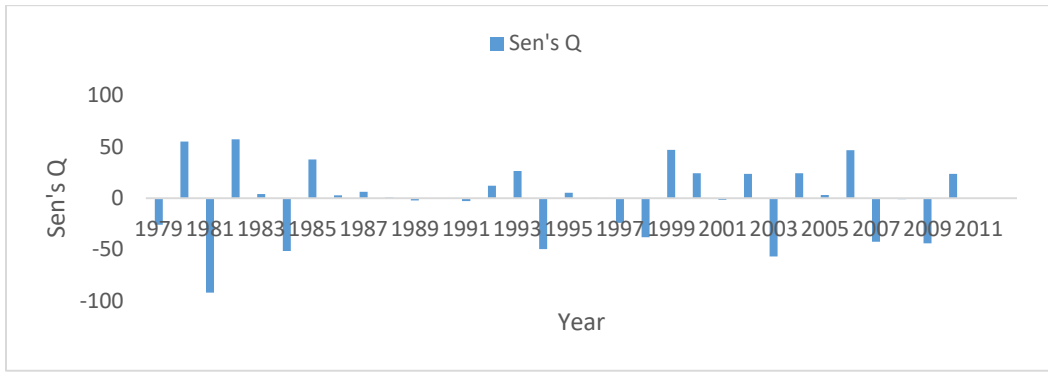
Ekirin Ade



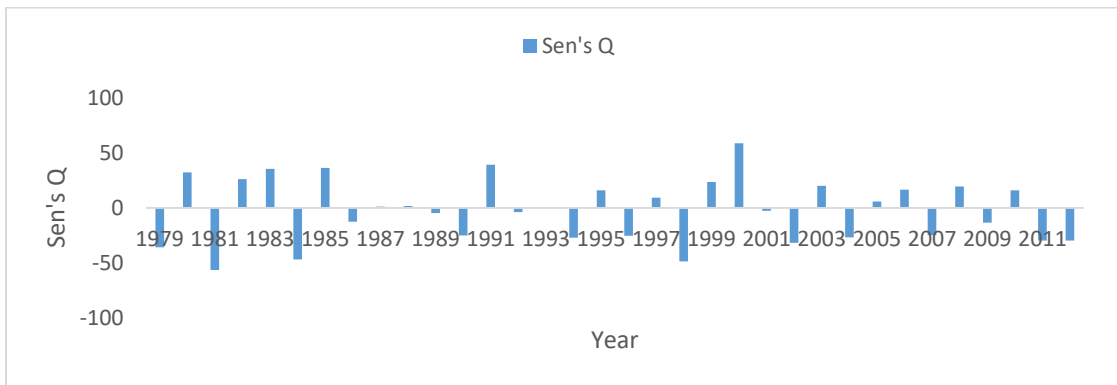
Ganaga



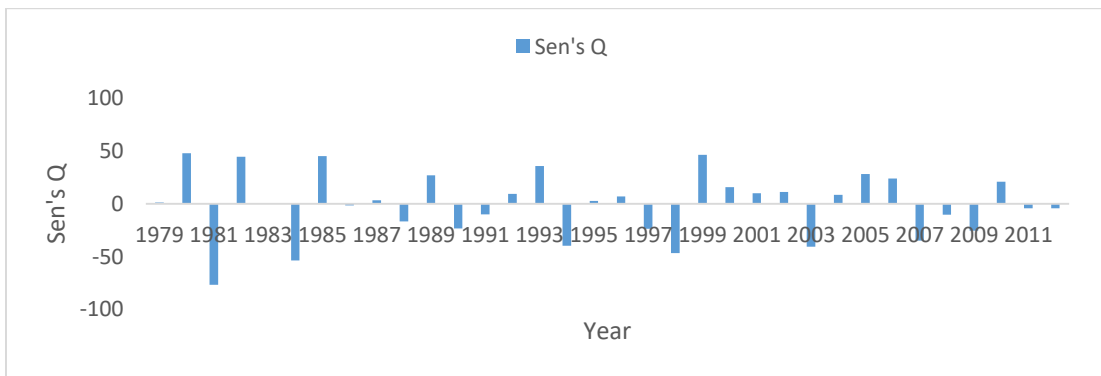
Lafiagi



Obangede



Oke Oyi



Olamaboro